

# Photo Reactions on the Deuteron in the $\Delta$ -Resonance Region

K. A. Bugaev<sup>1,2</sup>, U. Oelfke<sup>1,3</sup> and P.U. Sauer<sup>1</sup>

<sup>1</sup>Institute for Theoretical Physics, University of Hannover  
30167 Hannover, Germany

<sup>2</sup>Bogolyubov Institute for Theoretical Physics  
Kiev, Ukraine

<sup>3</sup> Theory Group, TRIUMF  
4004 Wesbrook Mall  
Vancouver, B.C.  
Canada V6T 2A3

## Abstract

Photo disintegration of the deuteron and photo pionproduction on the deuteron are described in the region of the  $\Delta$ -resonance. The two reactions are unitarily coupled. A novel definition of electromagnetic exchange currents in the presence of pionproduction is given. Numerical predictions are done for spin-independent and spin-dependent observables of both reactions. The sensitivity of the results with respect to the nucleon- $\Delta$  transition current and with respect to the irreducible nucleon- $\Delta$  potential is studied.

**Key words:** Photo disintegration, photo pionproduction, electromagnetic exchange currents

**PACS:** 25.20; 13.60.L

# 1. Introduction

The two-nucleon system above pion threshold is the simplest many-nucleon system which can be studied at intermediate-energy excitation. At those energies the pion ( $\pi$ ) and the  $\Delta$ -isobar degrees of freedom become active and are clearly seen in elastic two-nucleon scattering and in its unitarily coupled inelastic channels with one pion, i.e., in the two-body pion-deuteron (d) channel and in the three-body  $\pi$ NN channel containing two free nucleons (N) and one pion. The hadronic properties of the two-nucleon system above pion threshold are often described in terms of hamiltonian force models [1, 2] with explicit pion and  $\Delta$ -isobar degrees of freedom or in terms of variants [3, 4, 5] of it, in which the pion-nucleon  $P_{33}$ -resonance is accounted for by the properties of a pion-nucleon potential. The theoretical description of the two-nucleon system above pion threshold is technically demanding due to its three-body aspect and unfortunately not always successful, since the building blocks of the employed force model are not tuned yet. An overview on the art of describing the hadronic processes in the two-nucleon system above pion threshold is given in Ref. [6]. At intermediate energies the pion and the  $\Delta$ -isobar can also be excited in electromagnetic (e.m.) reactions, i.e., in inelastic electron scattering or by the absorption of real photons ( $\gamma$ ). Bremsstrahlung in two-nucleon scattering is the corresponding process of photon emission. This paper develops a description for both photo reactions in the two-nucleon system. The description is attempted to be consistent with the description of hadronic reactions given previously [1]. The paper applies the description to photo disintegration of the deuteron and to photo pionproduction on the deuteron.

The simultaneous description of hadronic and e.m. reactions requires the conceptual consistency between hadronic interaction operators and e.m. current operators. That consistency is the underlying theme of this paper. It completes work started in Ref. [7] by two of the present authors. In their pioneering work Arenhövel and Leidemann [8] studied deuteron disintegration in e.m. reactions and beautifully proved the importance of meson-exchange currents and isobar-excitation for a successful description. Wilhelm *et al.* [9, 10, 11] extended that work to a simultaneous description of photo pionproduction on the deuteron. Parallel theoretical developments can be found in Ref. [12]. More recent theoretical results on this subject can also be found in Ref. [13]. The present paper will therefore be unable to add much to our understanding of those processes. However, we believe that a thorough discussion of a consistent treatment of all pionic and e.m. reactions from the deuteron is a worthwhile enterprise.

Sect. 2 describes the conceptual characteristics of the model used for the hadronic interaction and for the e.m. current. It discusses in some length the constraint of current conservation and the redefinition of exchange currents in a coupled-channel theory which considers the pion as an active degree of freedom. It gives the e.m. multi-channel transition matrix for photon reactions in the two-nucleon system. Sect. 3 describes the actual parameterization of the force and of the current in our practical calculations. Sect. 4 applies the theoretical apparatus to photo disintegration of the deuteron and to photo

pionproduction on the deuteron. It gives results for both types of reactions. Sect. 5 contains our conclusions.

## 2. Theoretical Framework

### 2.1 Force Model and Hadronic Reactions

Our approach for studying e.m. reactions in the two-nucleon system employs the hadronic interaction of Ref. [1]. That interaction describes the two-nucleon system below and above pion-threshold and its coupled inelastic channels with at most one pion, i.e., the reactions  $NN \rightarrow NN$ ,  $NN \leftrightarrow \pi d$ ,  $NN \rightarrow \pi NN$ ,  $\pi d \rightarrow \pi d$  and  $\pi d \rightarrow \pi NN$ . The inclusion of inelastic channels with at most one pion limits [1] the validity of the force model to c.m. energies below 500 MeV. The force model is defined in the framework of nonrelativistic quantum mechanics. This section briefly reviews its basic ideas. Appendix A provides the details needed for the objectives of this paper.

The Hilbert space for the description of hadronic and e.m. reactions at intermediate energies has the purely nucleonic sector  $\mathcal{H}_N$  and two additional sectors  $\mathcal{H}_\Delta$  and  $\mathcal{H}_\pi$  with non-nucleonic content. In  $\mathcal{H}_\Delta$  one of the nucleons is replaced by a  $\Delta$ -isobar. The third sector  $\mathcal{H}_\pi$  contains one additional pion besides nucleons. The projection operators on the three different sectors  $\mathcal{H}_N$ ,  $\mathcal{H}_\Delta$  and  $\mathcal{H}_\pi$  are labeled  $P_N$ ,  $P_\Delta$  and  $Q$ , respectively, with  $P_N + P_\Delta + Q = 1$ .

The hamiltonian  $H$  consists of the kinetic energy  $H_0$  and of the interaction  $H_1$ , i.e.,  $H = H_0 + H_1$ . The eigenstates of the kinetic energy  $H_0$  make up the different Hilbert sectors. The interaction hamiltonian  $H_1$  is given in terms of instantaneous potentials and is decomposed according to its action within and between the three different Hilbert sectors, i.e.,

$$H_1 = (P_N + P_\Delta)H_1(P_N + P_\Delta) + P_\Delta H_1 Q + Q H_1 P_\Delta + Q H_1 Q. \quad (2.1)$$

The various contributions to  $H_1$  are shown in Fig. 2.1 for a system of baryon number two. The potentials  $P_a H_1 P_b$  with  $a, b = N, \Delta$  act in the purely baryonic sectors, i.e.,  $P_N H_1 P_N$  is the two-nucleon potential of Fig. 2.1(a),  $P_\Delta H_1 P_N$  the transition potential from two-nucleon to nucleon- $\Delta$  states of Fig. 2.1(b) and  $P_\Delta H_1 P_\Delta$  the potential between nucleon- $\Delta$  states of Figs. 2.1(c) and 2.1(d). The two-baryon states are coupled to the pionic states by the one-baryon  $\pi N \Delta$  vertex  $Q H_1 P_\Delta$  of Fig. 2.1(e). The hermitian conjugate parts  $P_N H_1 P_\Delta$  and  $P_\Delta H_1 Q$  are not shown in Fig. 2.1. In the three-particle Hilbert sector  $\mathcal{H}_\pi$  the interaction  $Q H_1 Q$  consists of the two-nucleon potential in the presence of a pion and of the pion-nucleon potential in nonresonant partial waves according to Figs. 2.1(f) and 2.1(g) respectively.

A special feature of the considered force model is its mechanism for pionproduction and pion absorption. Pionic states are not coupled directly to purely nucleonic ones, i.e.,  $P_N H_1 Q = Q H_1 P_N = 0$ . Pion production and pion absorption are assumed to proceed

through the excitation and deexcitation of an  $\Delta$ -isobar in two-nucleon processes. The  $\Delta$ -isobar is a bare particle of spin and isospin  $\frac{3}{2}$ . It is unobservable and gets dressed to the physical  $P_{33}$ -resonance of pion-nucleon scattering by self-energy corrections due to coupling to pion-nucleon states. This force model assumes the  $P_{33}$  partial wave to dominate pion-nucleon scattering in the region up to 300 MeV pion lab energy. Its standard realization assumes  $P_{33}$  pion-nucleon scattering to proceed exclusively through the  $\Delta$ -isobar as shown in Fig. 2.2, i.e., a possible nonresonant potential  $QH_1Q$  is taken to be zero in that partial wave. The  $P_{33}$  pion-nucleon transition matrix  $t_{\pi N}(\varepsilon_\Delta + i0)$  therefore takes the particular form [1, 2, 14]

$$t_{\pi N}(\varepsilon_\Delta + i0)|\mathbf{k}_\Delta\rangle = QH_1P_\Delta \frac{1}{\varepsilon_\Delta + i0 - \frac{k_\Delta^2}{2m_\Delta^0} - M_\Delta(\varepsilon_\Delta, k_\Delta) + \frac{i}{2}\Gamma_\Delta(\varepsilon_\Delta, k_\Delta)} P_\Delta H_1 Q |\mathbf{k}_\Delta\rangle. \quad (2.2)$$

In Eq. (2.2)  $m_\Delta^0 = 1315.8$  MeV is the bare mass of the  $\Delta$ -isobar according to [1], whereas  $M_\Delta(\varepsilon_\Delta, k_\Delta)$  and  $\Gamma_\Delta(\varepsilon_\Delta, k_\Delta)$  are its renormalized mass and width. The latter quantities depend on the energy  $\varepsilon_\Delta$  available for and on the total momentum  $\mathbf{k}_\Delta$  of the pion-nucleon system; they become identical with the mass and the width of the physical  $P_{33}$ -resonance for  $\varepsilon_\Delta = 1232$  MeV at resonance and for  $\mathbf{k}_\Delta = 0$  in the pion-nucleon c.m. system.

The explicit parameterization of the hamiltonian (2.1) will be given in Sect. 3.2. Its application to the two-nucleon system above pion threshold leads to a complex multi-channel scattering problem. The employed scattering theory is an extended version of the Alt-Grassberger-Sandhas (AGS) formulation [15], extended to particle production in Ref. [1]. In Ref. [1] methods for the practical solution of the resulting equations are also given. Details of the theoretical apparatus are repeated in Appendix A in order to make the present paper self-contained. This section reviews only some further essentials:

The reaction channels differ by their particle content. There are two-baryon channels without a pion, i.e., two-nucleon and nucleon- $\Delta$  channels,  $N$  and  $\Delta$ , respectively, denoted by the small Latin letters  $a, b, c \dots$  in the following, there are two-body channels in the three-particle Hilbert sector  $\mathcal{H}_\pi$ , in which two particles form a bound pair, denoted by small Greek letters  $\alpha, \beta, \gamma \dots$ , the label for the spectating particle, and there are three-particle channels in  $\mathcal{H}_\pi$ , in which all three particles are free, denoted by the subscript 0. In the two-nucleon system above pion threshold only three different reaction channels are experimentally observable, i.e.,

1. the two-nucleon channel  $a = N$  with the asymptotic states  $|\phi_N(\mathbf{p}_N)\rangle$  of relative momentum  $\mathbf{p}_N$ ,  $E_N(\mathbf{p}_N)$  being the corresponding energy,
2. the pion-deuteron channel  $\alpha = \pi$  with asymptotic states  $|\phi_\pi(\mathbf{q}_\pi)\rangle$  of relative pion-deuteron momentum  $\mathbf{q}_\pi$ ,  $E_\pi(\mathbf{q}_\pi)$  being the corresponding energy and
3. the three-particle break-up channel 0 of two free nucleons and one free pion with the asymptotic  $\pi NN$  states  $|\phi_0(\mathbf{p}, \mathbf{q})\rangle$  of internal momenta  $\mathbf{p}$  and  $\mathbf{q}$ ,  $E_0(\mathbf{p}, \mathbf{q})$  being the corresponding energy.

When no confusion arises, we shall omit the arguments of the channel energy, i.e., we shall use  $E_N$ ,  $E_\pi$  and  $E_0$ .

The  $S$ -matrix elements between the different kinds of initial and final states  $|\phi_i\rangle$  and  $|\phi_f\rangle$  of energy  $E_i$  and  $E_f$  with  $i, f = N, \pi, 0$  referring to the three distinct channels are given in terms of the on-shell multi-channel transition matrix  $U(z)$ , i.e.,

$$\langle\phi_f|S|\phi_i\rangle = \langle\phi_f|\phi_i\rangle - 2\pi i\delta(E_f - E_i)\langle\phi_f|U_{fi}(E_i + i0)|\phi_i\rangle. \quad (2.3)$$

The various channel components of the off-shell transition matrix  $U(z)$  follow from an appropriate decomposition of the full resolvent

$$G(z) = \frac{1}{z - H_0 - H_1} \quad (2.4)$$

according to Eq. (A.1) of Appendix A. They satisfy integral equations. The multi-channel transition matrix  $U(z)$  contains the complete information about the dynamics generated by the hamiltonian (2.1). E.g., it allows to construct the fully correlated scattering states

$$\begin{aligned} |\Psi_N^{(\pm)}(\mathbf{p}_N)\rangle &= \pm i0G(E_N \pm i0)P_N|\phi_N(\mathbf{p}_N)\rangle, \\ |\Psi_\pi^{(\pm)}(\mathbf{q}_\pi)\rangle &= \pm i0G(E_\pi \pm i0)Q|\phi_\pi(\mathbf{q}_\pi)\rangle, \\ |\Psi_0^{(\pm)}(\mathbf{p}, \mathbf{q})\rangle &= \pm i0G(E_0 \pm i0)Q|\phi_0(\mathbf{p}, \mathbf{q})\rangle, \end{aligned} \quad (2.5)$$

in terms of the uncorrelated channel states  $|\phi_N(\mathbf{p}_N)\rangle$ ,  $|\phi_\pi(\mathbf{q}_\pi)\rangle$  and  $|\phi_0(\mathbf{p}, \mathbf{q})\rangle$ , i.e.,

$$P_b|\Psi_N^{(\pm)}(\mathbf{p}_N)\rangle = [\delta_{bN} + g_{b0}^P(E_N \pm i0)U_{bN}(E_N \pm i0)]P_N|\phi_N(\mathbf{p}_N)\rangle, \quad (2.6a)$$

$$Q|\Psi_N^{(\pm)}(\mathbf{p}_N)\rangle = g_\beta^Q(E_N \pm i0)U_{\beta N}(E_N \pm i0)P_N|\phi_N(\mathbf{p}_N)\rangle, \quad (2.6b)$$

$$P_b|\Psi_\pi^{(\pm)}(\mathbf{q}_\pi)\rangle = g_{b0}^P(E_\pi \pm i0)U_{b\pi}(E_\pi \pm i0)Q|\phi_\pi(\mathbf{q}_\pi)\rangle, \quad (2.7a)$$

$$Q|\Psi_\pi^{(\pm)}(\mathbf{q}_\pi)\rangle = [\delta_{\beta\pi} + g_\beta^Q(E_\pi \pm i0)U_{\beta\pi}(E_\pi \pm i0)]Q|\phi_\pi(\mathbf{q}_\pi)\rangle, \quad (2.7b)$$

$$P_b|\Psi_0^{(\pm)}(\mathbf{q}, \mathbf{p})\rangle = g_{b0}^P(E_0 \pm i0)U_{b0}(E_0 \pm i0)Q|\phi_0(\mathbf{q}, \mathbf{p})\rangle, \quad (2.8a)$$

$$Q|\Psi_0^{(\pm)}(\mathbf{q}, \mathbf{p})\rangle = g_\beta^Q(E_0 \pm i0)U_{\beta 0}(E_0 \pm i0)Q|\phi_0(\mathbf{q}, \mathbf{p})\rangle, \quad (2.8b)$$

$$= [1 + g_0^Q(E_0 \pm i0)U_{00}(E_0 \pm i0)]Q|\phi_0(\mathbf{q}, \mathbf{p})\rangle. \quad (2.8c)$$

The quantities  $g_{b0}^P(z)$ ,  $g_\beta^Q(z)$  and  $g_0^Q(z)$  are partial resolvents defined in Eq. (A.2) of Appendix A. The form of Eqs. (2.6) - (2.8) for the hadronic scattering states is needed in Sect. 2.3 to derive the corresponding transition amplitudes for the e.m. processes in the two-nucleon system. That information is unnecessary for the  $S$ -matrix (2.3) of hadronic reactions.

## 2.2 The E.M. Current and the Constraint of Current Conservation

The e.m. interaction of a system of nucleons whose dynamics is controlled by the force model of Sect. 2.1 is described in this section. The presentation is split into three parts: First, the general structure of the current acting in and between the different Hilbert sectors  $\mathcal{H}_N$ ,  $\mathcal{H}_\Delta$  and  $\mathcal{H}_\pi$  is explained and the corresponding e.m. hamiltonian  $H_1^\gamma$  for the emission and absorption of real photons is constructed. Second, the constraint of current conservation is discussed. Third, the interaction-dependent contributions to the current are constructed. We consider Subsects. 2.2.2 and 2.2.3 the conceptually most important ones of this paper.

### 2.2.1 Structure of the E.M. Interaction

The photon field  $A^\mu(x)$  couples to the e.m. current operator  $j^\mu(x) = (\rho(x), \mathbf{j}(x))$  of hadrons and forms the e.m. hamiltonian  $H_1^\gamma$  by

$$H_1^\gamma = \int d^3x A_\mu(\mathbf{x}, 0) j^\mu(\mathbf{x}, 0). \quad (2.9)$$

The photon field  $A^\mu(\mathbf{x}, 0)$  is employed in Coulomb gauge, i.e.,  $A^\mu(\mathbf{x}, 0) = (0, \mathbf{A}(\mathbf{x}, 0))$  with  $\nabla \cdot \mathbf{A}(\mathbf{x}, 0) = 0$ . Consequently, the e.m. hamiltonian  $H_1^\gamma$  couples the photon field only to the spatial components  $\mathbf{j}(\mathbf{x}, 0)$  of the current  $j^\mu(x)$ . The e.m. hamiltonian is used in one-photon exchange approximation, i.e., in lowest-order perturbation theory. In this paper it will be applied to reactions with real photons only. Thus, the operator of the e.m. field  $A^\mu(\mathbf{x}, 0)$  takes the form

$$A^\mu(\mathbf{x}, 0) = \frac{1}{(2\pi)^{\frac{3}{2}}} \int \frac{d^3k}{2\omega} \sum_{\lambda=\pm 1} \varepsilon^\mu(\mathbf{k}, \lambda) [a(\mathbf{k}, \lambda) e^{i\mathbf{k}\mathbf{x}} + a^\dagger(\mathbf{k}, \lambda) e^{-i\mathbf{k}\mathbf{x}}], \quad (2.10)$$

where  $a(\mathbf{k}, \lambda)$  and  $a^\dagger(\mathbf{k}, \lambda)$  are the annihilation and creation operators for a photon of momentum  $\mathbf{k}$ , of energy  $\omega = |\mathbf{k}|$  and of helicity  $\lambda$  with  $\varepsilon^\mu(\mathbf{k}, \lambda)$  being the polarization vector. The conventions of Ref. [16] for commutation rules and normalization are adopted.

Though real photons in Coulomb gauge couple only to the spatial components of the current, we nevertheless discuss the e.m. current in full – in anticipation of the theoretical needs when describing general e.m. reactions. The current will be employed in the Fourier-transformed form

$$j^\mu(\mathbf{k}_\gamma) = \int d^3x e^{i\mathbf{k}_\gamma \mathbf{x}} j^\mu(\mathbf{x}, 0). \quad (2.11)$$

It couples the various sectors of the Hilbert space considered, i.e.,

$$j^\mu(\mathbf{k}_\gamma) = (P_N + P_\Delta + Q) j^\mu(\mathbf{k}_\gamma) (P_N + P_\Delta + Q), \quad (2.12)$$

and it consists of one-baryon and at least two-baryon pieces,  $j^{[1]\mu}(\mathbf{k}_\gamma)$  and  $j^{[2]\mu}(\mathbf{k}_\gamma)$ , i.e.,

$$j^\mu(\mathbf{k}_\gamma) = j^{[1]\mu}(\mathbf{k}_\gamma) + j^{[2]\mu}(\mathbf{k}_\gamma). \quad (2.13)$$

It has to be consistent with the underlying hadronic interaction and has at least to satisfy current conservation

$$\mathbf{k}_\gamma \cdot \mathbf{j}(\mathbf{k}_\gamma) = [H_0 + H_1, \rho(\mathbf{k}_\gamma)] \quad (2.14)$$

as one consistency condition. All calculations will be done in the c.m. system; nevertheless, the current operator  $j^\mu(\mathbf{k}_\gamma)$  also has to be a Lorentz four-vector; boost properties of the current are therefore additional consistency conditions, but will not be considered here, as usual. The one-nucleon current  $P_N j^{[1]\mu}(\mathbf{k}_\gamma) P_N$  is seen in elastic electron-nucleon scattering, the current  $(P_\Delta + Q) j^{[1]\mu}(\mathbf{k}_\gamma) P_N$  in electro pionproduction on the nucleon. The considered hadronic hamiltonian of Subsect. 2.1 requires interaction-dependent exchange currents of many-baryon nature. Only currents of one-baryon and two-baryon characteristics are considered according to Eq. (2.13).

### 2.2.2 Channel Decomposition and Baryon-Number Decomposition

This subsection analyzes the condition (2.14) of current conservation. The condition (2.14) has the form

$$\begin{aligned} \mathbf{k}_\gamma \cdot (P_N + P_\Delta + Q) \left[ \mathbf{j}^{[1]}(\mathbf{k}_\gamma) + \mathbf{j}^{[2]}(\mathbf{k}_\gamma) \right] (P_N + P_\Delta + Q) = \\ (P_N + P_\Delta + Q) [H_0^{[1]} + H_1^{[1]} + H_1^{[2]}, \rho^{[1]}(\mathbf{k}_\gamma) + \rho^{[2]}(\mathbf{k}_\gamma)] (P_N + P_\Delta + Q), \end{aligned} \quad (2.15)$$

once the coupling between channels and the baryon-number characteristics of the hamiltonian and of the current are made explicit. The kinetic energy operator  $H_0^{[1]}$  is of one-baryon nature and that fact is notationally indicated in this subsection by the superscript one in square brackets in contrast to the remainder of the paper. However, also the interaction part of the hamiltonian has one-baryon pieces  $H_1^{[1]}$  besides the irreducible two-baryon ones  $H_1^{[2]}$ . In one-baryon pieces one nucleon does not participate in any interaction: One-baryon pieces are the  $\pi N \Delta$  vertex of process (e) in Fig. 2.1 and the pion-nucleon potential of process (g) in Fig. 2.1. Thus, we use the hadronic hamiltonian whose interaction structure is given in Eq. (2.1) in the form

$$\begin{aligned} H = & P_N H_0^{[1]} P_N + P_\Delta H_0^{[1]} P_\Delta + Q H_0^{[1]} Q + \\ & P_\Delta H_1^{[1]} Q + Q H_1^{[1]} P_\Delta + Q H_1^{[1]} Q + \\ & (P_N + P_\Delta) H_1^{[2]} (P_N + P_\Delta) + Q H_1^{[2]} Q. \end{aligned} \quad (2.16)$$

The condition of current conservation splits up into eighteen separate constraints differentiated by channel coupling and baryon number. Only twelve among the eighteen

constraints are independent, the other six are related to the independent ones by the hermiticity of the hamiltonian and of the current operator. As an example two constraints are spelt out in detail for one particular channel coupling, the coupling of purely nucleonic to pion-nucleon states, i.e.,

$$\mathbf{k}_\gamma \cdot Q \mathbf{j}^{[1]}(\mathbf{k}_\gamma) P_N = Q H_0^{[1]} Q Q \rho^{[1]}(\mathbf{k}_\gamma) P_N - Q \rho^{[1]}(\mathbf{k}_\gamma) P_N P_N H_0^{[1]} P_N + Q H_1^{[1]}(P_\Delta + Q) (P_\Delta + Q) \rho^{[1]}(\mathbf{k}_\gamma) P_N, \quad (2.17)$$

$$\begin{aligned} \mathbf{k}_\gamma \cdot Q \mathbf{j}^{[2]}(\mathbf{k}_\gamma) P_N = & Q H_0^{[1]} Q Q \rho^{[2]}(\mathbf{k}_\gamma) P_N - Q \rho^{[2]}(\mathbf{k}_\gamma) P_N P_N H_0^{[1]} P_N + \\ & Q H_1^{[1]} Q Q \rho^{[1]}(\mathbf{k}_\gamma) P_N + \\ & Q H_1^{[1]}(P_\Delta + Q) (P_\Delta + Q) \rho^{[2]}(\mathbf{k}_\gamma) P_N + \\ & Q H_1^{[2]} Q Q [\rho^{[1]}(\mathbf{k}_\gamma) + \rho^{[2]}(\mathbf{k}_\gamma)] P_N - \\ & Q [\rho^{[1]}(\mathbf{k}_\gamma) + \rho^{[2]}(\mathbf{k}_\gamma)] (P_N + P_\Delta) (P_N + P_\Delta) H_1^{[2]} P_N. \end{aligned} \quad (2.18)$$

The split into constraints of one-baryon and two-baryon nature is not straightforward. E.g., the term  $Q H_1^{[1]} Q Q \rho^{[1]}(\mathbf{k}_\gamma) P_N$  in Eqs. (2.17) and (2.18) has one-baryon *and* two-baryon contributions depending on whether the pion interacts with the same nucleon on which the e.m. charge produced it or whether it is exchanged between the nucleons. The constraints following from Eq. (2.15), e.g., the special constraints (2.17) and (2.18), are still quite general for the employed force model.

Compared with the coupled-channel current model of Ref. [17], the employed current also has a coupling to pionic states, i.e.,  $Q j^\mu(\mathbf{k}_\gamma) (P_N + P_\Delta)$ . In contrast to the employed hadronic interaction there is coupling from the nucleonic to the pionic sector due to  $Q j^\mu(\mathbf{k}_\gamma) P_N$ . Since the hadronic interaction treats the pion degree of freedom explicitly, there is a competition between the reducible two-baryon contribution due to the explicit e.m. mechanism for the pionproduction  $(P_\Delta + Q) H_1^{[1]} Q g_0^Q(z) Q j^{[1]\mu}(\mathbf{k}_\gamma) P_N$  and the corresponding irreducible one-baryon and two-baryon currents  $(P_\Delta + Q) [j^{[1]\mu}(\mathbf{k}_\gamma) + j^{[2]\mu}(\mathbf{k}_\gamma)] P_N$ . E.g., parts of traditional exchange currents are resolved into simpler building blocks due to the explicit propagation of the pion, in the same way as parts of the three-nucleon force and of the two-nucleon current become reducible due to the explicit propagation of the  $\Delta$ -isobar. In the considered force model, the purely nucleonic currents  $P_N [j^{[1]\mu}(\mathbf{k}_\gamma) + j^{[2]\mu}(\mathbf{k}_\gamma)] P_N$  remain unaltered and irreducible. That property gets changed in a force model with an explicit  $\pi NN$  vertex [3 – 6, 18, 19], which therefore has different e.m. properties. The competition between the e.m. mechanism of pion production and of exchange currents of pion range is the further theme of this section, a general conceptual problem to be respected in actual parameterizations of the current.

### 2.2.3 Construction of Interaction-Dependent Contributions to the Current

Appendix B gives the example of a coupled-channel current which satisfies the constraints of Subsect. 2.2.2 exactly. However, that example is purely phenomenological. In contrast, this subsection develops a current with physics content. The current is supposed to describe e.m. processes with the inclusion of pionproduction and absorption off nucleonic states. Only the parts  $(P_N + P_\Delta + Q)[j^{[1]\mu}(\mathbf{k}_\gamma) + j^{[2]\mu}(\mathbf{k}_\gamma)]P_N$  of the current are therefore required. The two-baryon part  $j^{[2]\mu}(\mathbf{k}_\gamma)$  is interaction-dependent. However, also the one-baryon current  $j^{[1]\mu}(\mathbf{k}_\gamma)$  contains an interaction-dependent part,  $j_{exchange}^{[1]\mu}(\mathbf{k}_\gamma)$ , besides the interaction-free one,  $j_{bare}^{[1]\mu}(\mathbf{k}_\gamma)$ , i.e.,

$$j^{[1]\mu}(\mathbf{k}_\gamma) = j_{bare}^{[1]\mu}(\mathbf{k}_\gamma) + j_{exchange}^{[1]\mu}(\mathbf{k}_\gamma). \quad (2.19)$$

The one- and two-baryon interaction-dependent currents are derived in the framework of the extended  $S$ -matrix method [20, 21]. They will be defined up to first order in the potentials  $H_1$ . Thus, we have to expect that also the continuity equation for the current can only be satisfied up to this order.

## A. One-Baryon Interaction-Dependent Current

The one-baryon current for the use in Schrödinger theory is defined. Its interaction-dependent part depends on the one-baryon potentials  $P_\Delta H_1^{[1]}Q$ ,  $QH_1^{[1]}P_\Delta$  and  $QH_1^{[1]}Q$  of Figs. 2.1(e) and 1(g) employed for the description of pion-nucleon scattering. Those potentials are derived from a field-theoretic Lagrangian  $\mathcal{L}_I$  which couples the same channels through  $P_\Delta \mathcal{L}_I Q$ ,  $Q \mathcal{L}_I P_\Delta$  and  $Q \mathcal{L}_I Q$ ; the potentials are defined to be instantaneous and to act between on-mass-shell particles. Fig. 2.3 shows all one-baryon Feynman processes up to first order in the interaction which contribute to the effective current. The effective field-theoretic current without interaction is denoted by  $J_{bare}^{[1]\mu}(k_\gamma)$ , those with interaction by  $J_{exchange}^{[1]\mu}(k_\gamma)$ .

The interaction-free current  $J_{bare}^{[1]\mu}(k_\gamma)$  contains the standard purely nucleonic contribution  $j_{NN}^\mu(k_\gamma)$ , the transition contribution  $j_{\Delta N}^\mu(k_\gamma)$  from the nucleon to the  $\Delta$ -isobar according to Ref. [22] and the Born current  $j_B^\mu(k_\gamma)$  which connects nucleonic states with pion-nucleon states. Fieldtheoretically, the Born current sums up five different processes which Fig. 2.4 makes explicit; however, the employed interaction model does not use an explicit  $\pi NN$ -vertex as mechanism for pion-production and pion-absorption, i.e.,  $P_N H_1^{[1]}Q = QH_1^{[1]}P_N = 0$ ; thus, no part of the Born current is reducible into simpler building blocks, e.g., into a purely e.m. and hadronic one. The Born current will therefore be used as an irreducible one-baryon current. It is proportional to the  $\pi NN$  coupling

constant or other meson nucleon-nucleon coupling constants, but it is considered to be interaction-free, a deliberately chosen wording, which should not be misleading. In the interaction-dependent processes (d) - (f) of Fig. 2.3 all intermediate particles propagate covariantly and off-mass-shell. The processes are considered of first order in the interaction. If the pion-nucleon interaction in process (f) is described by a field-theoretic four-point vertex, process (f) is manifestly first-order in the interaction Lagrangian  $\mathcal{L}_I$ ; if it were defined by meson exchange, it were second order in  $\mathcal{L}_I$ ; even in the latter case we shall consider process (f) as of first order in the interaction and lump it together with processes (d) and (e). The amplitudes for the effective field-theoretic current depend on the four-momentum transfer  $k_\gamma$ ; they are assumed to satisfy the continuity equation individually, i.e.,

$$k_{\gamma\mu} J_{bare}^{[1]\mu}(k_\gamma) = 0, \quad (2.20a)$$

$$k_{\gamma\mu} J_{exchange}^{[1]\mu}(k_\gamma) = 0. \quad (2.20b)$$

As the one-baryon potential  $H_1^{[1]}$ , the interaction-free current  $j_{bare}^{[1]\mu}(\mathbf{k}_\gamma)$  is defined for the purpose of Schrödinger theory by the corresponding field-theoretic processes between on-mass-shell states, i.e., by the processes (a) – (c) of Fig. 2.3 with amplitude  $J_{bare}^{[1]\mu}(k_\gamma)$ ,

$$\langle \mathbf{k}'_f | j_{bare}^{[1]\mu}(\mathbf{k}_\gamma) | \mathbf{k}_N \rangle = \langle \mathbf{k}'_f | J_{bare}^{[1]\mu}(k'_f - k_N) | \mathbf{k}_N \rangle, \quad (2.21a)$$

$$\mathbf{k}_\gamma \cdot (P_N + P_\Delta + Q) j_{bare}^{[1]\mu}(\mathbf{k}_\gamma) P_N = (P_N + P_\Delta + Q) [H_0^{[1]}, \rho_{bare}^{[1]}(\mathbf{k}_\gamma)] P_N, \quad (2.21b)$$

with  $\mathbf{k}_\gamma = \mathbf{k}'_f - \mathbf{k}_N$ . In Eq. (2.21a)  $\mathbf{k}'_f$  denotes the total on-mass-shell momentum in the final state. Thus,  $\mathbf{k}'_f$  is  $\mathbf{k}'_N$ ,  $\mathbf{k}'_\Delta$  or  $\mathbf{k}'_\pi + \mathbf{k}'_N$ , respectively, depending on the final channel; since initial and final particles are on their mass shells, i.e.,  $k_\gamma^0 = k_f^0 - k_N^0$ ,  $k^0$  being the relativistic on-mass-shell energy, the defined interaction-free current depends on the three-momentum transfer  $\mathbf{k}_\gamma$  only. The noncovariant continuity equation (2.21b) follows from the field-theoretic one (2.20a) for  $J_{bare}^{[1]\mu}(k_\gamma)$ .

Fig. 2.5 lists all one-baryon processes up to first order in the noncovariant potentials  $QH_1^{[1]}P_\Delta$ ,  $P_\Delta H_1^{[1]}Q$  and  $QH_1^{[1]}Q$  which a description in terms of Schrödinger theory yields. There are three different types of processes. Their sum is required to exactly account for the one-baryon Feynman processes described by Fig. 2.3, i.e.,

$$\begin{aligned} & \langle \mathbf{k}'_f | j_{bare}^{[1]\mu}(\mathbf{k}_\gamma) + j_{exchange}^{[1]\mu}(\mathbf{k}_\gamma) + J_{oms}^{[1]\mu}(\mathbf{k}_\gamma) | \mathbf{k}_N \rangle = \\ & \langle \mathbf{k}'_f | J_{bare}^{[1]\mu}(k'_f - k_N) + J_{exchange}^{[1]\mu}(k'_f - k_N) | \mathbf{k}_N \rangle. \end{aligned} \quad (2.22)$$

The above requirement defines the interaction-dependent part  $j_{exchange}^{[1]\mu}(\mathbf{k}_\gamma)$  of the one-baryon current. Fig. 2.6 makes that definition explicit. According to Eq. (2.21a) the interaction-free current  $j_{bare}^{[1]\mu}(\mathbf{k}_\gamma)$ , contained in the first three processes of Fig. 2.5, is chosen to account for the corresponding first three Feynman processes of Fig. 2.3. Processes

(d) – (f) in Fig. 2.5 are the second type of processes; they stand for the effective current  $J_{oms}^{[1]\mu}(\mathbf{k}_\gamma)$ , first order in the noncovariant potentials. Though these processes of Fig. 2.5 look identical to the corresponding Feynman processes (d) - (f) of Fig. 2.3, they cannot account for them in full: In contrast to the Feynman processes, the building blocks of  $J_{oms}^{[1]\mu}(\mathbf{k}_\gamma)$ , the noncovariant potentials and the interaction-free current  $j_{bare}^{[1]\mu}(\mathbf{k}_\gamma)$ , are defined between on-mass-shell states; furthermore, the intermediate states are of positive energy and propagate on-mass-shell, but off-energy-shell according to the global propagators of Schrödinger theory. Since the effective current  $J_{oms}^{[1]\mu}(\mathbf{k}_\gamma)$  with on-mass-shell (oms) intermediate states cannot account for the corresponding Feynman processes in full, a correction  $j_{exchange}^{[1]\mu}(\mathbf{k}_\gamma)$  is required. Thus, it is defined according to Eq. (2.22) by

$$\langle \mathbf{k}'_f | j_{exchange}^{[1]\mu}(\mathbf{k}_\gamma) | \mathbf{k}_N \rangle := \langle \mathbf{k}'_f | J_{exchange}^{[1]\mu}(k'_f - k_N) | \mathbf{k}_N \rangle - \langle \mathbf{k}'_f | J_{oms}^{[1]\mu}(\mathbf{k}_\gamma) | \mathbf{k}_N \rangle. \quad (2.23)$$

It is represented also by the processes (a) – (c) in Fig. 2.5; they can graphically not be differentiated from the interaction-free ones  $j_{bare}^{[1]\mu}$ , since the external parameters are the same, but their dynamic content is entirely different. They are the third type of processes in Fig. 2.5. Since the divergence of the effective current  $J_{oms}^{[1]\mu}(\mathbf{k}_\gamma)$  can easily be shown to be

$$\langle \mathbf{k}'_f | (k'_f - k_N)_\mu J_{oms}^{[1]\mu}(\mathbf{k}_\gamma) | \mathbf{k}_N \rangle = \langle \mathbf{k}'_f | [H_1^{[1]}, \rho_{bare}^{[1]}(\mathbf{k}_\gamma)] | \mathbf{k}_N \rangle, \quad (2.24)$$

the continuity equation for the complete one-baryon current connecting nucleonic states with all other sectors of Hilbert space is derived from the following sequence of steps:

$$\begin{aligned} & \mathbf{k}_\gamma \cdot \langle \mathbf{k}'_f | \mathbf{j}_{bare}^{[1]}(\mathbf{k}_\gamma) + \mathbf{j}_{exchange}^{[1]}(\mathbf{k}_\gamma) | \mathbf{k}_N \rangle \\ &= \langle \mathbf{k}'_f | [H_0^{[1]}, \rho_{bare}^{[1]}(\mathbf{k}_\gamma)] - (k'_f - k_N)_\mu j_{exchange}^{[1]\mu}(\mathbf{k}_\gamma) + (k'_f - k_N)^0 \rho_{exchange}^{[1]}(\mathbf{k}_\gamma) | \mathbf{k}_N \rangle \\ &= \langle \mathbf{k}'_f | [H_0^{[1]}, \rho_{bare}^{[1]}(\mathbf{k}_\gamma)] + (k'_f - k_N)_\mu J_{oms}^{[1]\mu}(\mathbf{k}_\gamma) + [H_0^{[1]}, \rho_{exchange}^{[1]}(\mathbf{k}_\gamma)] | \mathbf{k}_N \rangle \\ &= \langle \mathbf{k}'_f | [H_0^{[1]} + H_1^{[1]}, \rho_{bare}^{[1]}(\mathbf{k}_\gamma) + \rho_{exchange}^{[1]}(\mathbf{k}_\gamma)] - [H_1^{[1]}, \rho_{exchange}^{[1]}(\mathbf{k}_\gamma)] | \mathbf{k}_N \rangle \end{aligned} \quad (2.25)$$

The last term on the right-hand side of Eq. (2.25) is of second order in the potential. Thus, the continuity equation is satisfied up to first order in the potential, i.e.,

$$\begin{aligned} & \mathbf{k}_\gamma \cdot (P_N + P_\Delta + Q) \left( \mathbf{j}_{bare}^{[1]}(\mathbf{k}_\gamma) + \mathbf{j}_{exchange}^{[1]}(\mathbf{k}_\gamma) \right) P_N = \\ & (P_N + P_\Delta + Q) [H_0^{[1]} + H_1^{[1]}, \rho_{bare}^{[1]}(\mathbf{k}_\gamma) + \rho_{exchange}^{[1]}(\mathbf{k}_\gamma)] P_N + \mathcal{O} \left[ (H_1^{[1]})^2 \right]. \end{aligned} \quad (2.26)$$

The definition of the exchange part  $j_{exchange}^{[1]\mu}(\mathbf{k}_\gamma)$  of the one-baryon current and the proof of validity of the continuity equation (2.26) for the one-baryon current rests on the current conservation (2.20) for the amplitudes of the corresponding Feynman processes. We called that condition an assumption; it has always to be demonstrated that it holds for the form of the field-theoretic interaction Lagrangian  $\mathcal{L}_I$  and of the field-theoretic currents  $j_{NN}^\mu(k_\gamma)$ ,  $j_{\Delta N}^\mu(k_\gamma)$  and  $j_B^\mu(k_\gamma)$  employed. Furthermore, the kinetic energy operator  $H_0^{[1]}$  used for the calculation of the relativistic Feynman amplitudes and for the noncovariant

Schrödinger theory has to be the same, i.e., it has to be based on the relativistic on-mass-shell relation between energy and three-momentum; the noncovariant potentials are to be defined through the field-theoretic Lagrangian  $\mathcal{L}_I$ .

## B. Two-Baryon Interaction-Dependent Current

We use the same strategy for the definition of the two-baryon exchange current as for the definition of the one-baryon exchange current. We only choose a different presentation.

Fig. 2.7 shows all connected but reducible processes which arise for the two-baryon current in the noncovariant framework of Schrödinger theory and which are based on the one-baryon current and the interaction  $H_1$  up to first order. The employed one-baryon current is the bare one, i.e.,  $j_{bare}^{[1]}(\mathbf{k}_\gamma)$ , since the one-baryon exchange part  $j_{exchange}^{[1]}(\mathbf{k}_\gamma)$  is itself already of first order in the interaction. The processes define the amplitudes  $(P_N + P_\Delta + Q)J_{oms}^{[2]\mu}(\mathbf{k}_\gamma)P_N$  which satisfy the condition

$$\begin{aligned} \langle \mathbf{k}'_{f_1} \mathbf{k}'_{f_2} | (k'_{f_1} + k'_{f_2} - k_{N_1} - k_{N_2})_\mu J_{oms}^{[2]\mu}(\mathbf{k}_\gamma) | \mathbf{k}_{N_1} \mathbf{k}_{N_2} \rangle = \\ \langle \mathbf{k}'_{f_1} \mathbf{k}'_{f_2} | [H_1^{[1]} + H_1^{[2]}, \rho_{bare}^{[1]}(\mathbf{k}_\gamma)] | \mathbf{k}_{N_1} \mathbf{k}_{N_2} \rangle. \end{aligned} \quad (2.27)$$

With respect to the commutator  $[H_1^{[1]}, \rho_{bare}^{[1]}(\mathbf{k}_\gamma)]$ , only its part which is of two-baryon nature contributes. We choose an ordering scheme in powers of the interaction  $H_1$ . However, one has to admit, that this ordering scheme treats processes which physically belong together differently. Fig. 2.8 demonstrates this fact: Process (a) of Fig. 2.8 is of first order in  $H_1$ , and therefore is included in the amplitudes  $J_{oms}^{[2]\mu}(\mathbf{k}_\gamma)$ , whereas process (b) is of second order in  $H_1$  and is therefore not considered there. We remind that the hadronic part of the process (b) is taken out from the instantaneous pion exchange of process (a) in the definition of the interaction  $H_1$  in order to avoid double counting of physical processes.

The processes of first order in the interaction  $H_1$ , depicted on Fig. 2.7, cannot account for all corresponding processes  $J_{exchange}^{[2]\mu}(k_\gamma)$  which arise in a field-theoretic description of the same order. The field-theoretic processes are assumed to satisfy current conservation  $k_{\gamma\mu} J_{exchange}^{[2]\mu}(\mathbf{k}_\gamma) = 0$  and are employed for a standard definition of exchange currents, i.e.,

$$\begin{aligned} \langle \mathbf{k}'_{f_1} \mathbf{k}'_{f_2} | j_{exchange}^{[2]\mu}(\mathbf{k}_\gamma) | \mathbf{k}_{N_1} \mathbf{k}_{N_2} \rangle = \\ \langle \mathbf{k}'_{f_1} \mathbf{k}'_{f_2} | J_{exchange}^{[2]\mu}(k'_{f_1} + k'_{f_2} - k_{N_1} - k_{N_2}) - J_{oms}^{[2]\mu}(\mathbf{k}_\gamma) | \mathbf{k}_{N_1} \mathbf{k}_{N_2} \rangle. \end{aligned} \quad (2.28)$$

Though that definition of exchange currents is standard, the resulting currents are not, since the underlying hadronic interaction is also not standard due to its coupled-channel nature and due to the treatment of the pion as an explicit degree of freedom. We do not list many field-theoretic processes in diagrams and give only one example in Fig. 2.9. It is argued traditionally, that the field-theoretic processes (a) - (d) of Fig. 2.9 are not accounted for by the Schrödinger processes (e) and (f) in full. That difference

defines the traditional two-body exchange current  $\langle \mathbf{k}'_{N_1} \mathbf{k}'_{\Delta_2} | j_{traditional}^{[2]\mu}(\mathbf{k}_\gamma) | \mathbf{k}_{N_1} \mathbf{k}_{N_2} \rangle$  with  $\Delta$ -isobar excitation of the second nucleon. However, the employed hamiltonian treats pionproduction and pion absorption explicitly. Thus, process (g) of Fig. 2.9 has to be taken out from the traditional exchange current in an energy-independent way. The appropriate definition of that particular part of the exchange current is

$$\begin{aligned} \langle \mathbf{k}'_{N_1} \mathbf{k}'_{\Delta_2} | j_{exchange}^{[2]\mu}(\mathbf{k}_\gamma) | \mathbf{k}_{N_1} \mathbf{k}_{N_2} \rangle := \\ \langle \mathbf{k}'_{N_1} \mathbf{k}'_{\Delta_2} | j_{traditional}^{[2]\mu}(\mathbf{k}_\gamma) - \\ P_\Delta H_1^{[1]} Q \frac{Q}{k_{N_1}^0 + k_{N_2}^0 + i0 - Q H_0^{[1]} Q} Q j_{bare}^{[1]\mu}(\mathbf{k}_\gamma) P_N | \mathbf{k}_{N_1} \mathbf{k}_{N_2} \rangle. \end{aligned} \quad (2.29)$$

In the definition (2.29) the one-baryon current  $j_{bare}^{[1]\mu}(\mathbf{k}_\gamma)$  acts on nucleon one, baryon interchange has to be added explicitly. This nonstandard definition of the interaction-dependent two-baryon currents solves the problem of internal consistency between the employed hadronic and e.m. mechanisms of pion production and absorption and the irreducible e.m. pion-exchange current. The definition of the e.m. exchange current is identical in spirit to the definition of the two-nucleon potential  $P_N H_1 P_N$  in the interaction of Eq. (2.1) according to Ref. [1]: Compared with a traditional potential  $V_{NN}$ ,  $P_N H_1 P_N$  is not allowed to contain those processes which the coupled-channel description adds explicitly to the effective two-nucleon interaction. Defining  $P_N H_1 P_N$  in terms of a traditional well-defined potential  $V_{NN}$ , those processes have to be taken out from  $V_{NN}$  in an energy-independent form.

The continuity equation for the two-baryon exchange current takes the form

$$\begin{aligned} \mathbf{k}_\gamma \cdot (P_N + P_\Delta + Q) \mathbf{j}_{exchange}^{[2]}(\mathbf{k}_\gamma) P_N = \\ (P_N + P_\Delta + Q) [H_0^{[1]} + H_1^{[1]} + H_1^{[2]}, \rho_{bare}^{[1]}(\mathbf{k}_\gamma) + \rho_{exchange}^{[1]}(\mathbf{k}_\gamma)] P_N + \mathcal{O}[(H_1)^2]. \end{aligned} \quad (2.30)$$

Again as expected, it is satisfied up to order  $(H_1)^2$  only.

The definition of the interaction-dependent one-baryon and two-baryon currents is so general that e.m. and hadronic form factors can be added without problems. On the other hand, we have to warn the reader in one respect: The current model with its nonstandard parts defined in this subsection could not yet been used for the actual calculation of photo reactions in this paper. The current used here is of traditional form; its parameterization will be given in Sect. 3.

## 2.3 Photo Reactions in the Two-Nucleon System

This section describes processes with real photons in the two-nucleon system whose dynamics is controlled by the force model of Subsect. 2.1. Examples for the considered reactions are the photo absorption processes on the deuteron, i.e.,  $\gamma d \rightarrow pn$ ,  $\gamma d \rightarrow \pi^0 d$  and

$\gamma d \rightarrow \pi NN$ , and nucleon-nucleon bremsstrahlung without and with pionproduction, i.e.,  $NN \rightarrow NN\gamma$ ,  $pn \rightarrow d\gamma$ ,  $NN \rightarrow \pi d\gamma$ ,  $NN \rightarrow \pi NN\gamma$ ,  $\pi d \rightarrow NN\gamma$ ,  $\pi d \rightarrow \pi d\gamma$  and  $\pi d \rightarrow \pi NN\gamma$ . Only the first bremsstrahlung reaction is traditionally measured.

Since the energy balance is different in the absorption of a photon with energy  $\omega_\gamma$  and in the emission of a photon with the same energy  $\omega_\gamma$ , both types of reactions have to be described slightly differently. As for the hadronic reactions of Subsect. 2.1, an e.m. multi-channel transition matrix  $U^{\gamma A}(z)$  for the photo absorption processes and the corresponding transition matrix  $U^{\gamma E}(z)$  for bremsstrahlung processes are introduced. They connect initial and final hadronic channel states  $|\phi_i\rangle$  and  $|\phi_f\rangle$ . The channel states are those of Subsect. 2.1, i.e., the two-nucleon states  $|\phi_N(\mathbf{p}_N)\rangle$ , the pion-deuteron states  $|\phi_\pi(\mathbf{q}_\pi)\rangle$  and the break-up states  $|\phi_0(\mathbf{p}, \mathbf{q})\rangle$  with two free nucleons and one pion. The deuteron state  $|\phi_d(\mathbf{k}_d)\rangle = |d\mathbf{k}_d\rangle$  with total momentum  $\mathbf{k}_d$  and energy  $E_d(\mathbf{k}_d)$  has to be added to that list of initial and final channel states; for that state we make the formal identification  $|\Psi_d^{(\pm)}(\mathbf{k}_d)\rangle = \pm i0G(E_d \pm i0)|\phi_d(\mathbf{k}_d)\rangle = |\phi_d(\mathbf{k}_d)\rangle$  for later ease in notation. The  $S$ -matrix for photo absorption and photo emission is related to the e.m. multi-channel transition matrices  $U^{\gamma A}(z)$  and  $U^{\gamma E}(z)$  by

$$\langle \phi_f | S | \phi_i \gamma \rangle = -2\pi i \delta(E_f - E_i - \omega_\gamma) \langle \phi_f | U_{fi}^{\gamma A}(E_i + \omega_\gamma + i0) | \phi_i \rangle, \quad (2.31a)$$

$$= -2\pi i \delta(E_f - E_i - \omega_\gamma) \langle \Psi_f^{(-)} | H_1^\gamma | \Psi_i^{(+)} \rangle, \quad (2.31b)$$

$$\langle \phi_f \gamma | S | \phi_i \rangle = -2\pi i \delta(E_f + \omega_\gamma - E_i) \langle \phi_f | U_{fi}^{\gamma E}(E_i + i0) | \phi_i \rangle, \quad (2.32a)$$

$$= -2\pi i \delta(E_f + \omega_\gamma - E_i) \langle \Psi_f^{(-)} | H_1^\gamma | \Psi_i^{(+)} \rangle. \quad (2.32b)$$

The e.m. transition matrix elements are completely determined by the hadronic and e.m. interactions of Eqs. (2.1) and (2.9). Eqs. (2.31b) and (2.32b) give the on-shell elements in one-photon exchange approximation. Their general off-shell elements have the same structure as the on-shell elements of Eqs. (2.31) and (2.32) which are determined by the Møller operators for the step from channel states to correlated wave functions according to Eqs. (2.6) - (2.8). Thus, the on-shell e.m. multi-channel transition matrices can be given in terms of the off-shell hadronic multi-channel transition matrix  $U(z)$  and the hamiltonian  $H_1^\gamma$  for the e.m. interaction. E.g., the e.m. multi-channel transition matrix  $U_{fd}^{\gamma A}$  for the absorption of real photons by the deuteron has the following form

$$U_{Nd}^{\gamma A}(z) = \sum_{a=N, \Delta} (\delta_{Na} + U_{Na}(z)g_{a0}^P(z)P_a H_1^\gamma P_N) + U_{N0}(z)g_0^Q(z)QH_1^\gamma P_N, \quad (2.33)$$

$$U_{\pi d}^{\gamma A}(z) = \sum_{a=N, \Delta} U_{\pi a}(z)g_{a0}^P(z)P_a H_1^\gamma P_N + U_{\pi 0}(z)g_0^Q(z)QH_1^\gamma P_N, \quad (2.34)$$

$$U_{0d}^{\gamma A}(z) = \sum_{a=N, \Delta} U_{0a}(z)g_{a0}^P(z)P_a H_1^\gamma P_N + (1 + U_{00}(z)g_0^Q(z))QH_1^\gamma P_N, \quad (2.35)$$

i.e., for the processes  $\gamma d \rightarrow pn$ ,  $\gamma d \rightarrow \pi^0 d$  and  $\gamma d \rightarrow \pi NN$  in turn. The derivation of Eqs. (2.33) - (2.35) exploits the special structure of the force model according to Subsect. 2.1: The deuteron is a purely nucleonic state; it does not have any components in the Hilbert sectors  $\mathcal{H}_\Delta$  and  $\mathcal{H}_\pi$ .

### 3. Parameterization of the Hamiltonian

We report our first calculations on photo reactions of the deuteron. We extend early attempts [7, 21] of ours. Our calculations are still incomplete and do not incorporate all subtleties of those of Ref. [9 – 12], but they have special features compared to [9 – 13] which should make them interesting to others already in their present stage.

The parameterization of the kinetic energy operator  $H_0$ , of the hadronic interaction hamiltonian  $H_1$  and of the e.m. interaction hamiltonian  $H_1^\gamma$  are given in this section.

#### 3.1 The Kinetic Energy Operator $H_0$

The single-particle masses and momenta are denoted by  $m_i$  and  $\mathbf{k}_i$  with  $i = N, \Delta, \pi$  and  $\gamma$ . The single-particle energies of the nucleon and the  $\Delta$ -isobar  $e_N(\mathbf{k}_N)$  and  $e_\Delta(\mathbf{k}_\Delta)$  are assumed to be nonrelativistic, i.e.,

$$e_N(\mathbf{k}_N) = m_N + \frac{\mathbf{k}_N^2}{2m_N}, \quad (3.1a)$$

$$e_\Delta(\mathbf{k}_\Delta) = m_\Delta^0 + \frac{\mathbf{k}_\Delta^2}{2m_\Delta^0}. \quad (3.1b)$$

The exact relativistic forms are used for the single-particle energies of the pion and the photon  $\omega_\pi(\mathbf{k}_\pi)$  and  $\omega_\gamma(\mathbf{k}_\gamma)$ , i.e.,

$$\omega_\pi(\mathbf{k}_\pi) = \sqrt{m_\pi^2 + \mathbf{k}_\pi^2}, \quad (3.2a)$$

$$\omega_\gamma(\mathbf{k}_\gamma) = |\mathbf{k}_\gamma|. \quad (3.2b)$$

The chosen values of the masses are  $m_N = 939$  MeV,  $m_\Delta^0 = 1315.8$  MeV and  $m_\pi = 139$  MeV. The value for  $m_\Delta^0$  was already chosen in the context of Eq. (2.2) such that the interaction hamiltonian (2.1) describes pion-nucleon scattering in the  $P_{33}$  partial wave.

The calculations are carried out in the c.m. system, in which the sum of all single-particle momenta  $\mathbf{k}_i$  is zero. Thus, Jacobi momenta are introduced for the relative motion between particles. The kinetic energies of the considered channels is reexpressed in terms of those momenta.

The kinetic energy of states in two-baryon channels is for two nucleons characterized by

$$P_N H_0 P_N |\mathbf{p}_N\rangle = E_N(\mathbf{p}_N) |\mathbf{p}_N\rangle, \quad (3.3a)$$

$$\mathbf{p}_N = \frac{1}{2}(\mathbf{k}_{N1} - \mathbf{k}_{N2}), \quad (3.3b)$$

$$\mathbf{K} = \mathbf{k}_{N1} + \mathbf{k}_{N2} = 0 \quad (3.3c)$$

with  $E_N(\mathbf{p}_N) = 2e_N(\mathbf{p}_N)$ , in case of nucleon- $\Delta$  states by

$$P_\Delta H_0 P_\Delta |\mathbf{p}_\Delta\rangle = E_\Delta(\mathbf{p}_\Delta) |\mathbf{p}_\Delta\rangle, \quad (3.4a)$$

$$\mathbf{p}_\Delta = \frac{m_\Delta^0 \mathbf{k}_N - m_N \mathbf{k}_\Delta}{m_N + m_\Delta^0}, \quad (3.4b)$$

$$\mathbf{K} = \mathbf{k}_N + \mathbf{k}_\Delta = 0 \quad (3.4c)$$

with  $E_\Delta(\mathbf{p}_\Delta) = e_N(\mathbf{p}_\Delta) + e_\Delta(\mathbf{p}_\Delta)$ . The basis states  $|\mathbf{p}_N\rangle$  and  $|\mathbf{p}_\Delta\rangle$  are antisymmetrized plane-wave states;  $|\mathbf{p}_N\rangle$  coincides with the channel state  $|\phi_N(\mathbf{p}_N)\rangle$  of Subsect. 2.1.

In the three-particle Hilbert sector with two nucleons and one pion, two different sets of Jacobi momenta are used. Either the pion or one of the nucleons is chosen to be the spectator. The corresponding momenta are distinguished by the label of the spectator particle, i.e.,

$$Q H_0 Q |\mathbf{p}_\pi \mathbf{q}_\pi\rangle = E_0(\mathbf{p}_\pi \mathbf{q}_\pi) |\mathbf{p}_\pi \mathbf{q}_\pi\rangle, \quad (3.5a)$$

$$\mathbf{p}_\pi = \frac{1}{2}(\mathbf{k}_{N1} - \mathbf{k}_{N2}), \quad (3.5b)$$

$$\mathbf{q}_\pi = \frac{\omega_\pi(\mathbf{k}_\pi)(\mathbf{k}_{N1} + \mathbf{k}_{N2}) - 2m_N \mathbf{k}_\pi}{2m_N + \omega_\pi(\mathbf{k}_\pi)}, \quad (3.5c)$$

$$\mathbf{K} = \mathbf{k}_{N1} + \mathbf{k}_{N2} + \mathbf{k}_\pi = 0, \quad (3.5d)$$

with  $E_0(\mathbf{p}_\pi \mathbf{q}_\pi) = 2e_N(\mathbf{p}_\pi) + \mathbf{q}_\pi^2/4m_N + \omega_\pi(\mathbf{q}_\pi)$ , and

$$Q H_0 Q |\mathbf{p}_{N1} \mathbf{q}_{N1}\rangle = E_0(\mathbf{p}_{N1} \mathbf{q}_{N1}) |\mathbf{p}_{N1} \mathbf{q}_{N1}\rangle, \quad (3.6a)$$

$$\mathbf{p}_{N1} = \frac{\omega_\pi(\mathbf{k}_\pi) \mathbf{k}_{N2} - m_N \mathbf{k}_\pi}{m_N + \omega_\pi(\mathbf{k}_\pi)}, \quad (3.6b)$$

$$\mathbf{q}_{N1} = \frac{m_N(\mathbf{k}_{N2} + \mathbf{k}_\pi) - (m_N + \omega_\pi(\mathbf{k}_\pi)) \mathbf{k}_{N1}}{2m_N + \omega_\pi(\mathbf{k}_\pi)}, \quad (3.6c)$$

$$\mathbf{K} = \mathbf{k}_{N1} + \mathbf{k}_{N2} + \mathbf{k}_\pi = 0 \quad (3.6d)$$

with  $E_0(\mathbf{p}_{N1}\mathbf{q}_{N1}) \approx e_N(\mathbf{p}_{N1}) + e_N(\mathbf{q}_{N1}) + \mathbf{q}_{N1}^2/2(\omega_\pi(\mathbf{p}_{N1}) + m_N) + \omega_\pi(\mathbf{p}_{N1})$ . The basis states  $|\mathbf{p}_\pi\mathbf{q}_\pi\rangle$  and  $|\mathbf{p}_{N1}\mathbf{q}_{N1}\rangle$  are identical with the break-up channel states  $|\phi_0(\mathbf{p}\mathbf{q})\rangle$  of Subsect. 2.1.

The pion-deuteron channel state  $|\phi_\pi(\mathbf{q}_\pi)\rangle$  of Subsect. 2.1 can be expanded in terms of the basis states  $|\mathbf{p}_\pi\mathbf{q}_\pi\rangle$ ; it has the energy  $E_\pi(\mathbf{q}_\pi) = 2m_N + \varepsilon_d + \mathbf{q}_\pi^2/4m_N + \omega_\pi(\mathbf{q}_\pi)$  with  $\varepsilon_d$  denoting the binding energy of the deuteron. The deuteron state  $|\phi_d(\mathbf{k}_d)\rangle = |d\mathbf{k}_d\rangle$  of Subsect. 2.3 is the tensor product of an internal wave function  $|d\rangle$  expanded in terms of the basis states  $|\mathbf{p}_N\rangle$  and of a two-nucleon c.m. state  $|\mathbf{k}_d\rangle$ ; it has the energy  $E_d(\mathbf{k}_d) = 2m_N + \varepsilon_d + \mathbf{k}_d^2/4m_N$ .

### 3.2 Parameterization of the Hadronic Interaction $H_1$

The hadronic interaction (2.1) employed is mainly taken from Ref. [1]. The parameterization of the  $\pi N \Delta$ -vertex in Fig. 2.1(e) is unchanged compared with Ref. [1]. The two-nucleon potential  $P_N H_1 P_N$  of Fig. 2.1(a) is also employed in the form of Ref. [1], i.e., approximately phase-equivalent with the Paris potential [23]. The transition potential  $P_\Delta H_1 P_N$  of Fig. 2.1(b) from two-nucleon to nucleon- $\Delta$  states is based on pion- and rho-exchange, i.e.,

$$P_\Delta H_1 P_N = V_{\Delta N}(\pi) + V_{\Delta N}(\rho) \quad (3.7)$$

with

$$\begin{aligned} \langle \mathbf{p}'_\Delta | V_{\Delta N}(\pi) | \mathbf{p}_N \rangle = & \frac{(-)}{(2\pi)^3} \frac{f_{\pi NN}}{m_\pi} \left( \frac{\Lambda_{\pi N}^2 - m_\pi^2}{\Lambda_{\pi N}^2 + (\mathbf{p}'_\Delta - \mathbf{p}_N)^2} \right) \frac{f_{\pi N \Delta}}{m_\pi} \left( \frac{\Lambda_{\pi \Delta}^2 - m_\pi^2}{\Lambda_{\pi \Delta}^2 + (\mathbf{p}'_\Delta - \mathbf{p}_N)^2} \right) \\ & \tau(1) \tau_{\Delta N}(2) \frac{[\boldsymbol{\sigma}(1) \cdot (\mathbf{p}'_\Delta - \mathbf{p}_N)][\boldsymbol{\sigma}_{\Delta N}(2) \cdot (\mathbf{p}'_\Delta - \mathbf{p}_N)]}{m_\pi^2 + (\mathbf{p}'_\Delta - \mathbf{p}_N)^2}, \end{aligned} \quad (3.8a)$$

$$\begin{aligned} \langle \mathbf{p}'_\Delta | V_{\Delta N}(\rho) | \mathbf{p}_N \rangle = & \frac{(-)}{(2\pi)^3} \frac{f_{\rho NN}}{m_\rho} \left( \frac{\Lambda_{\rho N}^2 - m_\rho^2}{\Lambda_{\rho N}^2 + (\mathbf{p}'_\Delta - \mathbf{p}_N)^2} \right) \frac{f_{\rho N \Delta}}{m_\rho} \left( \frac{\Lambda_{\rho \Delta}^2 - m_\rho^2}{\Lambda_{\rho \Delta}^2 + (\mathbf{p}'_\Delta - \mathbf{p}_N)^2} \right) \\ & \tau(1) \tau_{\Delta N}(2) \frac{[\boldsymbol{\sigma}(1) \times (\mathbf{p}'_\Delta - \mathbf{p}_N)][\boldsymbol{\sigma}_{\Delta N}(2) \times (\mathbf{p}'_\Delta - \mathbf{p}_N)]}{m_\rho^2 + (\mathbf{p}'_\Delta - \mathbf{p}_N)^2} \end{aligned} \quad (3.8b)$$

where  $\boldsymbol{\sigma}(\boldsymbol{\sigma}_{\Delta N})$  and  $\boldsymbol{\tau}(\boldsymbol{\tau}_{\Delta N})$  are the nucleonic ( $N\Delta$ -transition) spin and isospin operators, respectively.

This form of the transition potential differs slightly from the one used in Refs. [19], the  $\delta$ -function contribution to the unregularized forms of the potential in configuration space is not removed in contrast to Refs. [19]; thus, no term proportional to  $\boldsymbol{\sigma}(1) \cdot \boldsymbol{\sigma}_{\Delta N}(2)$  appears in Eqs. (3.8); that change in the transition potential is according to Ref. [19]

immaterial except for the inelasticity in the  $^3P_0$  partial wave of two-nucleon scattering. The parameters

$$\begin{aligned} \frac{f_{\pi NN}^2}{4\pi} &= 0.08, & \frac{f_{\pi N\Delta}^2}{4\pi} &= 0.35, \\ \frac{f_{\rho NN}^2}{4\pi} &= 3.21, & \frac{f_{\rho N\Delta}^2}{4\pi} &= 9.13, \\ \Lambda_{\pi N} = \Lambda_{\pi\Delta} = \Lambda_{\rho N} = \Lambda_{\rho\Delta} &= 650 \text{ MeV}, \end{aligned} \quad (3.9)$$

in the transition potential yield a reasonable fit [19] to the total proton-proton cross sections up to 500 MeV in the c.m. system. The nucleon- $\Delta$  potential  $P_\Delta H_1 P_\Delta$  consists of a direct and an exchange part according to the processes (d) and (c) of Fig. 2.1. One time ordering of the pion-mediated exchange part, however, is generated dynamically by the explicit  $\pi N\Delta$ -vertex. Therefore, only the instantaneous approximation for the pion contribution to the remaining time ordering is contained in  $P_\Delta H_1 P_\Delta$ . As in Ref. [1], the direct part of  $P_\Delta H_1 P_\Delta$  is altogether put to zero for most calculations. Only the calculations of Subsect. 4.3 will go beyond this choice. Furthermore, all interactions in the Hilbert space with one pion are chosen to be zero, i.e.,  $QH_1Q = 0$ .

### 3.3 Parameterization of the E.M. Interaction

This section gives the actual parameterization of the current  $j^\mu(\mathbf{k}_\gamma)$  in its Fourier-transformed form and of the e.m. hamiltonian  $H_1^\gamma$  used in the calculations of this paper. The description of photo reactions from the deuteron requires only the part  $(P_N + P_\Delta + Q)\mathbf{j}(\mathbf{k}_\gamma)P_N$  of the full e.m. current. The actual form of the e.m. current will be given by its matrixelements in momentum space. According to Eq. (2.13) one-body and two-body parts,  $\mathbf{j}^{[1]}(\mathbf{k}_\gamma)$  and  $\mathbf{j}^{[2]}(\mathbf{k}_\gamma)$ , will be distinguished. The currents  $P_\Delta \mathbf{j}^{[1]}(\mathbf{k}_\gamma)P_N$  and  $Q\mathbf{j}^{[1]}(\mathbf{k}_\gamma)P_N$  describe photo pionproduction on the single nucleon. They are well tuned in Appendix C. Compared to the Refs. [10, 11] they are chosen energy-independently and therefore do not spoil the unitarity of the theory. However, for the photo reactions of the deuteron they are employed only in simplified form as described in this section. Of course, the parameters found in Appendix C, are then not optimal anymore. This is why we shall explore the sensitivity of our results on the strength of the nucleon- $\Delta$  transition current  $P_\Delta \mathbf{j}^{[1]}(\mathbf{k}_\gamma)P_N$ .

#### 3.3.1 The E.M. One-Baryon Current

For the one-nucleon part of the current  $P_N \mathbf{j}^{[1]}(\mathbf{k}_\gamma)P_N$  of Fig. 2.5(a) the nonrelativistic convection and spin contributions

$$\begin{aligned} \langle \mathbf{k}'_N | P_N \mathbf{j}^{[1]}(\mathbf{k}_\gamma) P_N | \mathbf{k}_N \rangle &= \delta(\mathbf{k}'_N - \mathbf{k}_N - \mathbf{k}_\gamma) e_P \\ &\quad \left[ e(\boldsymbol{\tau}_0) \frac{\mathbf{k}'_N + \mathbf{k}_N}{2m_N} + \frac{\mu(\boldsymbol{\tau}_0)}{2m_N} i(\boldsymbol{\sigma} \times \mathbf{k}_\gamma) \right] \end{aligned} \quad (3.10)$$

are used with  $e(\boldsymbol{\tau}_0) = \frac{1}{2}(1 + \boldsymbol{\tau}_0)$  and  $\mu(\boldsymbol{\tau}_0) = \mu_s + \boldsymbol{\tau}_0 \mu_v$ ,  $e_P$  being the positive elementary charge,  $\mu_s = 0.44$  and  $\mu_v = 2.35$ ,  $\mu_s$  and  $\mu_v$  being the isoscalar and isovector magnetic moments of the nucleon. Relativistic corrections to this single-nucleon current, especially the ones generated by the spin-orbit term, are known to be important for the process of  $\gamma d \rightarrow pn$  at low energies in forward direction [22, 24, 25]. However, the influence of these additional currents on the observables is expected to be small at energies in the regime of the  $\Delta$ -resonance [22] and therefore are neglected in our present parameterization.

In the single-baryon transition current  $P_{\Delta} \mathbf{j}^{[1]}(\mathbf{k}_{\gamma}) P_N$  of Fig. 2.5(b) we keep only its dominant part due to magnetic dipole transition. The smaller contribution arising from the electric quadrupole transition is neglected, i.e.,

$$\begin{aligned} \langle \mathbf{k}'_{\Delta} | P_{\Delta} \mathbf{j}^{[1]}(\mathbf{k}_{\gamma}) P_N | \mathbf{k}_N \rangle &= \delta(\mathbf{k}'_{\Delta} - \mathbf{k}_N - \mathbf{k}_{\gamma}) e_P \\ &(\boldsymbol{\tau}_{\Delta N})_0 \frac{G_{M1}^{\Delta N}}{2\mu_{\Delta N}} i \left( \boldsymbol{\sigma}_{\Delta N} \times \frac{m_N \mathbf{k}'_{\Delta} - m_{\Delta}^0 \mathbf{k}_N}{m_N + m_{\Delta}^0} \right). \end{aligned} \quad (3.11)$$

Appendix C suggests  $G_{M1}^{\Delta N} = 3.65$  as optimal value; however, we shall employ a range of values in order to explore sensitivities. In contrast to the form of Appendix C, the current (3.11) is not fully transverse, i.e.,  $\mathbf{k}_{\gamma} \cdot P_{\Delta} \mathbf{j}^{[1]}(\mathbf{k}_{\gamma}) P_N \neq 0$ . Here  $\mu_{\Delta N}$  denotes the reduced mass of the nucleon and of the  $\Delta$ -isobar.

The one-baryon part of the e.m. current  $Q \mathbf{j}^{[1]}(\mathbf{k}_{\gamma}) P_N$  in Fig. 2.5(c) describes the Born process of photo pionproduction from the nucleon as displayed in Fig. 2.4. It includes  $\rho$ - and  $\omega$ -exchanges. Its parameterization is defined explicitly in Appendix C. However, only its contribution to the  $P_{33}$ -partial wave is kept in the present calculations, it is kept without any rescattering there. Thus, it does not contribute to photo disintegration in our calculations. Retained and omitted contributions arising from the Born process are displayed in Fig. 3.1.

### 3.3.2 The E.M. Two-Baryon Current

The two-nucleon current  $P_N \mathbf{j}^{[2]}(\mathbf{k}_{\gamma}) P_N$  is approximated by its traditional pion contribution which we assume to be dominant. The corresponding current contains the pair and the pion-in-flight parts which are shown in Fig. 3.2(a) and 3.2(b). They are used in their nonrelativistic forms [17]:

$$\begin{aligned} \langle \mathbf{k}'_{N1} \mathbf{k}'_{N2} | P_N \mathbf{j}_{\pi, pair}^{[2]}(\mathbf{k}_{\gamma}) P_N | \mathbf{k}_{N1} \mathbf{k}_{N2} \rangle &= i \frac{1}{(2\pi)^3} e_P \\ &\delta(\mathbf{k}'_{N1} + \mathbf{k}'_{N2} - \mathbf{k}_{N1} - \mathbf{k}_{N2} - \mathbf{k}_{\gamma}) \left( \frac{f_{\pi NN}}{m_{\pi}} \right)^2 (\boldsymbol{\tau}_1 \times \boldsymbol{\tau}_2)_0 \\ &\left( \frac{\Lambda_{\pi N}^2 - m_{\pi}^2}{\Lambda_{\pi N}^2 + (\mathbf{k}'_{N1} - \mathbf{k}_{N1})^2} \frac{\boldsymbol{\sigma}_2 [\boldsymbol{\sigma}_1 \cdot (\mathbf{k}'_{N1} - \mathbf{k}_{N1})]}{(\mathbf{k}'_{N1} - \mathbf{k}_{N1})^2 + m_{\pi}^2} - \right. \end{aligned}$$

$$\frac{\Lambda_{\pi N}^2 - m_\pi^2}{\Lambda_{\pi N}^2 + (\mathbf{k}'_{N2} - \mathbf{k}_{N2})^2} \frac{\boldsymbol{\sigma}_1 [\boldsymbol{\sigma}_2 \cdot (\mathbf{k}'_{N2} - \mathbf{k}_{N2})]}{(\mathbf{k}'_{N2} - \mathbf{k}_{N2})^2 + m_\pi^2} \Bigg) , \quad (3.12a)$$

$$\begin{aligned} \langle \mathbf{k}'_{N1} \mathbf{k}'_{N2} | P_N \mathbf{j}_{\pi, pion}^{[2]}(\mathbf{k}_\gamma) P_N | \mathbf{k}_{N1} \mathbf{k}_{N2} \rangle &= i \frac{1}{(2\pi)^3} e_P \\ \delta(\mathbf{k}'_{N1} + \mathbf{k}'_{N2} - \mathbf{k}_{N1} - \mathbf{k}_{N2} - \mathbf{k}_\gamma) \left( \frac{f_{\pi NN}}{m_\pi} \right)^2 (\boldsymbol{\tau}_1 \times \boldsymbol{\tau}_2)_0 \\ (\mathbf{k}'_{N1} - \mathbf{k}_{N1} - \mathbf{k}'_{N2} + \mathbf{k}_{N2}) \left[ \frac{\Lambda_{\pi N}^2 - m_\pi^2}{\Lambda_{\pi N}^2 + (\mathbf{k}'_{N1} - \mathbf{k}_{N1})^2} \cdot \frac{\Lambda_{\pi N}^2 - m_\pi^2}{\Lambda_{\pi N}^2 + (\mathbf{k}'_{N2} - \mathbf{k}_{N2})^2} \right]^{\frac{1}{2}} \\ \frac{[\boldsymbol{\sigma}_1 \cdot (\mathbf{k}'_{N1} - \mathbf{k}_{N1})]}{(\mathbf{k}'_{N1} - \mathbf{k}_{N1})^2 + m_\pi^2} \frac{[\boldsymbol{\sigma}_2 \cdot (\mathbf{k}'_{N2} - \mathbf{k}_{N2})]}{(\mathbf{k}'_{N2} - \mathbf{k}_{N2})^2 + m_\pi^2} , \end{aligned} \quad (3.12b)$$

with  $\Lambda_{\pi N} = 200$  MeV. All other two-baryon currents are neglected.

The currents of Subsect. 3.3.1 are bare ones in the definition of Sect. 2.2. None of the nontraditional interaction-dependent currents defined in Sect. 2.2 are included in the present calculations.

## 4. Results

Photo disintegration of the deuteron and photo pionproduction on the deuteron are unitarily coupled reactions. A simultaneously consistent description of both processes is required in order to be conceptually satisfactory; such a description is given with the interactions of Sect. 3.

### 4.1 Photo Disintegration of the Deuteron

We show some characteristic results of our calculations in Figs. 4.1 – 4.3. We give them for the kinematic region in which resonance production becomes important in the unitarily coupled pionic channel. We present the total cross-section as function of the photon lab energy as well as the unpolarised differential cross-section  $d\sigma/d\Omega$  and the photon asymmetry for the photon lab energies 260 MeV and 300 MeV.

The dependence of our results on the magnetic dipole strength  $G_{M1}^{\Delta N}$  in the nucleon- $\Delta$  transition current is studied. Results for three values are displayed. We note that the value  $G_{M1}^{\Delta N} = 3.65$  suggested in Appendix C by the single-nucleon data yields a rather poor agreement with experimental results. Of course, the strength parameter  $G_{M1}^{\Delta N}$  has to be increased compared with 3.65 when other mechanisms for  $\Delta$ -isobar excitation as done in the present calculation, i.e., the electric quadrupole resonance production and the rescattering of the pion produced in a Born process are left out, as explained in Subsect. 3.3.1. The value of  $G_{M1}^{\Delta N}$ , preferable for this reaction, is essentially suggested by Fig. 4.1, and it is slightly above 5.16.

## 4.2 Photo Pionproduction on the Deuteron

We show some characteristic results of our calculations in Figs. 4.4 – 4.6 and give them for the kinematic region in which resonance pionproduction becomes important. We present the unpolarized differential cross-section  $d\sigma/d\Omega$  and the deuteron vector polarization  $t_{11}$  for the photon lab energies 260 MeV and 300 MeV.

The dependence of our results on the magnetic dipole strength  $G_{M1}^{\Delta N}$  in the nucleon- $\Delta$  transition current is studied. Results for three values are displayed. We note that – in contrast to photo disintegration – the value suggested in Appendix C seems to yield a reasonable account of the few existing experimental data. Of course, the strength parameter  $G_{M1}^{\Delta N}$  has to be increased slightly when other mechanisms for pion production as done in the present calculation, i.e., the electric quadrupole resonance production and the rescattering of the pion produced in a Born process are left out as explained in Subsect. 3.3.1. With respect to the small-angle results of the Fig. 4.6 the calculation does not appear fully converged with respect to the inclusion of two-baryon angular momentum. The vector polarization  $t_{11}$  is not sensitive with respect to the choice of  $G_{M1}^{\Delta N}$ .

## 4.3 The Role of Irreducible Nucleon- $\Delta$ Potential

Ref. [26] noted the dependence of some observables for the two-nucleon system above pion threshhold on the choice of the irreducible nucleon- $\Delta$  potentials of Figs. 1(c) and 1(d). Sensitivity occured when the observables were described without such a potential as done for the results of Subsects. 4.2 and 4.3, and, alternatively, with two distinct nucleon- $\Delta$  potentials derived either from a one-boson exchange model or from a nonrelativistic quark model [27]. Ref. [26] noted that dependence for photo reactions of the deuteron, too. We study it as well and show characteristic results in Figs. 4.7 – 4.11 for the kinematic region in which  $\Delta$ -resonance contributions are important.

We present the total photo disintegration cross section as function of the photon lab energy, the unpolarized differential cross section  $d\sigma/d\Omega$  and the photon asymmetry  $\Sigma^\gamma$  at 260 MeV and 300 MeV photon lab energy for photo disintegration. We also present the unpolarized differential cross section  $d\sigma/d\Omega$  and the vector polarization  $t_{11}$  for photo pionproduction at 260 MeV and 300 MeV photon lab energy. Though no clear preference for one particular nucleon- $\Delta$  potential arises, we conclude: The quark-model based potential is smoother and therefore yields physically smoother corrections without apparently unphysical structures.

## 5. Conclusions

We are used to the fact that interaction-dependent meson-exchange currents arise in a theoretical description of e.m. processes, when meson degrees of freedom are frozen.

When, however, mesons become active, the traditional definition of interaction-dependent currents has to be revised. E.g., such a revision becomes necessary for e.m. pionproduction. The paper gives a redefinition of interaction-dependent currents when theoretically describing pionproduction. We think this is the conceptual value of the paper; its value remains, even if the quantitative significance of the novel interaction-dependent currents could not be checked yet in actual calculations.

The practical calculations performed employ traditional currents with well-known exchange contributions. In contrast to Ref. [10, 11] the currents are energy-independent thus, hermitian, in order to preserve the unitarity of the theoretical description. Photo disintegration of the deuteron and photo pionproduction on the deuteron are calculated simultaneously in a consistent frame work. The sensitivity of results on the parameters of the nucleon- $\Delta$  transition current and on the form of the irreducible nucleon- $\Delta$  potential got well established. We hope that the sensitivity will allow at a later, more refined, stage of theoretical description to learn more about the important parts of the e.m. current and on the nucleon- $\Delta$  potential from photo reactions on the deuteron.

## Appendix A: Hadronic Scattering Theory

The  $S$ -matrix needed for describing the hadronic reactions in the two-nucleon system above pion threshold are determined by the on-shell elements of the multi-channel transition matrix  $U(z)$ . Its various components  $U_{fi}(z)$  are defined by appropriate decompositions of the full hadronic resolvent  $G(z)$  of Eq. (2.4), i.e.,

$$\begin{aligned}
P_b G(z) P_a &= \delta_{ba} g_{a0}^P(z) + g_{b0}^P(z) U_{ba}(z) g_{a0}^P(z), \\
Q G(z) P_a &= g_{\beta}^Q(z) U_{\beta a}(z) g_{a0}^P(z), \\
Q G(z) P_a &= g_0^Q(z) U_{0a}(z) g_{a0}^P(z), \\
P_b G(z) Q &= g_{b0}^P(z) U_{b\beta}(z) g_{\beta}^Q(z), \\
Q G(z) Q &= \delta_{\beta\alpha} g_{\alpha}^Q(z) + g_{\beta}^Q(z) U_{\beta\alpha}(z) g_{\alpha}^Q(z), \\
Q G(z) Q &= g_0^Q(z) U_{0\alpha}(z) g_{\alpha}^Q(z), \\
Q G(z) Q &= g_0^Q(z) + g_0^Q(z) U_{00}(z) g_0^Q(z).
\end{aligned} \tag{A.1}$$

In Eq. (A.1)

$$\begin{aligned}
g_{a0}^P(z) &= \frac{P_a}{z - P_a H_0 P_a}, \\
g_0^Q(z) &= \frac{Q}{z - Q H_0 Q}, \\
g_{\alpha}^Q(z) &= \frac{Q}{z - Q H_0 Q - v_{\alpha}^Q}
\end{aligned} \tag{A.2}$$

represent partial resolvents,  $v_{\alpha}^Q$  being the potential between the pair of particles  $\alpha$  in the Hilbert sector  $\mathcal{H}_{\pi}$  as illustrated in Figs. 2.1(f) and 2.1(g) and as notationally defined in Eq. (A.4). The resulting relations between the  $S$ -matrix elements and the on-shell multi-channel transition matrix  $U(z)$  are

$$\begin{aligned}
\langle \phi_N(\mathbf{p}'_N) | S | \phi_N(\mathbf{p}_N) \rangle &= \delta(\mathbf{p}'_N - \mathbf{p}_N) - 2\pi i \delta(E_N(\mathbf{p}'_N) - E_N(\mathbf{p}_N)) \\
&\quad \langle \phi_N(\mathbf{p}'_N) | U_{NN}(E_N(\mathbf{p}_N) + i0) | \phi_N(\mathbf{p}_N) \rangle, \\
\langle \phi_{\pi}(\mathbf{q}'_{\pi}) | S | \phi_N(\mathbf{p}_N) \rangle &= -2\pi i \delta(E_{\pi}(\mathbf{q}'_{\pi}) - E_N(\mathbf{p}_N)) \\
&\quad \langle \phi_{\pi}(\mathbf{q}'_{\pi}) | U_{\pi N}(E_N(\mathbf{p}_N) + i0) | \phi_N(\mathbf{p}_N) \rangle, \\
\langle \phi_0(\mathbf{q}', \mathbf{p}') | S | \phi_N(\mathbf{p}_N) \rangle &= -2\pi i \delta(E_0(\mathbf{q}', \mathbf{p}') - E_N(\mathbf{p}_N)) \\
&\quad \langle \phi_0(\mathbf{q}', \mathbf{p}') | U_{0N}(E_N(\mathbf{p}_N) + i0) | \phi_N(\mathbf{p}_N) \rangle, \\
\langle \phi_N(\mathbf{p}'_N) | S | \phi_{\pi}(\mathbf{q}_{\pi}) \rangle &= -2\pi i \delta(E_N(\mathbf{p}'_N) - E_{\pi}(\mathbf{q}_{\pi})) \\
&\quad \langle \phi_N(\mathbf{p}'_N) | U_{N\pi}(E_{\pi}(\mathbf{q}_{\pi}) + i0) | \phi_{\pi}(\mathbf{q}_{\pi}) \rangle, \\
\langle \phi_{\pi}(\mathbf{q}'_{\pi}) | S | \phi_{\pi}(\mathbf{q}_{\pi}) \rangle &= \delta(\mathbf{q}'_{\pi} - \mathbf{q}_{\pi}) - 2\pi i \delta(E_{\pi}(\mathbf{q}'_{\pi}) - E_{\pi}(\mathbf{q}_{\pi})) \\
&\quad \langle \phi_{\pi}(\mathbf{q}'_{\pi}) | U_{\pi\pi}(E_{\pi}(\mathbf{q}_{\pi}) + i0) | \phi_{\pi}(\mathbf{q}_{\pi}) \rangle,
\end{aligned} \tag{A.3}$$

$$\begin{aligned}\langle \phi_0(\mathbf{q}', \mathbf{p}') | S | \phi_\pi(\mathbf{q}_\pi) \rangle &= -2\pi i \delta(E_0(\mathbf{q}', \mathbf{p}') - E_\pi(\mathbf{q}_\pi)) \\ &\quad \langle \phi_0(\mathbf{q}', \mathbf{p}') | U_{0\pi}(E_\pi(\mathbf{q}_\pi) + i0) | \phi_\pi(\mathbf{q}_\pi) \rangle.\end{aligned}$$

All on-shell and off-shell elements of the multi-channel transition matrix  $U(z)$  are determined by the hamiltonian (2.1) through integral equations. Ref. [1] chooses the integral equation for its two-baryon components  $U_{ba}(z)$  as fundamental equation and relates all other components of the multi-channel transition matrix to those. Redefining the various interaction terms in the hamiltonian (2.1) for compactness, i.e.,

$$H_1 = (P_N + P_\Delta)H_1(P_N + P_\Delta) + P_\Delta H_1 Q + QH_1 P_\Delta + QH_1 Q, \quad (\text{A.4a})$$

$$H_1 = \sum_{a,b=N,\Delta} v_{ab}^P + \sum_{a=N,\Delta} v_a^{PQ} + \sum_{a=N,\Delta} v_a^{QP} + \sum_\alpha v_\alpha^Q, \quad (\text{A.4b})$$

the integral equation for the two-baryon components  $U_{ba}(z)$  takes the form

$$U_{ba}(z) = \sum_{c=N,\Delta} [v_{bc}^P + v_b^{PQ} g^Q(z) v_c^{QP}] [\delta_{ca} + g_{c0}^P(z) U_{ca}(z)]. \quad (\text{A.5})$$

The remaining components are related to the baryonic ones by quadrature, i.e., by

$$\begin{aligned}U_{\beta a}(z) &= u_{\beta 0}(z) g_0^Q(z) \sum_b v_b^{QP} [\delta_{ba} + g_{b0}^P(z) U_{ba}(z)], \\ U_{0a}(z) &= [1 + u_{00}(z) g_0^Q(z)] \sum_b v_b^{QP} [\delta_{ba} + g_{b0}^P(z) U_{ba}(z)], \\ U_{b\alpha}(z) &= \sum_a [\delta_{ba} + U_{ba}(z) g_{a0}^P(z)] v_a^{PQ} g_0^Q(z) u_{0\alpha}(z), \\ U_{\beta\alpha}(z) &= u_{\beta\alpha}(z) + u_{\beta 0}(z) g_0^Q(z) \\ &\quad \{ \sum_{ba} v_b^{PQ} [\delta_{ba} g_{a0}^P(z) + g_{b0}^P(z) U_{ba}(z) g_{a0}^P(z)] v_a^{PQ} \} g_0^Q(z) u_{0\alpha}(z), \\ U_{0\alpha}(z) &= u_{0\alpha}(z) + [1 + u_{00}(z) g_0^Q(z)] \\ &\quad \{ \sum_{ba} [\delta_{ba} g_{a0}^P(z) + g_{b0}^P(z) U_{ba}(z) g_{a0}^P(z)] v_a^{PQ} \} g_0^Q(z) u_{0\alpha}(z), \\ U_{00}(z) &= u_{00}(z) + [1 + u_{00}(z) g_0^Q(z)] \\ &\quad \{ \sum_{ba} [\delta_{ba} g_{a0}^P(z) + g_{b0}^P(z) U_{ba}(z) g_{a0}^P(z)] v_a^{PQ} \} g_0^Q(z) [1 + u_{00}(z)].\end{aligned} \quad (\text{A.6})$$

The relations (A.5) and (A.6) also require the solution of the three-particle scattering problem in the pionic sector  $\mathcal{H}_\pi$  of the Hilbert space without pion production and absorption. That solution is given by the full propagator

$$g^Q(z) = \frac{1}{z - QH_0Q - \sum_\alpha v_\alpha^Q} \quad (\text{A.7})$$

and its corresponding multi-channel three-body transition matrix  $u(z)$  determined by the usual form of the AGS-equations. Once all components of the multi-channel transition matrix  $U(z)$  are determined, the scattering wave functions  $|\Psi_N^{(\pm)}(\mathbf{p}_N)\rangle$ ,  $|\Psi_\pi^{(\pm)}(\mathbf{q}_\pi)\rangle$  and  $|\Psi_0^{(\pm)}(\mathbf{p}, \mathbf{q})\rangle$  of Eq. (2.5) can be given according to Eqs. (2.6) - (2.8).

## Appendix B: Example for a Coupled-Channel Interaction-Dependent Current

This appendix proves that a coupled-channel e.m. current for the description of disintegration of and pionproduction on the deuteron , i.e.,  $(P_N + P_\Delta + Q) [\mathbf{j}^{[1]}(\mathbf{k}_\gamma) + \mathbf{j}^{[2]}(\mathbf{k}_\gamma)] P_N$  can be given which satisfies the condition (2.15) of Subsection 2.2.2 exactly. The example is purely phenomenological and therefore is not and should not be used in practical calculations. However, the example proves that the coupled-channel current has to have interaction-dependent pieces already in its one-baryon part, and its two-baryon part receives additional nontraditional contributions.

We make some simplifying assumptions: There be no interactions in the Hilbert sector with a pion, i.e.,  $QH_1^{[1]}Q = 0$  and  $QH_1^{[2]}Q = 0$ ; Siegert's hypothesis hold exactly, i.e.,  $\rho^{[2]}(\mathbf{k}_\gamma) = 0$ , and the remaining one-baryon charge density has the vanishing components  $P_\Delta \rho^{[1]}(\mathbf{k}_\gamma) P_N = 0$  and  $Q \rho^{[1]}(\mathbf{k}_\gamma) P_\Delta = 0$ . Under these assumptions the constraints (2.15) for the required parts of the current are

$$\mathbf{k}_\gamma \cdot P_N \mathbf{j}^{[1]}(\mathbf{k}_\gamma) P_N = P_N H_0^{[1]} P_N P_N \rho^{[1]}(\mathbf{k}_\gamma) P_N - P_N \rho^{[1]}(\mathbf{k}_\gamma) P_N P_N H_0^{[1]} P_N, \quad (\text{B.1a})$$

$$\mathbf{k}_\gamma \cdot P_\Delta \mathbf{j}^{[1]}(\mathbf{k}_\gamma) P_N = P_\Delta H_1^{[1]} Q Q \rho^{[1]}(\mathbf{k}_\gamma) P_N, \quad (\text{B.1b})$$

$$\mathbf{k}_\gamma \cdot Q \mathbf{j}^{[1]}(\mathbf{k}_\gamma) P_N = Q H_0^{[1]} Q Q \rho^{[1]}(\mathbf{k}_\gamma) P_N - Q \rho^{[1]}(\mathbf{k}_\gamma) P_N P_N H_0^{[1]} P_N, \quad (\text{B.1c})$$

$$\mathbf{k}_\gamma \cdot P_N \mathbf{j}^{[2]}(\mathbf{k}_\gamma) P_N = P_N H_1^{[2]} P_N P_N \rho^{[1]}(\mathbf{k}_\gamma) P_N - P_N \rho^{[1]}(\mathbf{k}_\gamma) P_N P_N H_1^{[2]} P_N, \quad (\text{B.2a})$$

$$\begin{aligned} \mathbf{k}_\gamma \cdot P_\Delta \mathbf{j}^{[2]}(\mathbf{k}_\gamma) P_N &= P_\Delta H_1^{[1]} Q Q \rho^{[1]}(\mathbf{k}_\gamma) P_N + P_\Delta H_1^{[2]} P_N P_N \rho^{[1]}(\mathbf{k}_\gamma) P_N - \\ &\quad P_\Delta \rho^{[1]}(\mathbf{k}_\gamma) P_\Delta P_\Delta H_1^{[2]} P_N, \end{aligned} \quad (\text{B.2b})$$

$$\mathbf{k}_\gamma \cdot Q \mathbf{j}^{[2]}(\mathbf{k}_\gamma) P_N = Q \rho^{[1]}(\mathbf{k}_\gamma) P_N P_N H_1^{[2]} P_N. \quad (\text{B.2c})$$

The constraints (B.1) and (B.2) are not entirely closed; they require knowledge on the one-baryon charge  $P_\Delta \rho^{[1]}(\mathbf{k}_\gamma) P_\Delta$  for the condition (B.2b). The fact that  $P_\Delta H_1^{[1]} Q Q \rho^{[1]}(\mathbf{k}_\gamma) P_N$  has one-baryon and two-baryon parts and therefore arises in Eqs. (B.1b) and (B.2b) has already been discussed in Subsect. 2.2.2.

The traditional nucleonic and Born currents of one-baryon nature,  $P_N j_{bare}^{[1]\mu}(\mathbf{k}_\gamma) P_N$  and  $Q j_{bare}^{[1]\mu}(\mathbf{k}_\gamma) P_N$ , satisfy Eqs. (B.1a) and (B.1c) respectively; there is no need for corresponding interaction-dependent contributions, i.e., for  $P_N j_{exchange}^{[1]\mu}(\mathbf{k}_\gamma) P_N = 0$  and  $Q j_{exchange}^{[1]\mu}(\mathbf{k}_\gamma) P_N = 0$ . The traditional transition current  $P_\Delta j_{bare}^{[1]\mu}(\mathbf{k}_\gamma) P_N$  is purely spatial and transverse, satisfying Eq. (B.1b) with vanishing right-hand side. The transition current requires an interaction-dependent contribution; a possible form satisfying Eq. (B.1b) is

$$P_\Delta \mathbf{j}_{exchange}^{[1]}(\mathbf{k}_\gamma) P_N | \mathbf{k}_N \rangle = -P_\Delta H_1^{[1]} Q \frac{1}{k_N^0 + i0 - Q H_0^{[1]} Q} Q \mathbf{j}_{bare}^{[1]}(\mathbf{k}_\gamma) P_N | \mathbf{k}_N \rangle; \quad (\text{B.3})$$

it depends on the interaction  $P_\Delta H_1^{[1]} Q$  and is, as the corresponding bare parts, also purely spatial. The interaction-dependent current  $P_\Delta \mathbf{j}_{exchange}^{[1]}(\mathbf{k}_\gamma) P_N$  is due to channel-coupling. The effective and reducible contribution to the transition current  $P_\Delta H_1^{[1]} Q(z - QH_0^{[1]} Q)^{-1} Qj^{[1]\mu}(\mathbf{k}_\gamma) P_N$  has to be taken out from its irreducible part in an averaged and energy-independent form.

The traditional two-nucleon exchange current  $P_N \mathbf{j}_{traditional}^{[2]}(\mathbf{k}_\gamma) P_N$  satisfies Eq. (B.2a). The traditional transition current of two-baryon nature  $P_\Delta \mathbf{j}_{traditional}^{[2]}(\mathbf{k}_\gamma) P_N$  solves Eq. (B.2b), with a right-hand side containing terms two and three only, taking

$$\langle \mathbf{k}'_\Delta | P_\Delta \rho^{[1]}(\mathbf{k}_\gamma) P_\Delta | \mathbf{k}_\Delta \rangle = \delta(\mathbf{k}'_\Delta - \mathbf{k}_N - \mathbf{k}_\gamma) e_P \frac{1}{2} (1 + \tau_{\Delta 3}). \quad (\text{B.4})$$

Thus, a nonstandard additional contribution is required, e.g.,

$$\begin{aligned} P_\Delta \mathbf{j}_{nonstandard}^{[2]}(\mathbf{k}_\gamma) P_N | \mathbf{k}_{N1} \mathbf{k}_{N2} \rangle = \\ - P_\Delta H_1^{[1]} Q \frac{1}{k_{N1}^0 + k_{N2}^0 + i0 - QH_0^{[1]} Q} Q \mathbf{j}_{bare}^{[1]}(\mathbf{k}_\gamma) P_N | \mathbf{k}_{N1} \mathbf{k}_{N2} \rangle; \end{aligned} \quad (\text{B.5})$$

it is of two-baryon nature and satisfies Eq. (B.2b) with only the first term on the right-hand side. Thus,

$$P_\Delta \mathbf{j}^{[2]}(\mathbf{k}_\gamma) P_N = P_\Delta \left[ \mathbf{j}_{traditional}^{[2]}(\mathbf{k}_\gamma) + \mathbf{j}_{nonstandard}^{[2]}(\mathbf{k}_\gamma) \right] P_N. \quad (\text{B.6})$$

The two-baryon current from nucleonic states to states with one pion is entirely nonstandard, i.e.,

$$\begin{aligned} \langle \mathbf{k}'_\pi \mathbf{k}'_{N1} \mathbf{k}'_{N2} | Q \mathbf{j}^{[2]}(\mathbf{k}_\gamma) P_N \\ - \langle \mathbf{k}'_\pi \mathbf{k}'_{N1} \mathbf{k}'_{N2} | Q \mathbf{j}_{bare}^{[1]}(\mathbf{k}_\gamma) P_N \frac{1}{k'_\pi^0 + k'_{N1}^0 + k'_{N2}^0 - P_N H_0^{[1]} P_N} P_N H_1^{[2]} P_N. \end{aligned} \quad (\text{B.7})$$

The interaction-dependent nonstandard irreducible two-baryon currents arise, since corresponding reducible ones are always generated and therefore have to be taken out from the corresponding traditional processes in an averaged energy-independent form; the traditional part of  $Q \mathbf{j}^{[2]}(\mathbf{k}_\gamma) P_N$  is zero.

## Appendix C: Photo Pionproduction on the Single Nucleon

A general description of photo pionproduction on the single nucleon is given. The process is used in order to fit phenomenological parameters in the parts  $P_{\Delta\mathbf{j}}^{[1]}(\mathbf{k}_\gamma)P_N$  and  $Q\mathbf{j}^{[1]}(\mathbf{k}_\gamma)P_N$  of the single-baryon current.

### C1. *S*-Matrix and E.M. Multipole Amplitudes of Photo Pionproduction

A detailed description of the photo pionproduction on the single nucleon can be found in the review of Berends et al. [28]. Our summary of formulae is based on the original work of Refs. [28 – 33].

We adopt the following kinematics: In the initial state a photon of momentum  $\mathbf{k}_\gamma$  and polarization vector  $\varepsilon^\mu(\mathbf{k}_\gamma)$  is absorbed by a nucleon of momentum  $\mathbf{k}_N$ . The momenta of the produced pion and the final nucleon are labeled by  $\mathbf{k}_\pi$  and  $\mathbf{k}'_N$ . The *S*-Matrix connecting the initial photon-nucleon and the final pion-nucleon states is related to the invariant scattering amplitude  $\mathcal{M}_{\pi N\gamma N}$  by

$$\langle \pi N | S | \gamma N \rangle = (-)i(2\pi)^4 \delta^4(k_\pi + k'_N - k_\gamma - k_N) \frac{\mathcal{M}_{\pi N\gamma N}}{\mathcal{N}}. \quad (\text{C.1})$$

The normalization constant

$$\mathcal{N} = (2\pi)^6 \sqrt{2E_\gamma(\mathbf{k}_\gamma)} \sqrt{2\omega_\pi(\mathbf{k}_\pi)} \sqrt{\frac{E_N(\mathbf{k}_N)}{m_N}} \sqrt{\frac{E_N(\mathbf{k}'_N)}{m_N}}, \quad (\text{C.2})$$

with  $E_\gamma(\mathbf{k}_\gamma)$ ,  $\omega_\pi(\mathbf{k}_\pi)$ ,  $E_N(\mathbf{k}_N)$  and  $E_N(\mathbf{k}'_N)$  being the energies of the corresponding particles, refers to the state normalization of Ref. [16]. We work in the c.m. system, i.e.,  $\mathbf{k}_N = -\mathbf{k}_\gamma$  and  $\mathbf{k}'_N = -\mathbf{k}_\pi$ . Energy conservation connects the momenta  $\mathbf{k}_\gamma$  and  $\mathbf{k}_\pi$ , i.e.,

$$W = |\mathbf{k}_\gamma| + \sqrt{m_N^2 + \mathbf{k}_\gamma^2} = \sqrt{m_\pi^2 + \mathbf{k}_\pi^2} + \sqrt{m_N^2 + \mathbf{k}_\pi^2}; \quad (\text{C.3})$$

$W$  is the energy available for the process; covariantly, it is the invariant mass defined by  $W^2 = (k_N + k_\gamma)^2$ . We use the Coulomb gauge for the photon field, i.e.,  $\varepsilon^\mu(\mathbf{k}_\gamma) = (0, \boldsymbol{\varepsilon}(\mathbf{k}_\gamma))$  with  $\boldsymbol{\varepsilon}(\mathbf{k}_\gamma) \cdot \mathbf{k}_\gamma = 0$ .

According to Lorentz symmetry and gauge invariance  $\mathcal{M}_{\pi N\gamma N}$  is built up from contributions of four independent operators acting in the nucleonic spin space; their relative

weight is controlled by four scalar functions  $\mathcal{F}_i(W, \cos \Theta)$ . Thus, the general form of the scattering amplitude is

$$\begin{aligned} \mathcal{M}_{\pi N\gamma N}(W, \cos \Theta) &= 4\pi \frac{W}{m_N} \chi'_s \left[ i\boldsymbol{\sigma} \cdot \boldsymbol{\varepsilon} \mathcal{F}_1(W, \cos \Theta) + \frac{\boldsymbol{\sigma} \cdot \mathbf{k}_\pi \boldsymbol{\sigma} \cdot (\mathbf{k}_\gamma \times \boldsymbol{\varepsilon})}{|\mathbf{k}_\pi||\mathbf{k}_\gamma|} \mathcal{F}_2(W, \cos \Theta) \right. \\ &\quad \left. + i \frac{\boldsymbol{\sigma} \cdot \mathbf{k}_\gamma \mathbf{k}_\pi \cdot \boldsymbol{\varepsilon}}{|\mathbf{k}_\gamma||\mathbf{k}_\pi|} \mathcal{F}_3(W, \cos \Theta) + i \frac{\boldsymbol{\sigma} \cdot \mathbf{k}_\pi \mathbf{k}_\pi \cdot \boldsymbol{\varepsilon}}{\mathbf{k}_\pi^2} \mathcal{F}_4(W, \cos \Theta) \right] \chi_s \end{aligned} \quad (\text{C.4})$$

with  $\chi_s$  and  $\chi'_s$  being the Pauli spinors of the nucleon in the initial and final states and with  $\boldsymbol{\varepsilon}$  abbreviating  $\boldsymbol{\varepsilon}(\mathbf{k}_\gamma)$ . The scattering amplitude is a function of the available energy  $W$  and of the scattering angle  $\Theta$  in the c.m. system.

The four independent spin operators depend on the scattering angle  $\Theta$ ; the four scalar functions  $\mathcal{F}_i(W, \cos \Theta)$  also depend on it. The latter dependence is usually expanded [30, 31] in terms of the Legendre polynomials  $P_l(\cos \Theta)$  and of the electric and magnetic multipole amplitudes  $E_{l\pm}$  and  $M_{l\pm}$ , i.e.,

$$\begin{aligned} \mathcal{F}_1(W, \cos \Theta) &= \sum_{l=0}^{\infty} \left[ [lM_{l+}(W) + E_{l+}(W)] P'_{l+1}(\cos \Theta) \right. \\ &\quad \left. + [(l+1)M_{l-}(W) + E_{l-}(W)] P'_{l-1}(\cos \Theta) \right], \end{aligned} \quad (\text{C.5a})$$

$$\mathcal{F}_2(W, \cos \Theta) = \sum_{l=1}^{\infty} \left[ [(l+1)M_{l+}(W) + lM_{l-}(W)] P'_l(\cos \Theta) \right], \quad (\text{C.5b})$$

$$\begin{aligned} \mathcal{F}_3(W, \cos \Theta) &= \sum_{l=1}^{\infty} \left[ [-M_{l+}(W) + E_{l+}(W)] P''_{l+1}(\cos \Theta) \right. \\ &\quad \left. + [M_{l-}(W) + E_{l-}(W)] P''_{l-1}(\cos \Theta) \right], \end{aligned} \quad (\text{C.5c})$$

$$\begin{aligned} \mathcal{F}_4(W, \cos \Theta) &= \sum_{l=1}^{\infty} \left[ [M_{l+}(W) - E_{l+}(W)] \right. \\ &\quad \left. - [M_{l-}(W) - E_{l-}(W)] P''_l(\cos \Theta) \right]. \end{aligned} \quad (\text{C.5d})$$

In Eq. (C.5)  $P'_l(P''_l)$  denotes the first (second) derivative of  $P_l(\cos \Theta)$  with respect to  $\cos \Theta$ . Eq. (C.5) can be inverted, i.e.,

$$\begin{aligned} E_{l+}(W) &= \frac{1}{2(l+1)} \int_{-1}^1 dx \left[ \mathcal{F}_1(W, x) P_l(x) - \mathcal{F}_2(W, x) P_{l+1}(x) - \mathcal{F}_3(W, x) \times \right. \\ &\quad \left. \frac{l}{2l+1} (P_{l+1}(x) - P_{l-1}(x)) - \mathcal{F}_4(W, x) \frac{l+1}{2l+3} (P_{l+2}(x) - P_l(x)) \right], \end{aligned} \quad (\text{C.6a})$$

$$\begin{aligned} E_{l-}(W) &= \frac{1}{2l} \int_{-1}^1 dx \left[ \mathcal{F}_1(W, x) P_l(x) - \mathcal{F}_2(W, x) P_{l-1}(x) + \mathcal{F}_3(W, x) \times \right. \\ &\quad \left. \frac{l+1}{2l+1} (P_{l+1}(x) - P_{l-1}(x)) - \mathcal{F}_4(W, x) \frac{l}{2l-1} (P_{l+2}(x) - P_l(x)) \right], \end{aligned} \quad (\text{C.6b})$$

$$\begin{aligned}
M_{l+}(W) &= \frac{1}{2(l+1)} \int_{-1}^1 dx \left[ \mathcal{F}_1(W, x) P_l(x) - \mathcal{F}_2(W, x) P_{l+1}(x) \right. \\
&\quad \left. + \mathcal{F}_3(W, x) \frac{1}{2l+1} (P_{l+1}(x) - P_{l-1}(x)) \right], \tag{C.6c}
\end{aligned}$$

$$\begin{aligned}
M_{l-}(W) &= \frac{1}{2l} \int_{-1}^1 dx \left[ -\mathcal{F}_1(W, x) P_l(x) + \mathcal{F}_2(W, x) P_{l-1}(x) \right. \\
&\quad \left. - \mathcal{F}_3(W, x) \frac{1}{2l+1} (P_{l+1}(x) - P_{l-1}(x)) \right]. \tag{C.6d}
\end{aligned}$$

In addition, the invariant scattering amplitude  $\mathcal{M}_{\pi N \gamma N}$  is built up from different isospin contributions distinct by the charge of the produced pion; the various parts show up in the scalar functions  $\mathcal{F}_i(W, \cos \Theta)$ , i.e.,

$$\mathcal{F}_i(W, \cos \Theta) = \mathcal{F}_i^{(+)}(W, \cos \Theta) \delta_{\alpha,0} + \mathcal{F}_i^{(-)}(W, \cos \Theta) \frac{1}{2} [\boldsymbol{\tau}_\alpha, \boldsymbol{\tau}_0] + \mathcal{F}_i^{(0)}(W, \cos \Theta) \boldsymbol{\tau}_\alpha. \tag{C.7}$$

The subscript  $\alpha$  refers to a specific isospin channel of the process, i.e.  $\alpha = (-)Q_\pi$  where  $Q_\pi$  is the charge of the pion,  $\boldsymbol{\tau}_\alpha$  being the usual nucleonic Pauli matrices. Instead of the amplitudes  $\mathcal{F}_i^{(+)}$  and  $\mathcal{F}_i^{(-)}$  the linear combinations

$$\mathcal{F}_i^{(\frac{1}{2})}(W, \cos \Theta) = \mathcal{F}_i^{(+)}(W, \cos \Theta) + 2\mathcal{F}_i^{(-)}(W, \cos \Theta) \tag{C.8a}$$

$$\mathcal{F}_i^{(\frac{3}{2})}(W, \cos \Theta) = \mathcal{F}_i^{(+)}(W, \cos \Theta) - \mathcal{F}_i^{(-)}(W, \cos \Theta) \tag{C.8b}$$

referring to definite total isospin of the final pion-nucleon state, i.e.,  $\frac{1}{2}$  and  $\frac{3}{2}$ , are introduced. The isospin contributions to the e.m. multipole amplitudes  $M_{l\pm}$  and  $E_{l\pm}$  will be explicitly indicated by the superscripts  $\beta = 0, \frac{1}{2}$ , or  $\frac{3}{2}$  of the scalar functions  $\mathcal{F}_i^{(\beta)}(W, \cos \Theta)$  and the multipoles  $M_{l\pm}^{(\beta)}$  and  $E_{l\pm}^{(\beta)}$ .

## C2. Single-Baryon Current to Be Fitted

The parts of the single-baryon current required for photo pionproduction are the transition current

$$\begin{aligned}
\langle \mathbf{k}_\Delta | P_\Delta \mathbf{j}^{[1]}(\mathbf{k}_\gamma) P_N | \mathbf{k}_N \rangle &= \delta(\mathbf{k}_\Delta - \mathbf{k}_N - \mathbf{k}_\gamma) \frac{e_p}{2m_N} (\boldsymbol{\tau}_{\Delta N})_0 \\
&\quad \left[ iG_{M1}^{\Delta N} [\boldsymbol{\sigma}_{\Delta N} \times \mathbf{k}_\gamma] + G_{E2}^{\Delta N} [\boldsymbol{\sigma}_{\Delta N} \boldsymbol{\sigma} \cdot \mathbf{k}_\gamma - \frac{i}{2} (\boldsymbol{\sigma}_{\Delta N} \times \mathbf{k}_\gamma)] \right] \tag{C.9}
\end{aligned}$$

and the Born current  $Q\mathbf{j}^{[1]}(\mathbf{k}_\gamma) P_N$ . The transition current has magnetic dipole and electric quadrupole contributions with the strength parameters  $G_{M1}^{\Delta N}$  and  $G_{E2}^{\Delta N}$ , respectively. In Eq. (C.9) the current is written in the pion-nucleon c.m. system, i.e., for  $\mathbf{k}_\Delta = 0$ ; the calculation of this appendix is done in that system. The Born current  $Q\mathbf{j}^{[1]}(\mathbf{k}_\gamma) P_N$  is taken

over from Ref. [32]; it is on its pion-nucleon side augmented by the phenomenological form factor

$$F_B(\mathbf{k}^2) = \frac{(\Lambda_B)^2}{(\Lambda_B)^2 + \mathbf{k}^2} . \quad (\text{C.10})$$

As for the corresponding form factor in the  $\pi N \Delta$ -vertex  $QH_1P_\Delta$ , the momentum  $\mathbf{k}$  is chosen to be the relative pion-nucleon momentum; it only becomes the true pion momentum in the pion-nucleon c.m. system.

Given the structure of the single-baryon current, the resonant multipole amplitudes have three contributions [34, 35],

$$M_{1+}^{(\frac{3}{2})}(W) = M_{1+}^{(\frac{3}{2})Res}(W) + M_{1+}^{(\frac{3}{2})Born}(W) + M_{1+}^{(\frac{3}{2})Inter}(W) , \quad (\text{C.11a})$$

$$E_{1+}^{(\frac{3}{2})}(W) = E_{1+}^{(\frac{3}{2})Res}(W) + E_{1+}^{(\frac{3}{2})Born}(W) + E_{1+}^{(\frac{3}{2})Inter}(W) , \quad (\text{C.11b})$$

the pure resonant, Born and interference (or often called rescattering) contributions being labeled with the superscript *Res*, *Born* and *Inter*, respectively. The three processes are displayed in Fig. C.1. They have the following analytic forms

$$M_{1+}^{(\frac{3}{2})Res}(W) = \frac{1}{6W} \left[ \frac{|\mathbf{k}_\pi|}{\sqrt{4\pi}} \frac{f_\Delta(\mathbf{k}_\pi^2)}{m_\pi} g^\Delta(W) G_{M1}^{\Delta N} \frac{e_p}{\sqrt{4\pi}} |\mathbf{k}_\gamma| \right] , \quad (\text{C.12a})$$

$$E_{1+}^{(\frac{3}{2})Res}(W) = \frac{-1}{12W} \left[ \frac{|\mathbf{k}_\pi|}{\sqrt{4\pi}} \frac{f_\Delta(\mathbf{k}_\pi^2)}{m_\pi} g^\Delta(W) G_{E2}^{\Delta N} \frac{e_p}{\sqrt{4\pi}} |\mathbf{k}_\gamma| \right] , \quad (\text{C.12b})$$

$$M_{1+}^{(\frac{3}{2})Born}(W) = F_B(\mathbf{k}_\pi^2) M_{1+bare}^{(\frac{3}{2})Born}(W) , \quad (\text{C.13a})$$

$$E_{1+}^{(\frac{3}{2})Born}(W) = F_B(\mathbf{k}_\pi^2) E_{1+bare}^{(\frac{3}{2})Born}(W) \quad (\text{C.13b})$$

and

$$M_{1+}^{(\frac{3}{2})Inter}(W) = g^\Delta(W) \left[ -\frac{i}{2} \Gamma_\Delta(W, 0) F_B(\mathbf{k}_\pi^2) + I_P(W) \right] M_{1+bare}^{(\frac{3}{2})Born}(W) , \quad (\text{C.14a})$$

$$E_{1+}^{(\frac{3}{2})Inter}(W) = g^\Delta(W) \left[ -\frac{i}{2} \Gamma_\Delta(W, 0) F_B(\mathbf{k}_\pi^2) + I_P(W) \right] E_{1+bare}^{(\frac{3}{2})Born}(W) , \quad (\text{C.14b})$$

with

$$f_\Delta(\mathbf{k}^2) = f_{\pi N \Delta} \frac{\Lambda_{\pi \Delta}^2 - m_\pi^2}{\Lambda_{\pi \Delta}^2 + \mathbf{k}^2} , \quad (\text{C.15a})$$

$$g^\Delta(W) = \frac{1}{W + i0 - M_\Delta(W, 0) + \frac{i}{2} \Gamma_\Delta(W, 0)} \quad (\text{C.15b})$$

according to Eq. (2.2). The last term in the brackets of the Eq. (C.14) is the principle value integral

$$I_P(W) = \frac{f_\Delta(\mathbf{k}_\pi^2)}{m_\pi} |\mathbf{k}_\pi| \frac{4\pi}{3} \frac{1}{(2\pi)^3} \mathcal{P} \int_0^\infty \frac{dp}{\omega_\pi(p)} \frac{f_\Delta(p^2)}{m_\pi} \frac{p^3 F_B(p^2)}{W - E_N(p) - \omega_\pi(p)} . \quad (\text{C.16})$$

The Born contribution of Eq. (C.13) is too lengthy to be given explicitly; it is taken over from Ref. [32]; only the additionally introduced form factor  $F_B(\mathbf{k}_\pi^2)$  has to be remembered.

By construction, the resonant multipole amplitudes satisfy Watson's theorem [36], i.e.,

$$M_{1+}^{(\frac{3}{2})}(W) = \left| M_{1+}^{(\frac{3}{2})}(W) \right| e^{i\delta_{P_{33}}(W)}, \quad (\text{C.17a})$$

$$E_{1+}^{(\frac{3}{2})}(W) = \left| E_{1+}^{(\frac{3}{2})}(W) \right| e^{i\delta_{P_{33}}(W)}. \quad (\text{C.17b})$$

In the last equations  $\delta_{P_{33}}(W)$  is the pion-nucleon phase shift in the  $P_{33}$  partial wave. This result gets obvious by using the equations above for the total multipoles, i.e.,

$$\begin{aligned} M_{1+}^{(\frac{3}{2})}(W) &= g^\Delta(W) \left[ \frac{1}{6W} \frac{|\mathbf{k}_\pi|}{\sqrt{4\pi}} \frac{f_\Delta(\mathbf{k}_\pi^2)}{m_\pi} G_{M1}^{\Delta N} \frac{e_p}{\sqrt{4\pi}} |\mathbf{k}_\gamma| \right. \\ &\quad \left. + ([W - M_\Delta(W, 0)] F_B(|\mathbf{k}_\pi|) + I_p(W)) M_{1+bare}^{(\frac{3}{2})Born}(W) \right], \end{aligned} \quad (\text{C.18a})$$

$$\begin{aligned} E_{1+}^{(\frac{3}{2})}(W) &= g^\Delta(W) \left[ \frac{-1}{12W} \frac{|\mathbf{k}_\pi|}{\sqrt{4\pi}} \frac{f_\Delta(\mathbf{k}_\pi^2)}{m_\pi} G_{E2}^{\Delta N} \frac{e_p}{\sqrt{4\pi}} |\mathbf{k}_\gamma| \right. \\ &\quad \left. + ([W - M_\Delta(W, 0)] F_B(|\mathbf{k}_\pi|) + I_p(W)) E_{1+bare}^{(\frac{3}{2})Born}(W) \right]. \end{aligned} \quad (\text{C.18b})$$

### C3. Results for Multipole Amplitudes

Sample results for multipole amplitudes in the kinematic regime up to 1.4 GeV c.m. energy  $W$  are given in Figs. C.2 - C.8. Figs. C.5 and C.6 display the resonant magnetic dipole  $M_{1+}^{(\frac{3}{2})}$ , Figs. C.7 and C.8 the electric quadrupole  $E_{1+}^{(\frac{3}{2})}$  and Figs. C.2 - C.4 some nonresonant multipoles.

Figs. C.5 - C.8 show results of our fit. We consider the fit satisfactory. The optimized parameters for the single-baryon current  $P_\Delta \mathbf{j}^{[1]}(\mathbf{k}_\gamma) P_N$  are  $G_{M1}^{\Delta N} = 3.65$  as magnetic dipole strength and  $G_{E2}^{\Delta N} = 0.10$  as electric quadrupole strength. The cut-off  $\Lambda_B$  of Eq. (C.10) for the Born current turns out to be better chosen differently for different multipoles, i.e.,  $\Lambda_B^{M1} = 245.5$  MeV and  $\Lambda_B^{E2} = 379.0$  MeV; no common satisfactory value could be found. In the Born current the  $\rho$ -meson does not contribute to either resonant multipole on symmetry grounds; in contrast, the  $\omega$ -meson does contribute but does so noticeably only for the magnetic dipole  $M_{1+}^{(\frac{3}{2})}$ .

Figs. C.2 - C.4 show sample results for nonresonant multipole amplitudes. The results do not use a cut-off form factor, i.e.,  $F_B(k^2) = 1$ . No distinct fit is carried out for each partial wave; thus, the results are predictions. The multipole  $E_{0+}^{(\frac{1}{2})}$  is an example in which the  $\rho$ -meson contributes markedly,  $M_{1-}^{(\frac{3}{2})}$  one in which the  $\omega$ -meson does so.

## Acknowledgements

The authors acknowledge helpful discussions with F. Fernandez, H. Garcilazo, A. Valcarce and P. Wilhelm. They thank K. Chmielewski and A. Kolezhuk for their help in using some software. The work benefitted from the DAAD grant, Contract No. 314/Al-e-dr, which allowed to upkeep the collaboration with the Nuclear Theory Group of the University of Salamanca; the warm hospitality of the Salamanca Nuclear Theory Group is greatly acknowledged. The work was supported in part by the Deutsche Forschungsgemeinschaft (DFG) under the Contract No. Sa 247/14-1.

## References

- [1] Pöpping, H., Sauer, P. U., Zhang, Xi-Zhen: *Nucl. Phys.* **A474**, 557 (1987); Erratum: *Nucl. Phys.* **A550**, 563 (1992)
- [2] Betz, M., Lee, T.-S. H.: *Phys. Rev.* **C23**, 375 (1981);  
Lee, T.-S. H., Matsuyama, A.: *Phys. Rev.* **C32**, 516 (1985); *Phys. Rev.* **C32**, 1986 (1985); *Phys. Rev.* **C34**, 1900 (1986)
- [3] Afnan, I.R., Blankleider, B.: *Phys. Rev.* **C22**, 1638 (1980); *Phys. Rev.* **C24**, 1572 (1981)
- [4] Fayard, C., Lamot, G. H., Mizutani, T.: *Phys. Rev. Lett.* **45**, 524 (1980)
- [5] Thomas, A. W., Rinat, A. S.: *Phys. Rev.* **C20**, 216 (1979);  
Rinat, A. S., Starkand, Y.: *Nucl. Phys.* **A397**, 381 (1983)
- [6] Garcilazo, H., Mizutani, T.:  $\pi$ NN Systems, Singapore: World Scientific 1990
- [7] Oelfke, U.: Elektromagnetische Reaktionen des Deuterons bei mittleren Energien: *Ph.D. Thesis*, University of Hannover 1990
- [8] Leidemann, W., Arenhövel, H.: *Nucl. Phys.* **A 465**, 573 (1987)
- [9] Wilhelm, P., Leidemann, W., Arenhövel, H.: *Few Body Systems* **3**, 111 (1988)
- [10] Wilhelm, P., Arenhövel, H.: *Phys. Lett.* **B 318**, 410 (1993)
- [11] Wilhelm, P., Arenhövel, H.: *Nucl. Phys.* **A593**, 435 (1995)
- [12] Tanabe, H., Ohta, K.: *Phys. Rev.* **C 40**, 1905 (1989)
- [13] Blaazer, F., Bakker, B. L. G., Boersma, H.J.: *Nucl. Phys.* **A568**, 681 (1994)
- [14] Dreissigacker, K., Furui, S., Hajduk, Ch., Sauer, P.U., Machleidt, R. : *Nucl. Phys.* **A375**, 334 (1982)
- [15] Alt, E. O., Grassberger, P., Sandhas, W. : *Nucl. Phys.* **B2**, 167 (1967)
- [16] Bjorken, J. D., Drell, S. D.: Relativistic Quatum Fields, New York: McGraw-Hill 1965
- [17] Strüve, W., Hajduk, Ch., Sauer, P.U., Theis, W.: *Nucl. Phys.* **A465**, 651 (1987)
- [18] Garcilazo, H., Mizutani, T.: *Few Body Systems* **5**, 127 (1988)
- [19] Bulla, A., Sauer, P. U.: *Few Body Systems* **12**, 141 (1992)

[20] Adam, J., Jr., Hajduk, Ch., Henning, H., Sauer, P. U., Truhlik, E.: *Nucl. Phys.* **A531**, 623 (1990)

[21] Sauer, P. U., Bugaev, K. A.: *Prog. Part. Nucl. Phys.* **34**, 147 (1995)

[22] Weber, H.J., Arenhövel, H.: *Phys. Rep.* **C 36**, 277 (1978)

[23] Lacombe, M., *et al.*: *Phys. Rev.* **C21**, 861 (1980)

[24] Friar, J. L., Gibson, B. F., Payne, G. L.: *Phys. Rev.* **C31**, 441 (1984)

[25] Jaus, W., Woolcock, W. S.: *Nucl. Phys.* **A431**, 669 (1984)

[26] Peña, M.T., Garcilazo, H., Oelfke, U., Sauer, P.U.: *Phys. Rev.* **C 45**, 1487 (1992)

[27] Valcarce, A., Fernandez, F., Garcilazo, H., Peña, M.T., Sauer, P.U.: *Phys. Rev.* **C49**, 1799 (1994)

[28] Berends, F. A., Donnachie, A., Weaver, D. L.: *Nucl. Phys.* **B4**, 1; 54; 103 (1967)

[29] Siegert, A. J. F.: *Phys. Rev.* **52**, 787 (1937)

[30] Chew, G. F., Goldberger, M.L., Low, F.E., Nambu, Y. : *Phys. Rev.* **106**, 1345 (1957)

[31] Goldberger, M. L., Watson, K. M.: Collision Theory, New York: Wiley 1964

[32] Olsson, M. G.: *Nucl. Phys.* **B78**, 55 (1974); Olsson, M. G., Osypowski, E. T.: *Nucl. Phys.* **B87**, 399 (1975)

[33] Nozawa, S., Blankleider, B., Lee, T.-S. H.: *Nucl. Phys.* **A513**, 459 (1990)

[34] Yang, S. N.: *J. of Phys.* **G11**, L205 (1985)

[35] Tanabe, H., Ohta, K.: *Phys. Rev.* **C31**, 1876 (1985)

[36] Watson, K. M.: *Phys. Rev.* **95**, 228 (1954)

[37] Kose, R., *et al.*: *Z. Phys.* **C 202**, 364 (1967)

[38] Arends, J., *et al.*: *Nucl. Phys.* **A 412**, 509 (1984)

[39] Gorbenko, V.G., *et al.*: *Nucl. Phys.* **A 381**, 330 (1982)

[40] von Holtey, G., *et al.*: *Z. Phys.* **C 259**, 51 (1973)

[41] Bouquet, B., *et al.*: *Nucl. Phys.* **B 79**, 45 (1974)

[42] Hilger, E., *et al.*: *Nucl. Phys.* **B 93**, 7 (1975)

[43] Pfeil, W., Schwela, D.: *Nucl. Phys.* **B45**, 379 (1972)

- [44] Berends, F. A., Donnachie, A.: *Nucl. Phys.* **B84**, 342 (1975)
- [45] Arndt, R.A., Strakovsky, I.I., Wozkman, R.L.: *Phys. Rev.* **C53**, 430 (1996); SAID data-base SM95

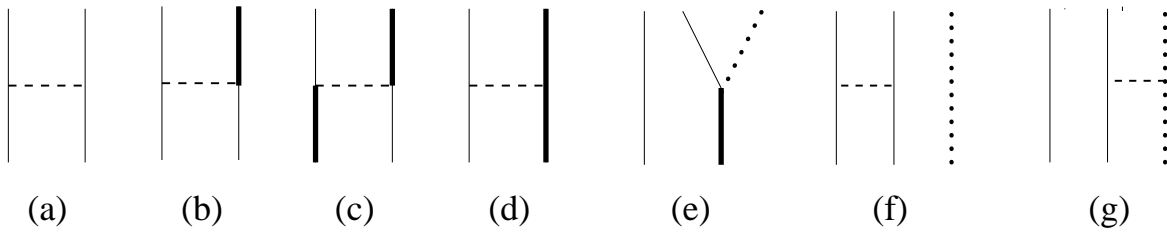


**Fig. 2.1.** Graphical definition of the interaction hamiltonian  $H_1$  in a Hilbert space of baryon number two. The solid vertical line denotes a nucleon, the thick one a  $\Delta$ -isobar, the dotted line a pion. Horizontal dashed lines represent the action of an instantaneous hermitian potential. Only process (a) contributes to the isospin-singlet partial waves.

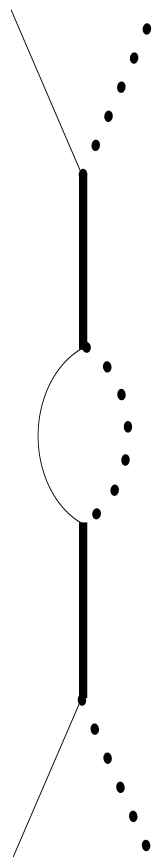


**Fig. 2.2.** Schematic representation of  $\pi N$  scattering in the  $P_{33}$  partial wave. Only one characteristic process of an infinite order is shown.

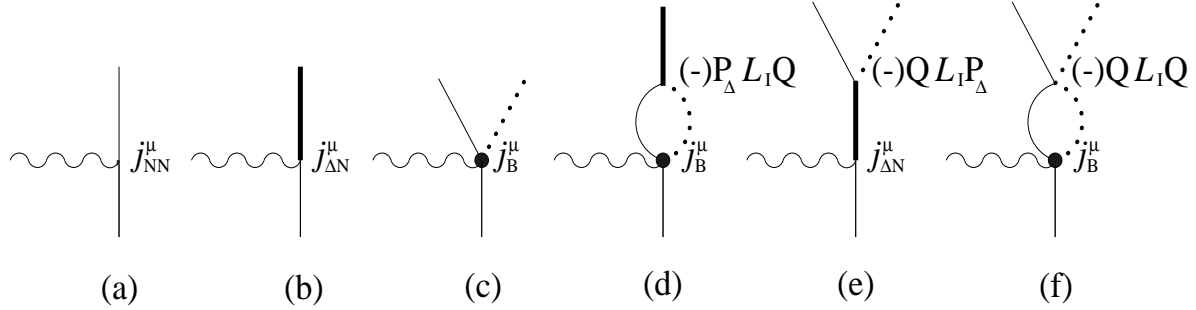


**Fig. 2.3.** Feynman processes for the one-baryon current up to first order in the field-theoretic Lagrangian  $\mathcal{L}_I$ . The first three processes are interaction-free; their amplitudes are denoted by  $J_{bare}^{[1]\mu}(k_\gamma)$ ; they are the purely nucleonic current  $j_{NN}^\mu(k_\gamma)$ , the transition one  $j_{\Delta N}^\mu(k_\gamma)$  from the nucleon to the  $\Delta$ -isobar and the Born one  $j_B^\mu(k_\gamma)$  which produces a pion on the nucleon; they are assumed to be conserved. The processes (d) to (f) are interaction-dependent; they are of first order in the interaction; their amplitudes are denoted by  $J_{exchange}^{[1]\mu}(k_\gamma)$ .

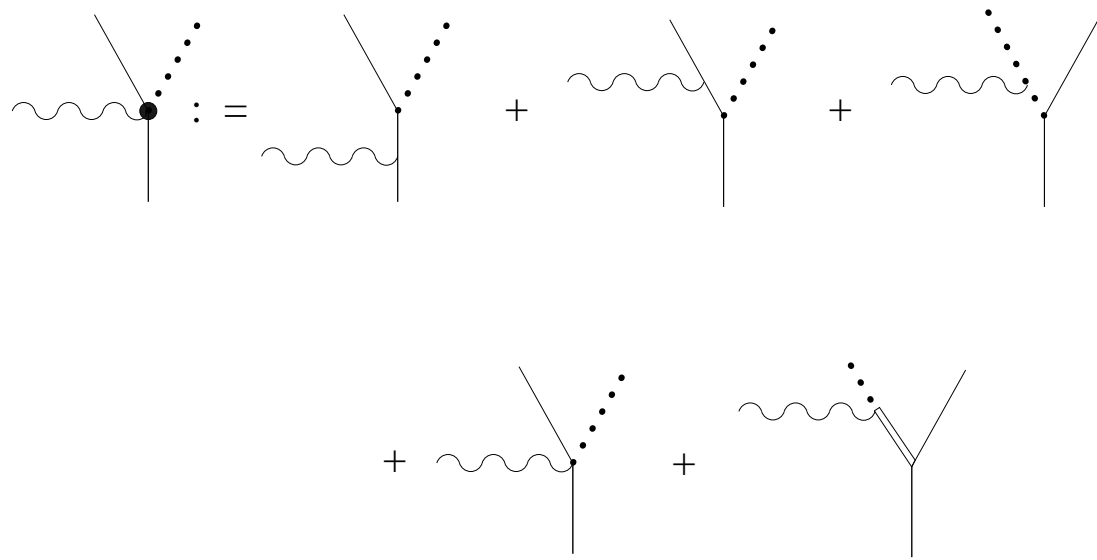
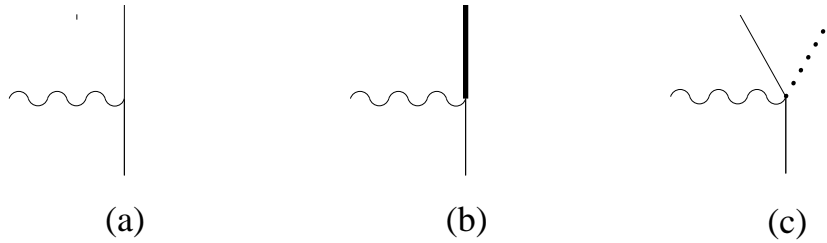


**Fig. 2.4.** Field-theoretic processes contained in the Born current  $j_B^\mu(k_\gamma)$ . The first four processes are solely derived from interactions with the pion. The fifth process involves rho- and omega-meson exchange; the vector mesons are diagrammatically indicated by double lines. Since the employed hadronic interaction does not use the pion-nucleon vertex as mechanism for the pion production and absorption, i.e.,  $QH_1^{[1]}P_N = 0$ , the current is not reducible.

$$(P_N + P_\Delta + Q)[j_{\text{bare}}^{[1]\mu} + j_{\text{exchange}}^{[1]\mu}]P_N :=$$



$$(P_N + P_\Delta + Q) J_{\text{oms}}^{[1]\mu} P_N :=$$

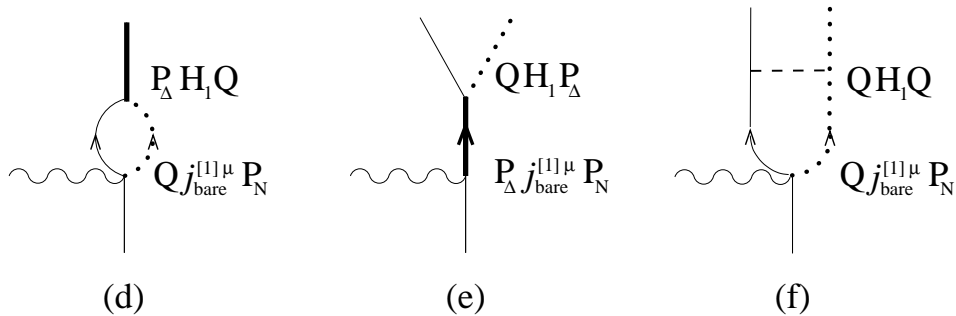


**Fig. 2.5.** Processes of Schrödinger theory for the one-baryon current up to first order in the interaction  $H_1^{[1]}$ . The arrows indicate that the corresponding particles in intermediate states are on their respective mass shells and propagate according to the global propagators of Schrödinger theory.

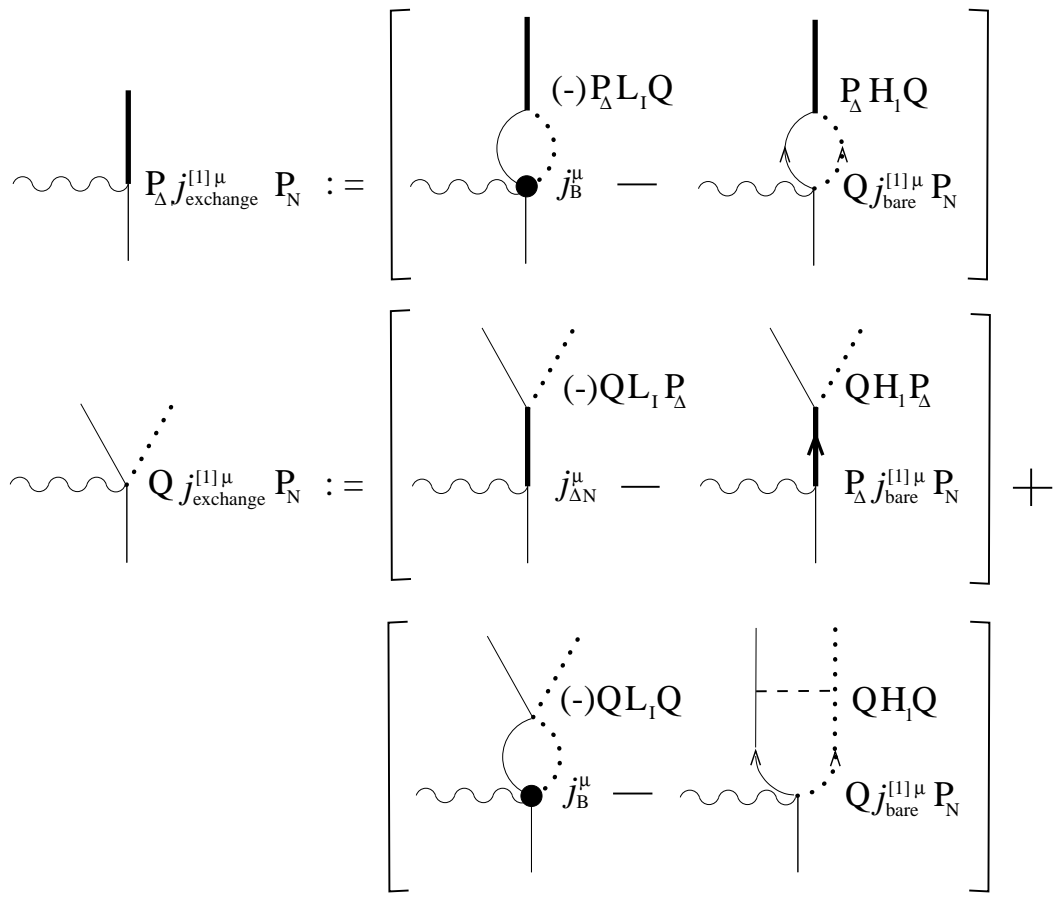


**Fig. 2.6.** Graphical definition of the multichannel one-baryon interaction-dependent current  $(P_\Delta + Q)j_{exchange}^{[1]\mu}(\mathbf{k}_\gamma)P_N$ . The meaning of the arrows for particles in intermediate states is given in Fig. 2.5.

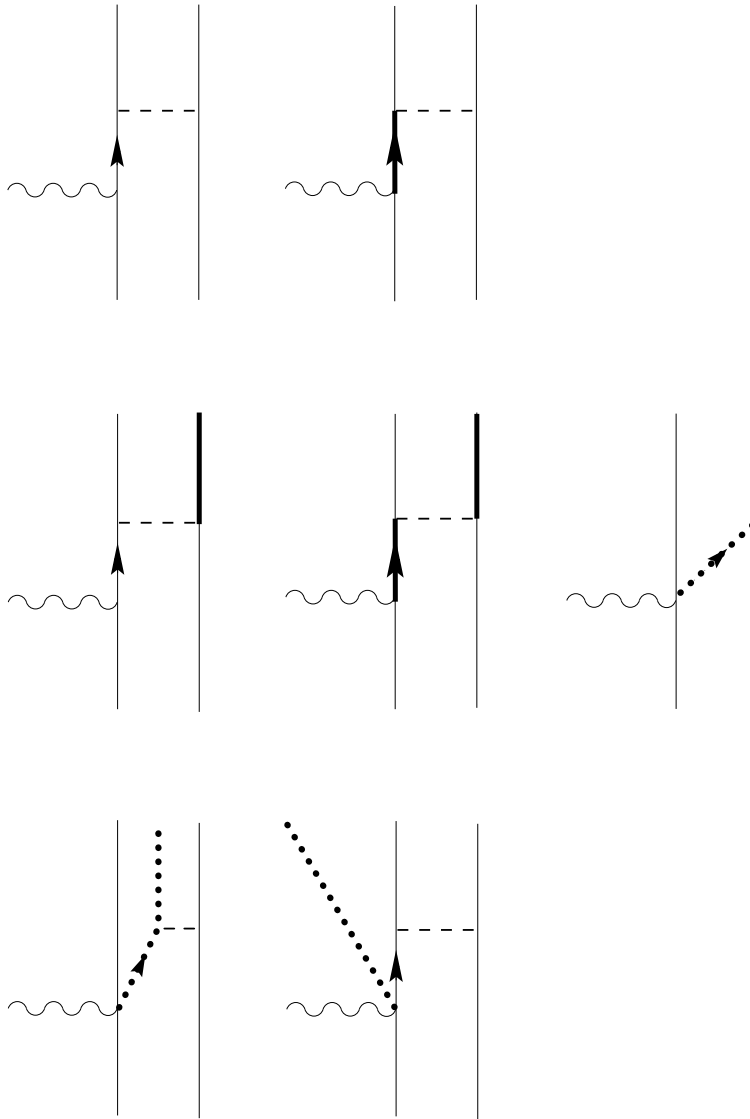


**Fig. 2.7.** Two-baryon current  $(P_N + P_\Delta + Q) J_{oms}^{[2]\mu}(\mathbf{k}_\gamma) P_N$  in the noncovariant framework of Schrödinger theory. They are based on the bare one-baryon current  $j_{bare}^{[1]\mu}(\mathbf{k}_\gamma)$  and on the interaction  $H_1^{[1]} + H_1^{[2]}$  up to first order. The meaning of the arrows for particles in intermediate states is given in Fig. 2.5. All connected, but reducible processes are shown in which the current acts first; exchange processes are not shown; furthermore, the processes in which the interaction  $H_1$  acts first are not shown for consistency of presentation. In the three rows the contributions  $P_N J_{oms}^{[2]\mu}(\mathbf{k}_\gamma) P_N$ ,  $P_\Delta J_{oms}^{[2]\mu}(\mathbf{k}_\gamma) P_N$  and  $Q J_{oms}^{[2]\mu}(\mathbf{k}_\gamma) P_N$  are given consecutively.

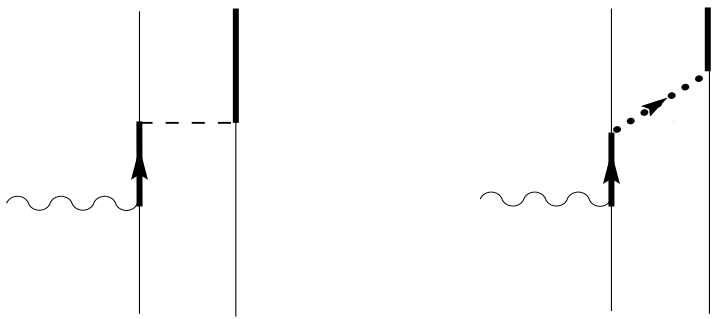


**Fig. 2.8.** Contributions to the two-baryon current  $P_\Delta J_{oms}^{[2]\mu}(\mathbf{k}_\gamma)P_N$  in the noncovariant framework of Schrödinger theory. In orders of the employed interaction  $H_1$ , the left process is of first in  $H_1^{[2]}$ , the right one of second order  $H_1^{[1]}$ . The meaning of the arrows for particles in intermediate states is given in Fig. 2.5.

$$P_\Delta j_{exchange}^{[2]\mu} P_N :=$$

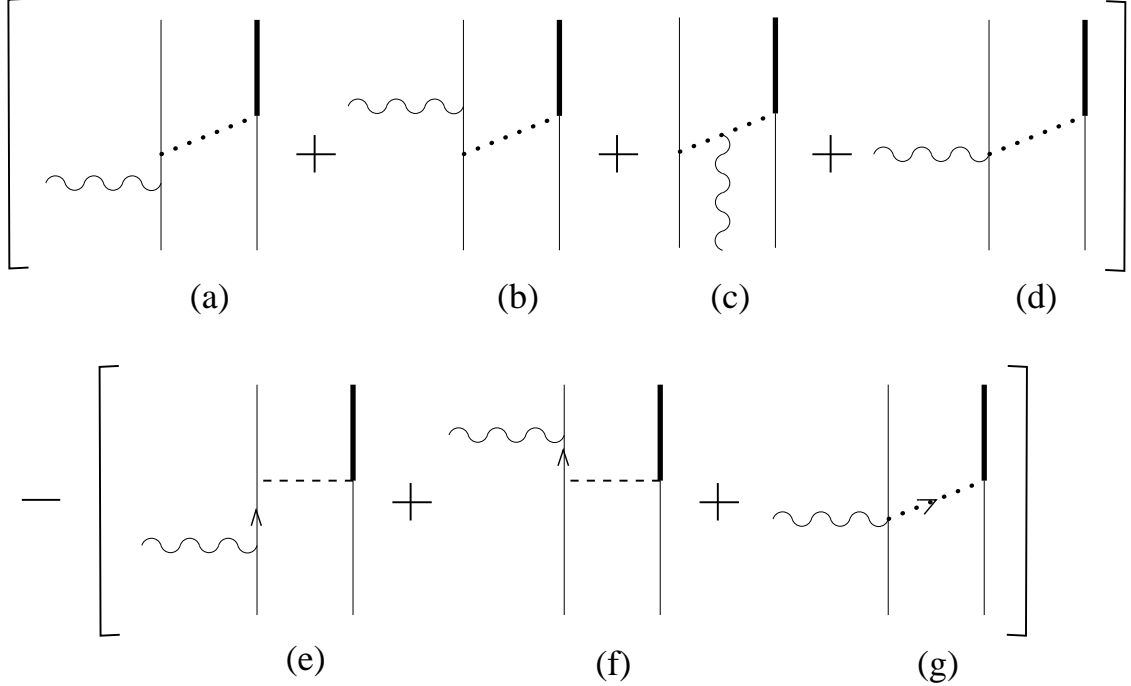


**Fig. 2.9.** Graphical definition of the two-baryon exchange current of pion range  $\langle \mathbf{k}'_{N_1} \mathbf{k}'_{\Delta_2} | j_{exchange}^{[2]\mu}(\mathbf{k}_\gamma) | \mathbf{k}_{N_1} \mathbf{k}_{N_2} \rangle$ . The meaning of the arrows for particles in intermediate states is given in Fig. 2.5. The four field-theoretic processes (a) - (d) of opposite time ordering in which the  $\pi N \Delta$ -vertex occurs prior to the  $\pi NN$ -vertex are required for the definition, but not shown.

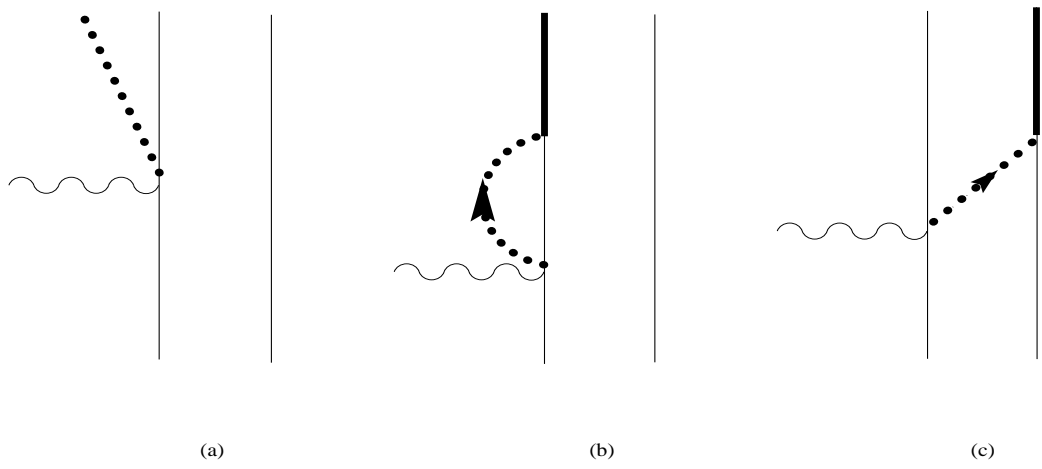


**Fig. 3.1.** Irreducible and reducible contributions arising from the Born current in the two-baryon system. Contribution (a), however only in the  $P_{33}$  partial wave, is retained in the present calculations for pion production without any further rescattering. The reducible processes (b) and (c) can contribute to disintegration and to pion production due to further final-state interaction; neither of these two processes is retained in the present calculations.

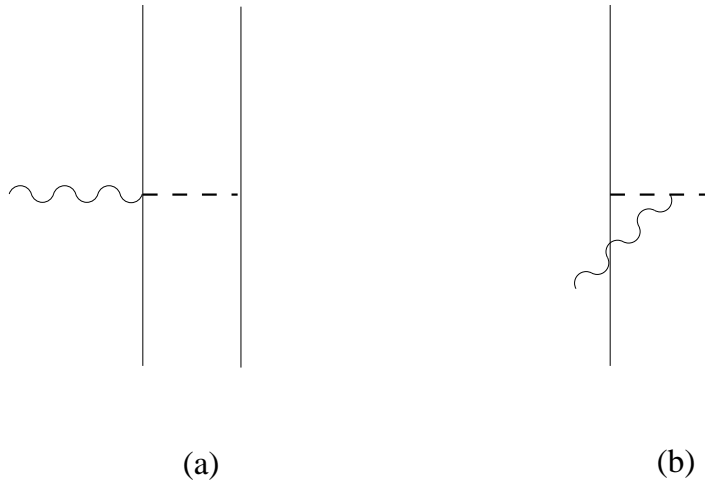


**Fig. 3.2.** Traditional meson-exchange currents. On the left side the contact or pair process is shown, on the right side the meson-in-flight one.

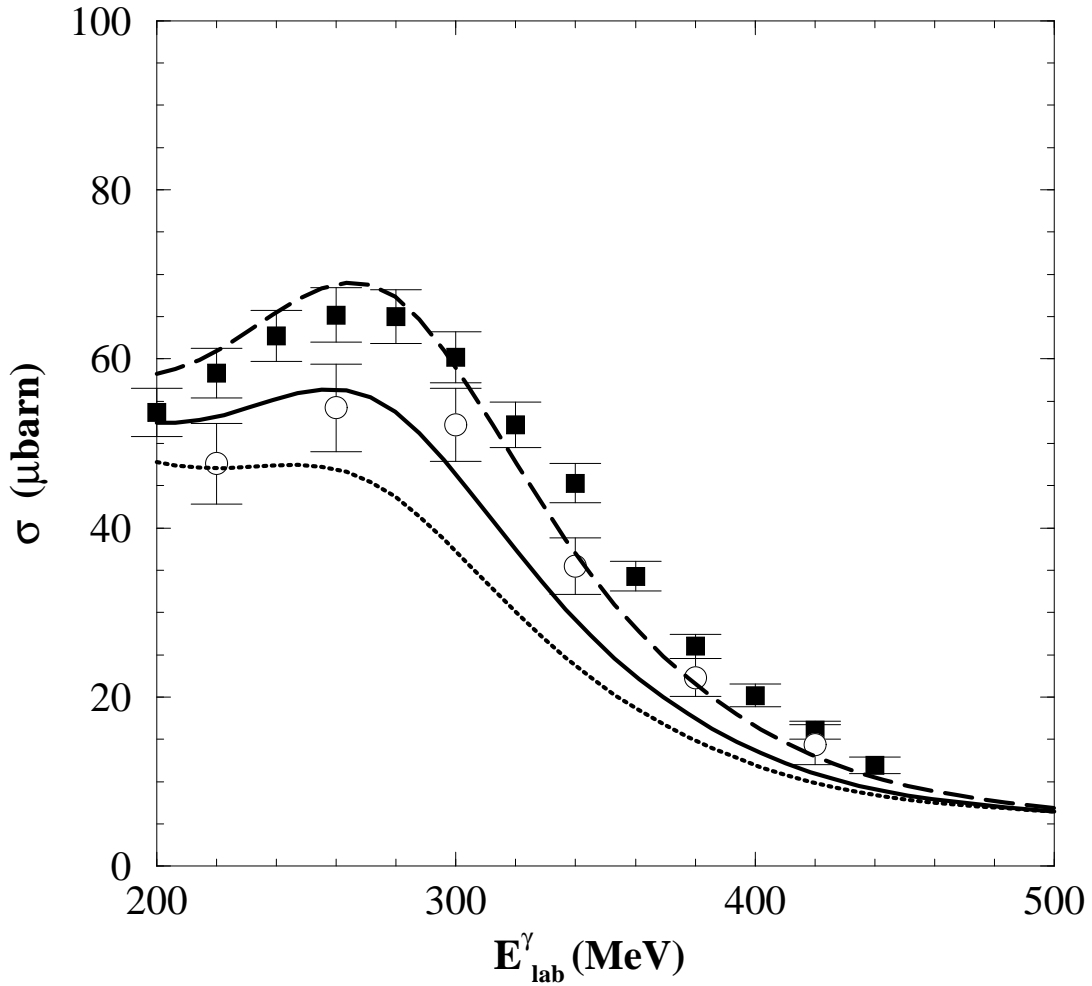


**Fig. 4.1.** Total cross-section of photo disintegration of the deuteron as a function of the photon lab energy. The sensitivity of the results on the coupling constant  $G_{M1}^{N\Delta}$  in the single-baryon current is shown. The results refer to three values of  $G_{M1}^{N\Delta}$ : 3.65 (dotted line), 5.16 (solid line) and 6.37 (long dashed one). The experimental data are from Ref. [37] (squares) and Ref. [38] (circles).

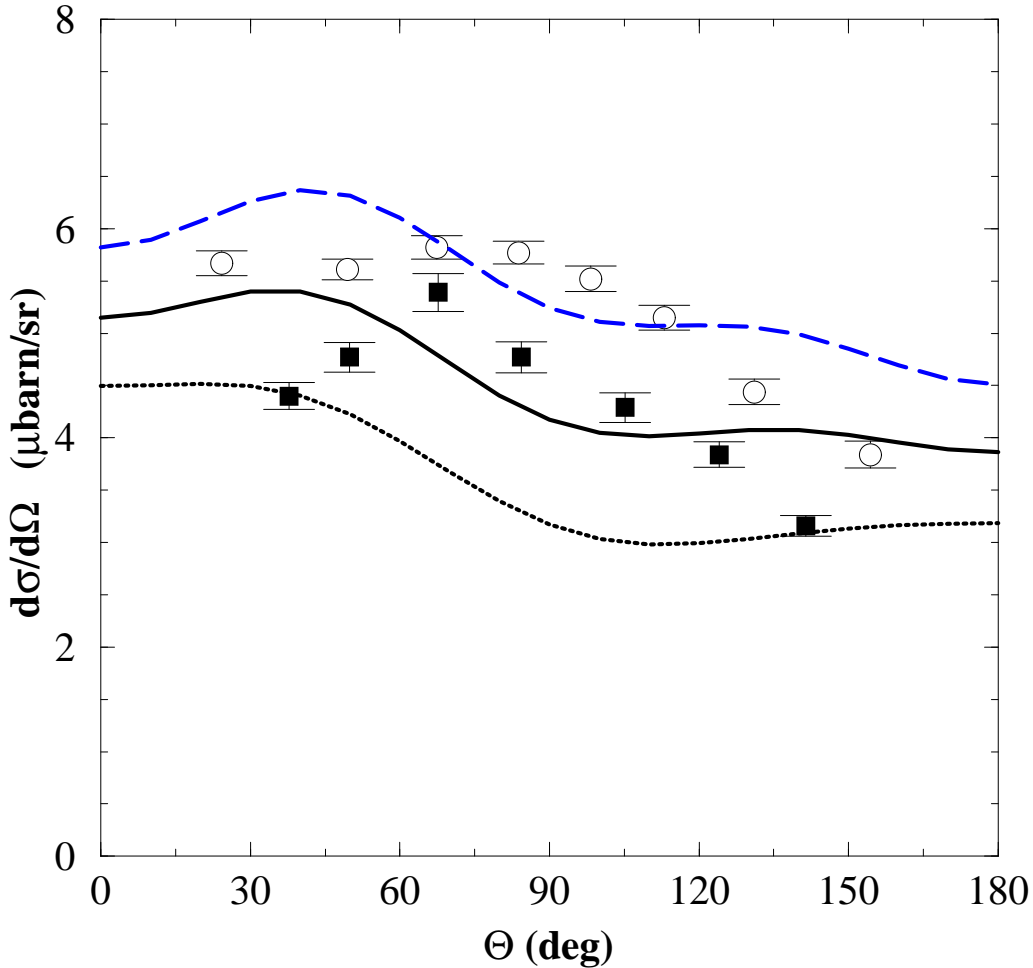


**Fig. 4.2(a).** Differential cross-section of photo disintegration of the deuteron for the photon energy  $E_{lab}^\gamma = 260$  MeV. The sensitivity of the results on the coupling constant  $G_{M1}^{N\Delta}$  in the single-baryon current is shown. The results refer to three values of  $G_{M1}^{N\Delta}$ : 3.65 (dotted line), 5.16 (solid line) and 6.37 (long dashed one). The experimental data are from Ref. [37] (squares) and Ref. [38] (circles).

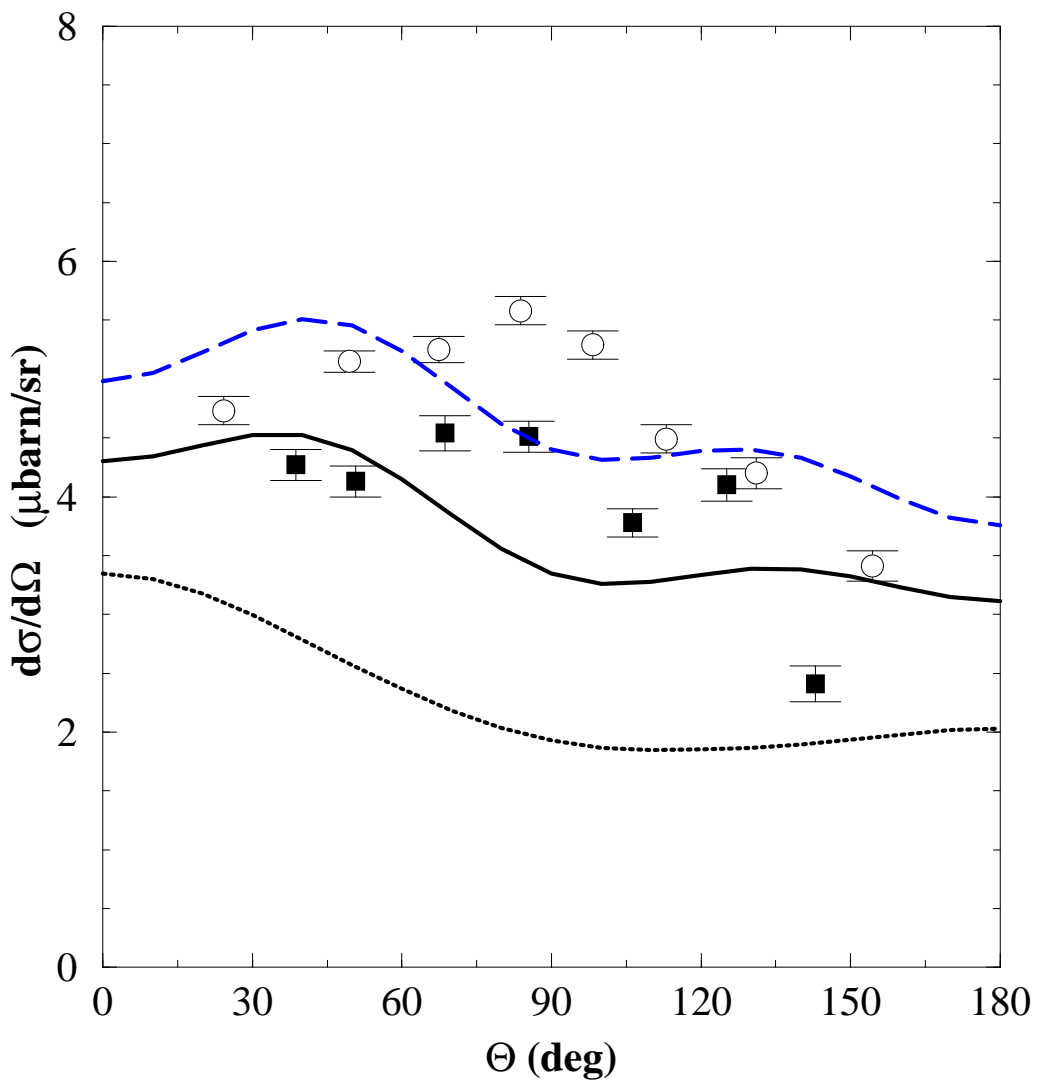


**Fig. 4.2(b).** Differential cross-section of photo disintegration of the deuteron for the photon lab energy  $E_{lab}^{\gamma} = 300$  MeV. The legend corresponds to Fig. 4.2(a).

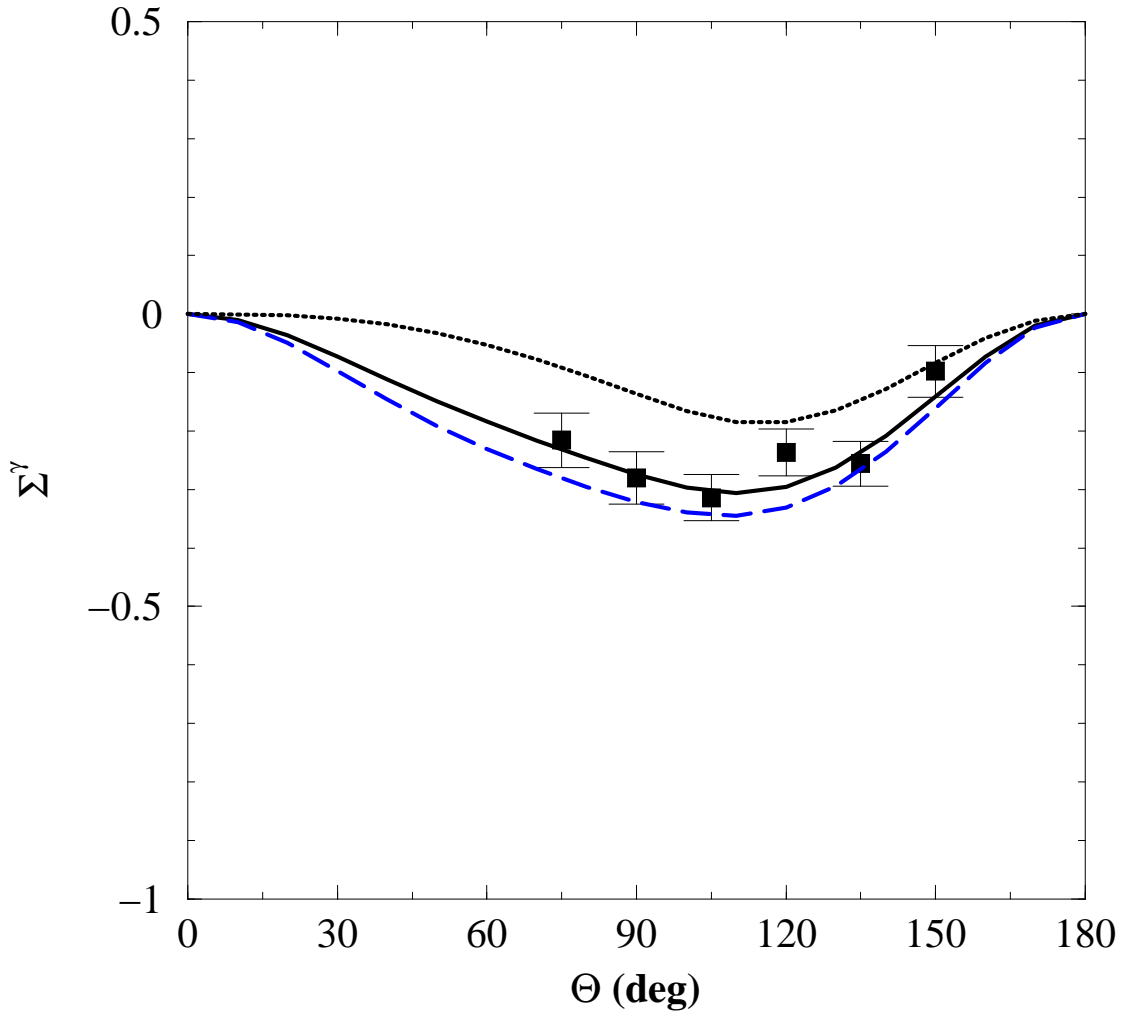


**Fig. 4.3(a).** Photon asymmetry of photo disintegration of the deuteron for the photon energy  $E_{lab}^\gamma = 260$  MeV. The sensitivity of the results on the coupling constant  $G_{M1}^{N\Delta}$  in the single-baryon current is shown. The results refer to three values of  $G_{M1}^{N\Delta}$ : 3.65 (dotted line), 5.16 (solid line) and 6.37 (long dashed one). The experimental data are from Ref. [39] (squares).

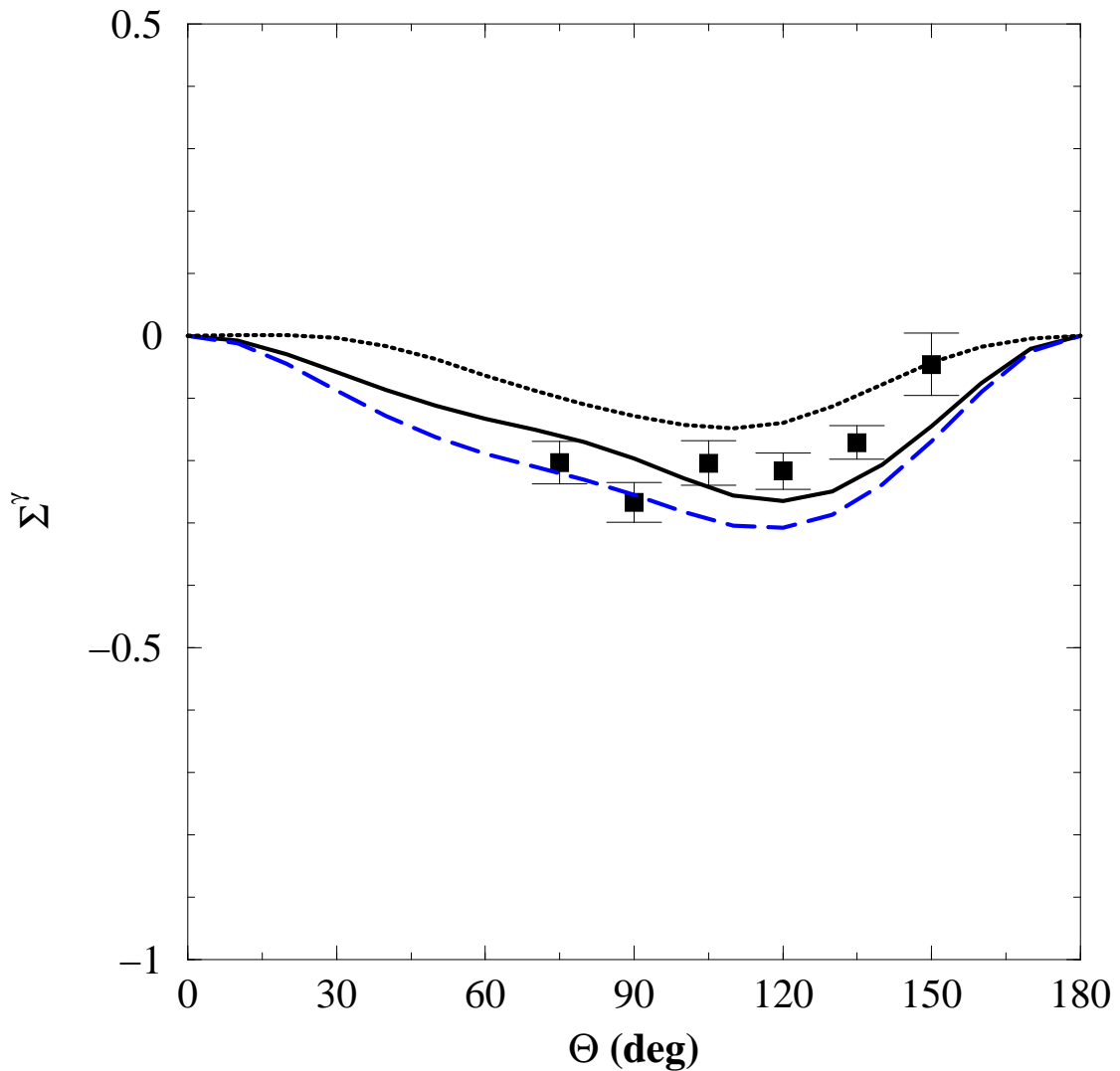


**Fig. 4.3(b).** Photon asymmetry of the photo disintegration of the deuteron for the photon energy photo disintegration for the photon energy  $E_{lab}^\gamma = 300$  MeV. The legend corresponds to Fig. 4.3(a).

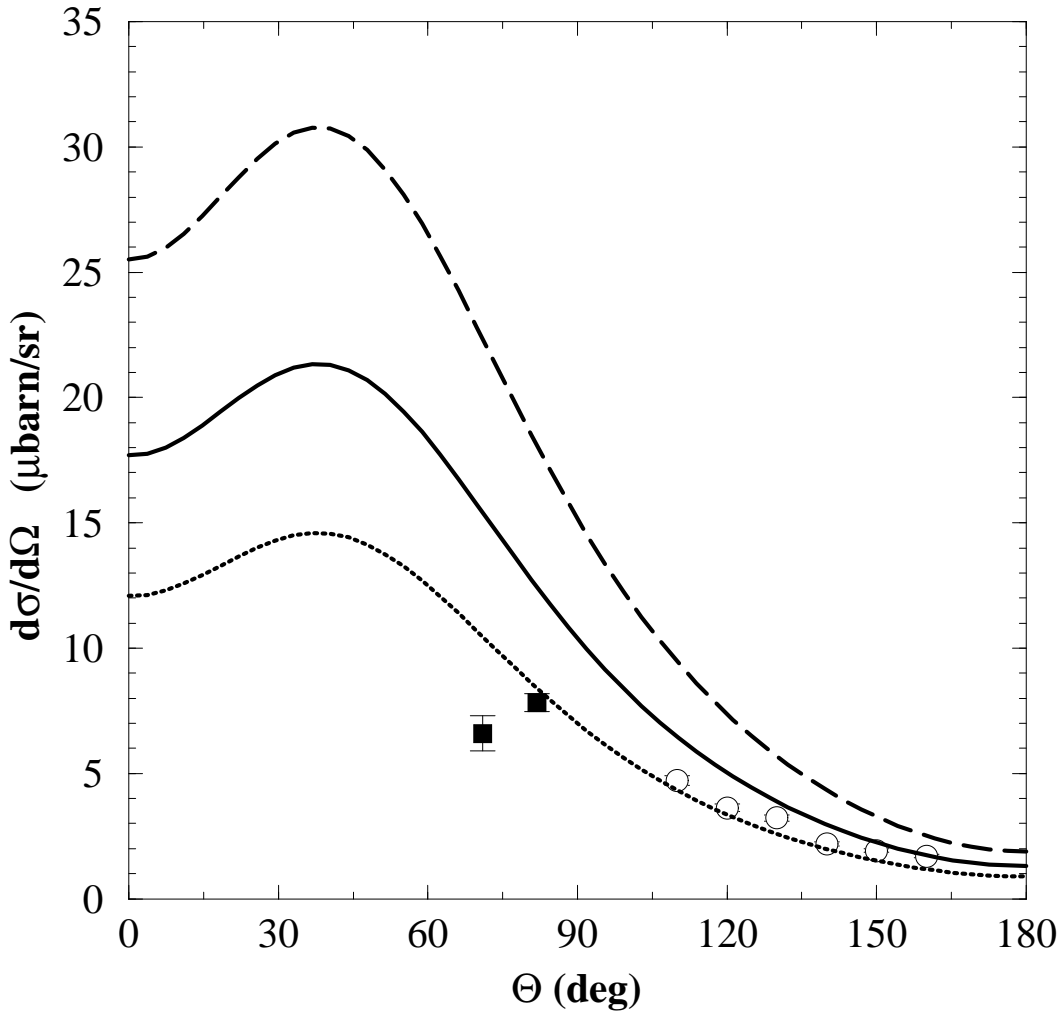


**Fig. 4.4(a).** Differential cross section of photo pionproduction on the deuteron for the photon energy  $E_{lab}^\gamma = 260$  MeV. The sensitivity of the results on the coupling constant  $G_{M1}^{N\Delta}$  in the single-baryon current is shown. The results refer to three values of  $G_{M1}^{N\Delta}$ : 3.65 (dotted line), 5.16 (solid line) and 6.37 (long dashed one). The experimental data are from Ref. [40] (circles) and Ref. [41] (squares).

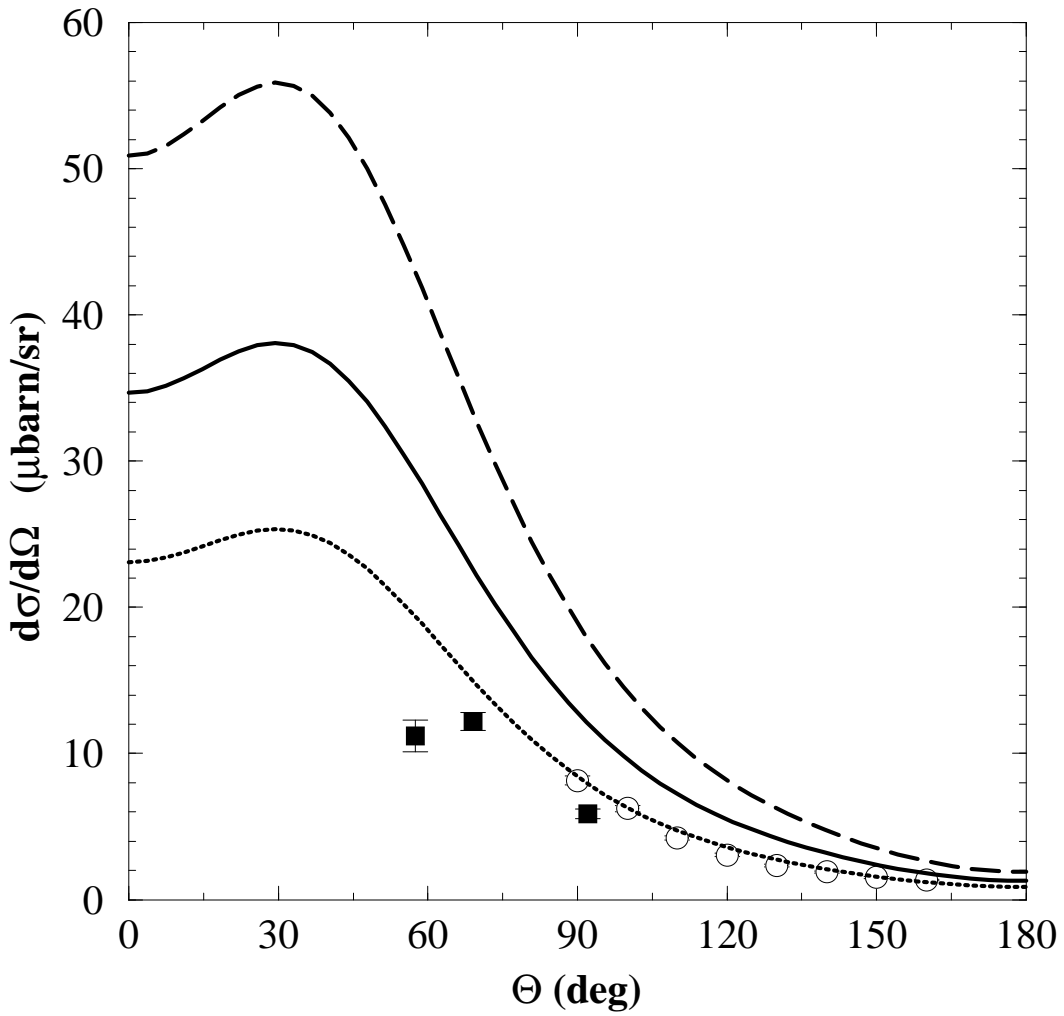


**Fig. 4.4(b).** Differential cross section of photo pion production on the deuteron for the photon energy  $E_{lab}^\gamma = 300$  MeV. The legend corresponds to Fig. 4.4(a).

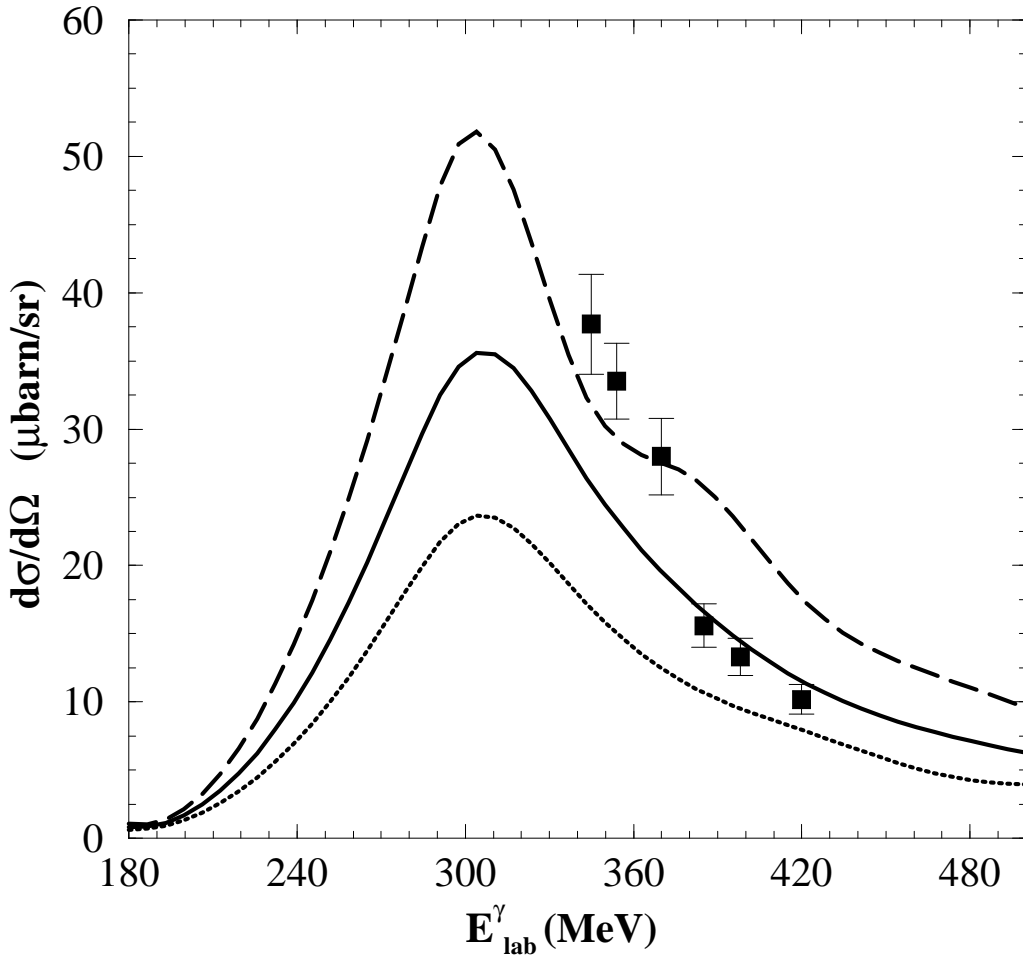


**Fig. 4.5.** Differential cross section of photo pionproduction on the deuteron at the fixed pion angle  $6^\circ$  in the c.m. system as a function of the photon energy. The sensitivity of the results on the coupling constant  $G_{M1}^{N\Delta}$  in the single-baryon current is shown. The results refer to three values of  $G_{M1}^{N\Delta}$ : 3.65 (dotted line), 5.16 (solid line) and 6.37 (long dashed one). The experimental data are from Ref. [42] (squares).

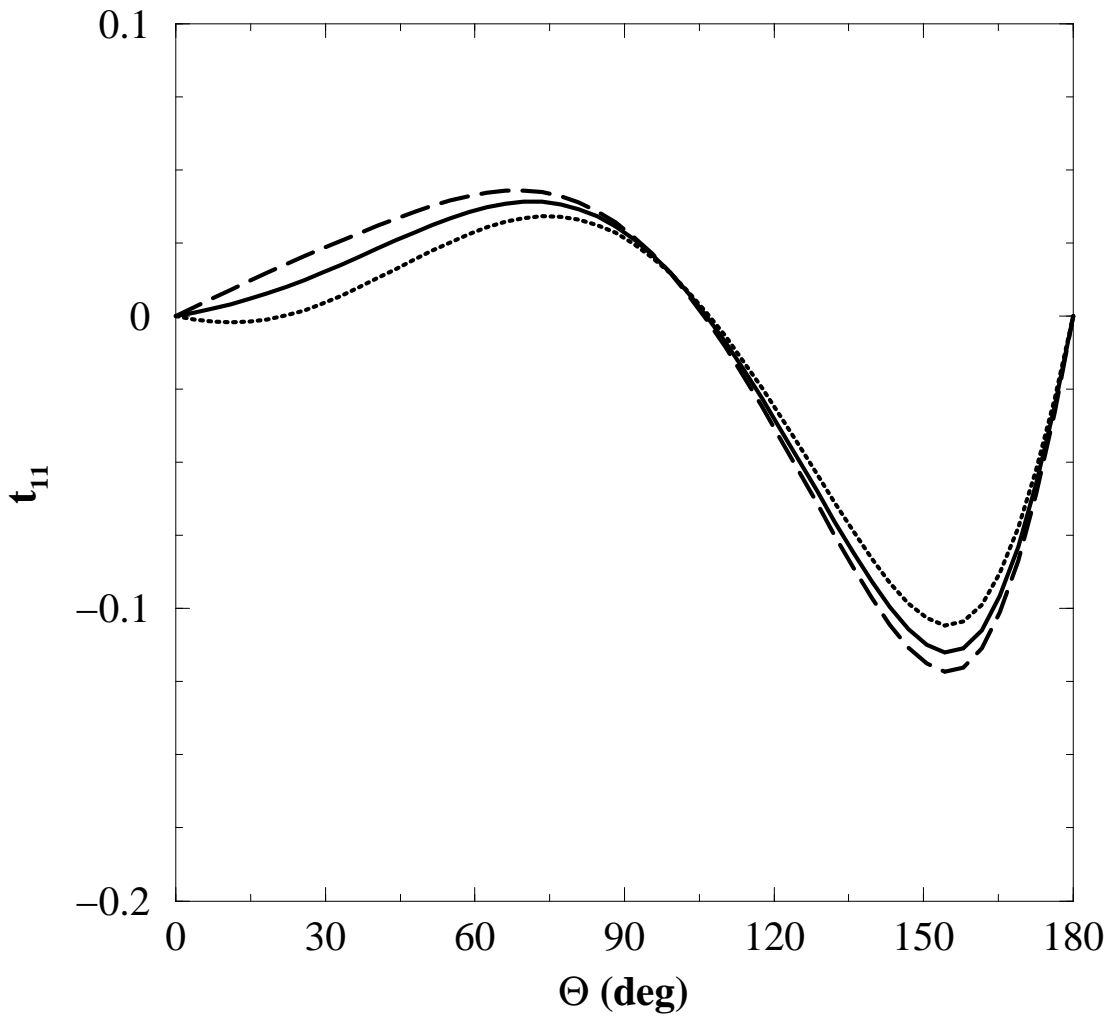


**Fig. 4.6(a).** Tensor polarization of photo pionproduction on the deuteron for the photon lab energy  $E_{lab}^\gamma = 260$  MeV. The sensitivity of the results on the coupling constant  $G_{M1}^{N\Delta}$  in the single-baryon current is shown. The results refer to three values of  $G_{M1}^{N\Delta}$ : 3.65 (dotted line), 5.16 (solid line) and 6.37 (long dashed one).

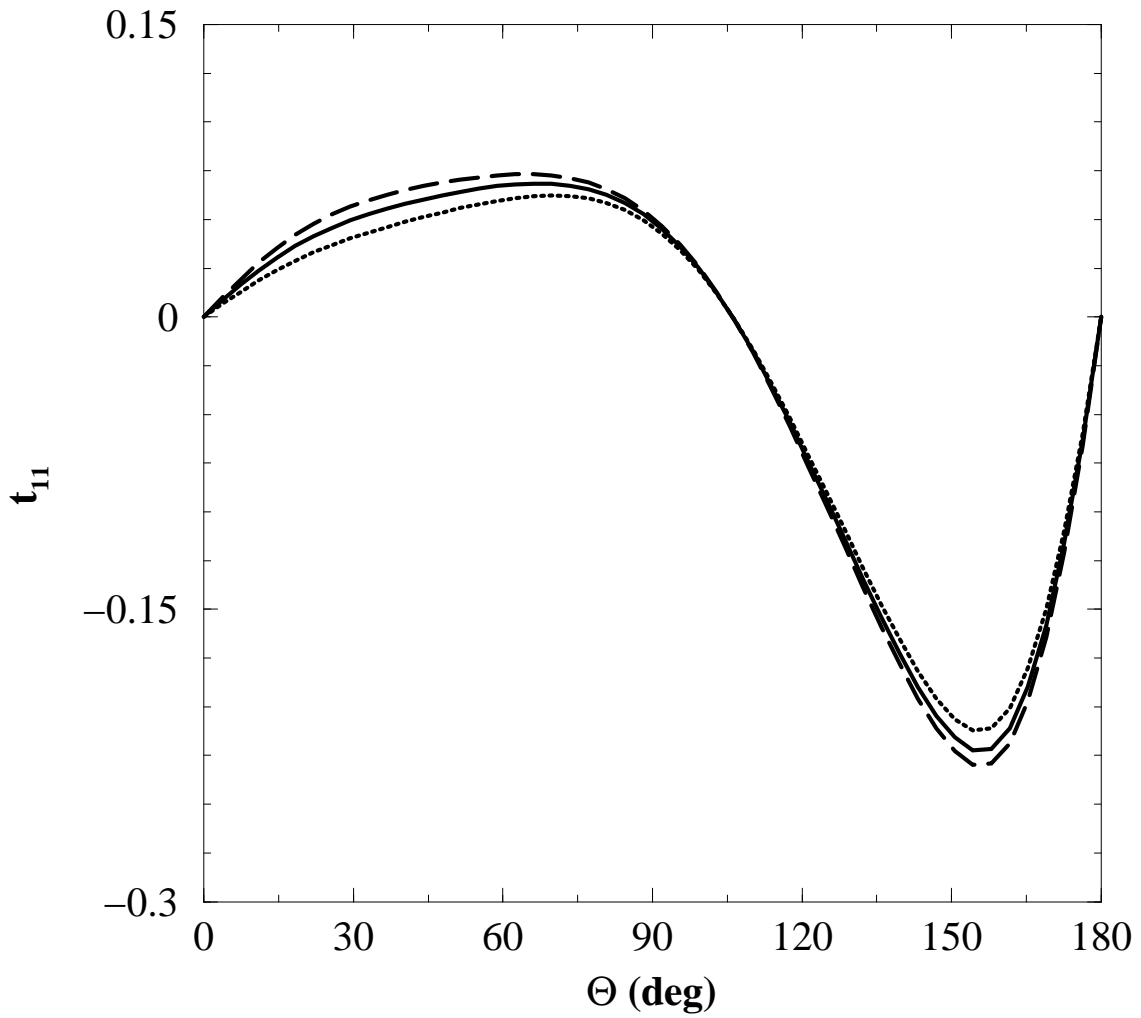


**Fig. 4.6(b).** Tensor polarization of photo pionproduction on the deuteron for the photon lab energy  $E_{lab}^\gamma = 300$  MeV. The legend corresponds to Fig. 4.6(a).

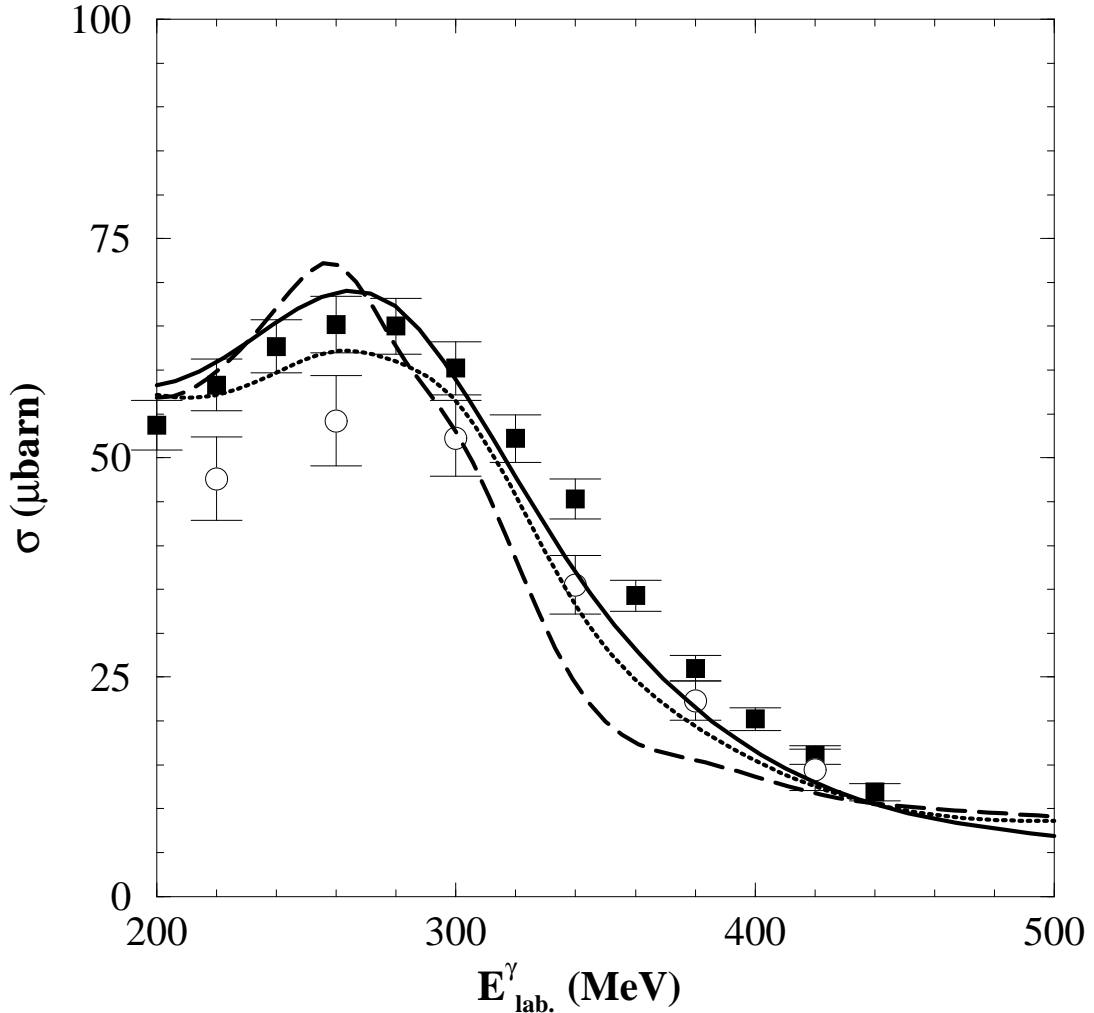


**Fig. 4.7.** Total cross section of photo disintegration of the deuteron as function of the photon lab energy. Sensitivity of results on three different choices of the nucleon- $\Delta$  potential in Figs. 1(c) and 1(d) is shown. They were chosen as follows: The nucleon- $\Delta$  potential as described in Subsect. 3.1 is the reference potential (solid line), the two others are based on meson exchange (long-dashed line) and on a nonrelativistic quark model (dotted line). The value of the coupling strength  $G_{M1}^{N\Delta}$  is 6.37. The experimental data are from Ref. [37] (squares) and Ref. [38] (circles).

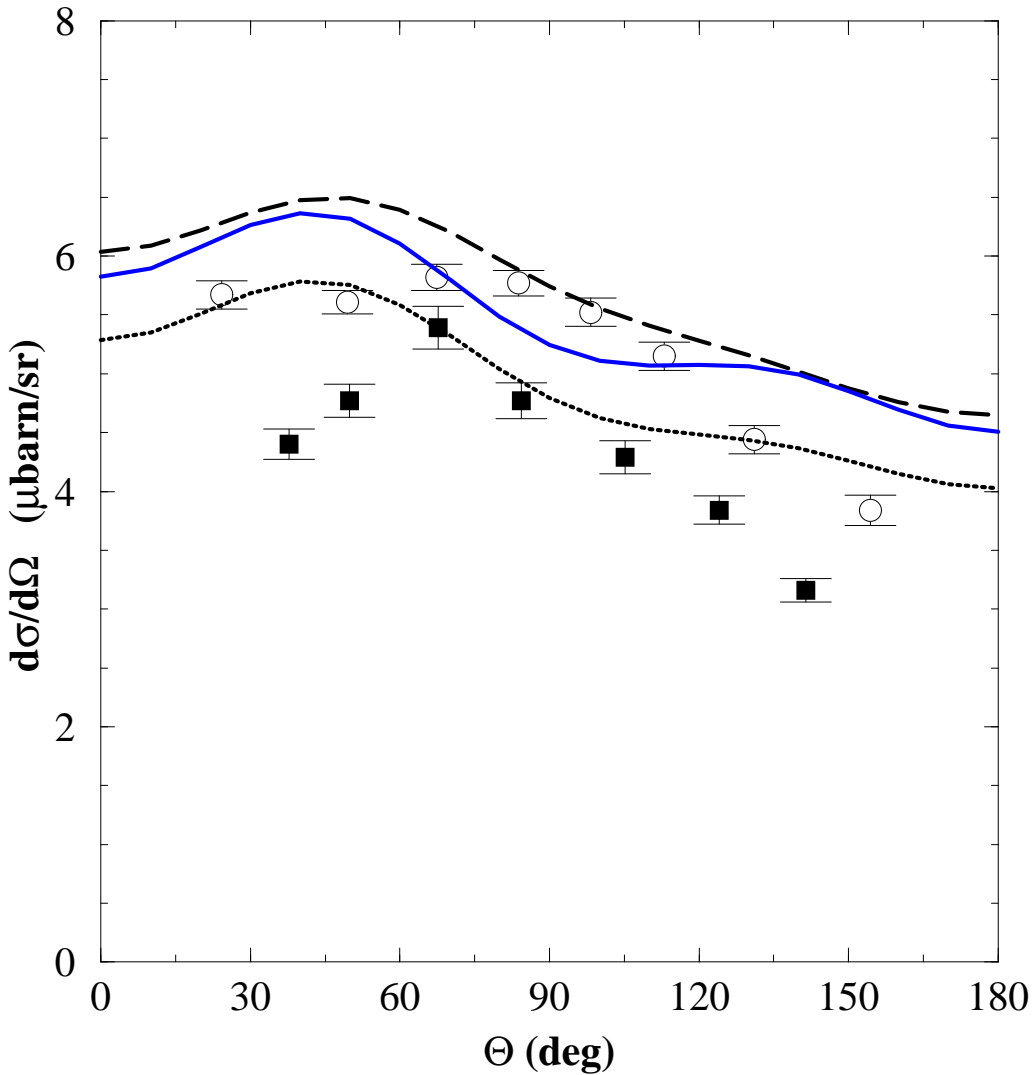


**Fig. 4.8(a).** Differential cross section of photo disintegration of the deuteron for the photon lab energy  $E_{lab}^\gamma = 260$  MeV. Sensitivity of results on three different choices of the nucleon- $\Delta$  potential in Figs. 1(c) and 1(d) is shown. They were chosen as follows: The nucleon- $\Delta$  potential as described in Subsect. 3.1 is the reference potential (solid line), the two others are based on meson exchange (long-dashed line) and on a nonrelativistic quark model (dotted line). The value of the coupling strength  $G_{M1}^{N\Delta}$  is 6.37. The experimental data are from Ref. [37] (squares) and Ref. [38] (circles).

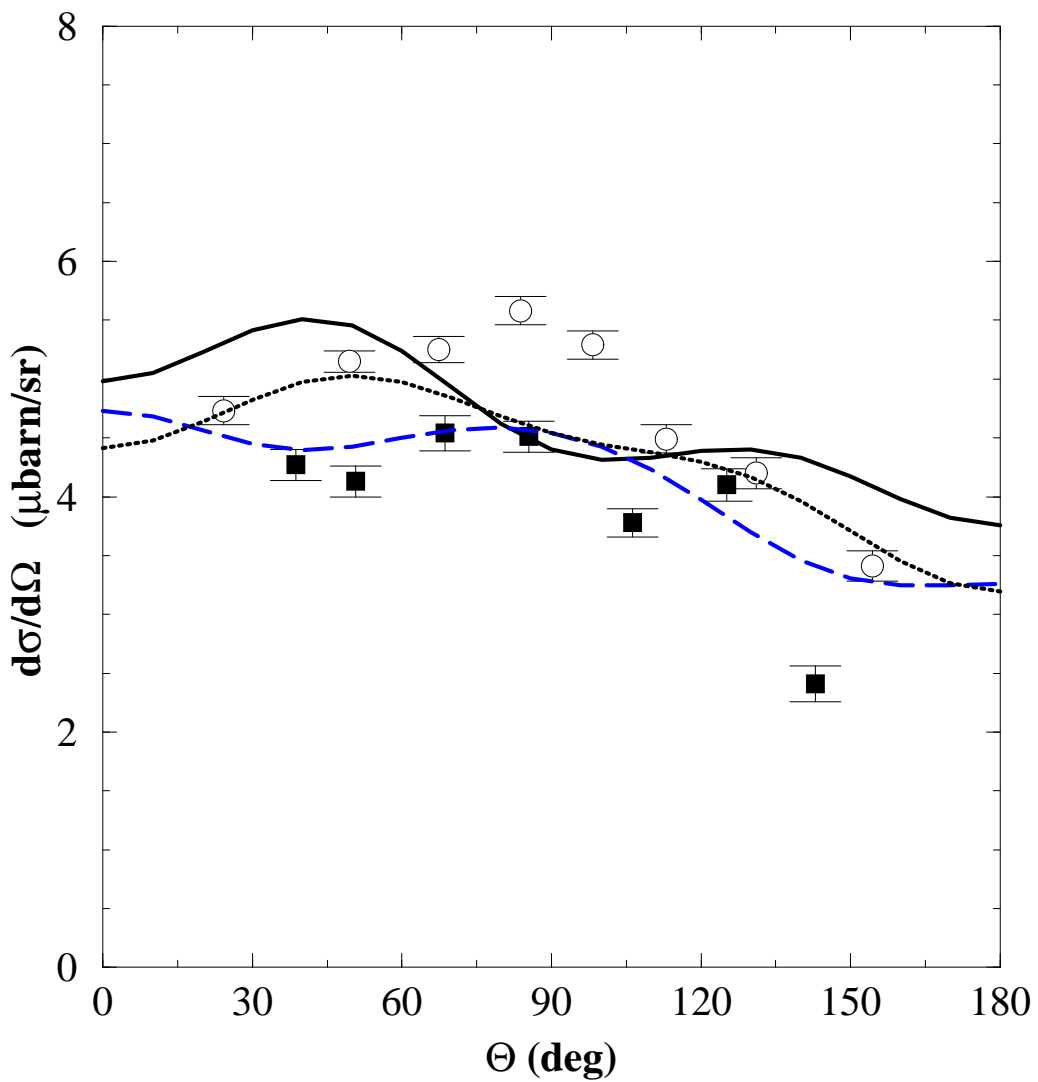


**Fig. 4.8(b).** Differential cross section of photo disintegration of the deuteron for the photon lab energy  $E_{lab}^\gamma = 300$  MeV. The legend corresponds to Fig. 4.8(a).

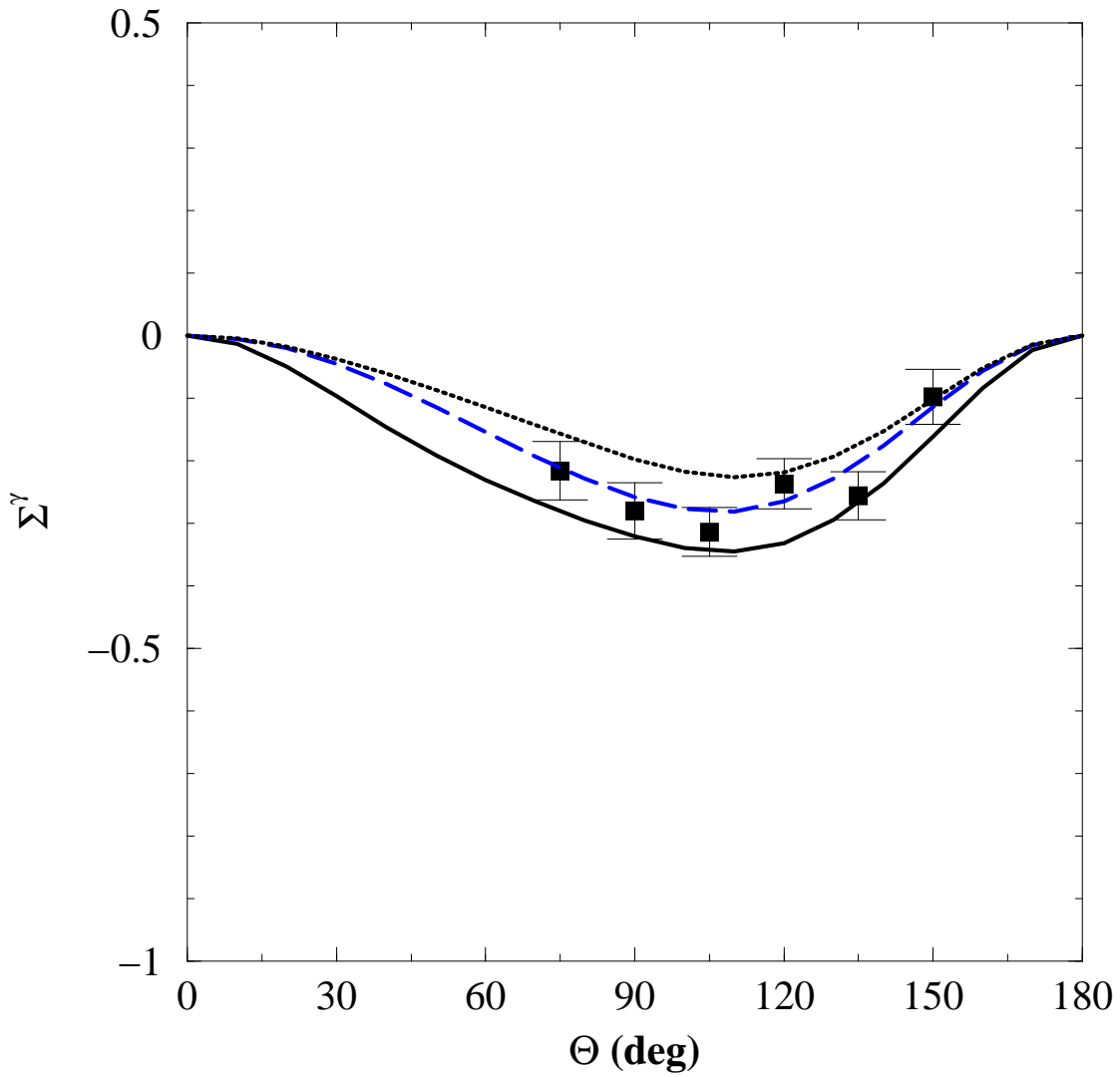


**Fig. 4.9(a).** Photon asymmetry of photo disintegration of the deuteron for the photon lab energy  $E_{lab}^\gamma = 260$  MeV. Sensitivity of results on three different choices of the nucleon- $\Delta$  potential in Figs. 1(c) and 1(d) is shown. They were chosen as follows: The nucleon- $\Delta$  potential as described in Subsect. 3.1 is the reference potential (solid line), the two others are based on meson exchange (long-dashed line) and on a nonrelativistic quark model (dotted line). The value of the coupling strength  $G_{M1}^{N\Delta}$  is 6.37. The experimental data are from Ref. [39].

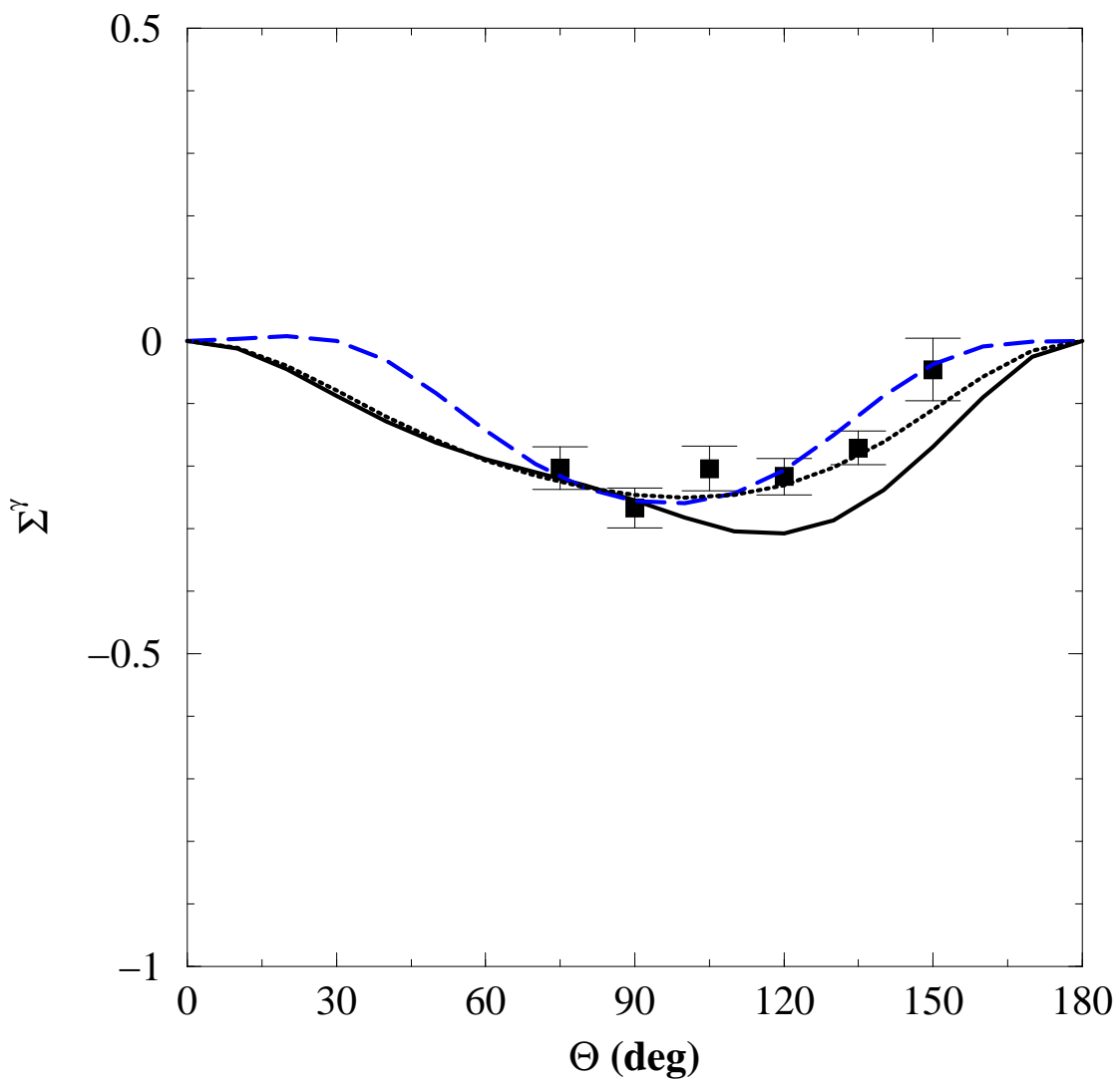


**Fig. 4.9(b).** Photon asymmetry of photo disintegration of the deuteron for the photon lab energy  $E_{lab}^\gamma = 300$  MeV. The legend corresponds to Fig. 4.9(a).

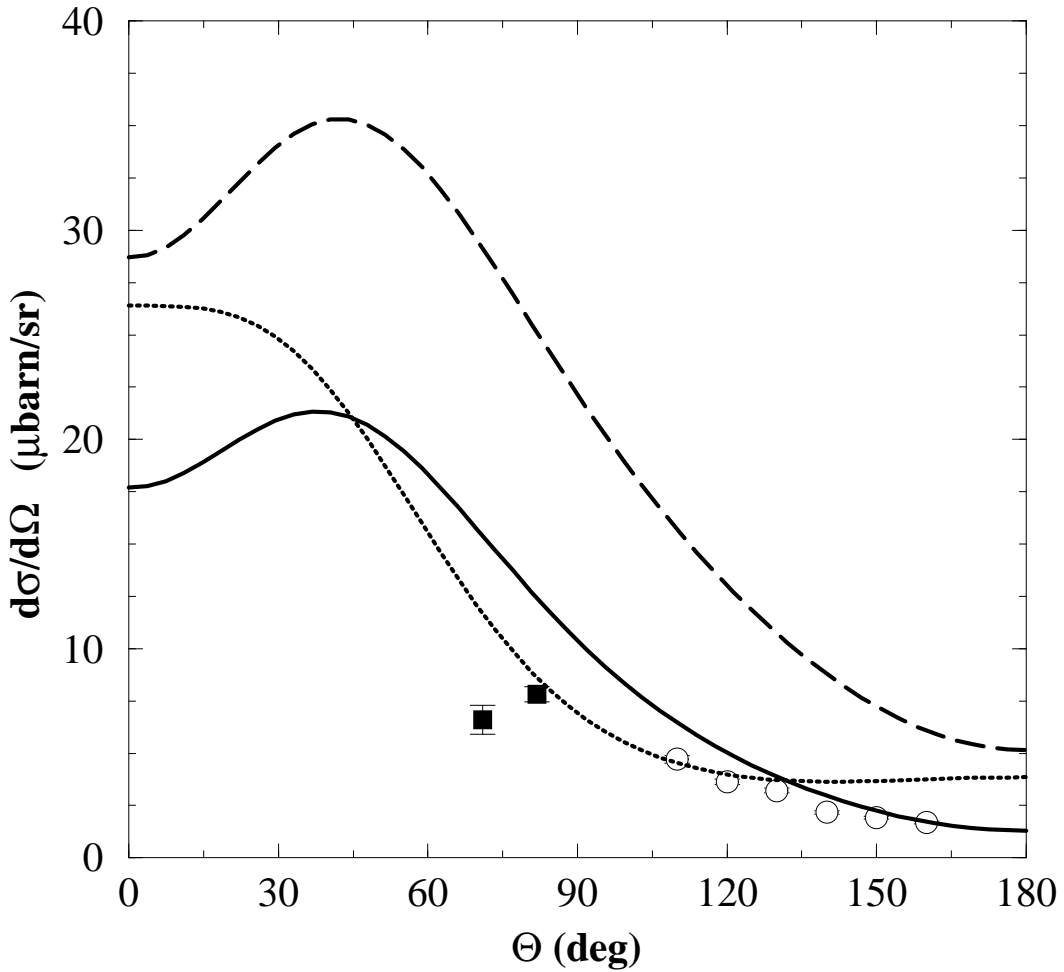


**Fig. 4.10(a).** Differential cross section of photo pion production on the deuteron for the photon lab energy  $E_{lab}^\gamma = 260$  MeV. Sensitivity of results on three different choices of the nucleon- $\Delta$  potential in Figs. 1(c) and 1(d) is shown. They were chosen as follows: The nucleon- $\Delta$  potential as described in Subsect. 3.1 is the reference potential (solid line), the two others are based on meson exchange (long-dashed line) and on a nonrelativistic quark model (dotted line). The value of the coupling strength  $G_{M1}^{N\Delta}$  is 5.16. The experimental data are from Ref. [40] (circles) and Ref. [41] (squares).

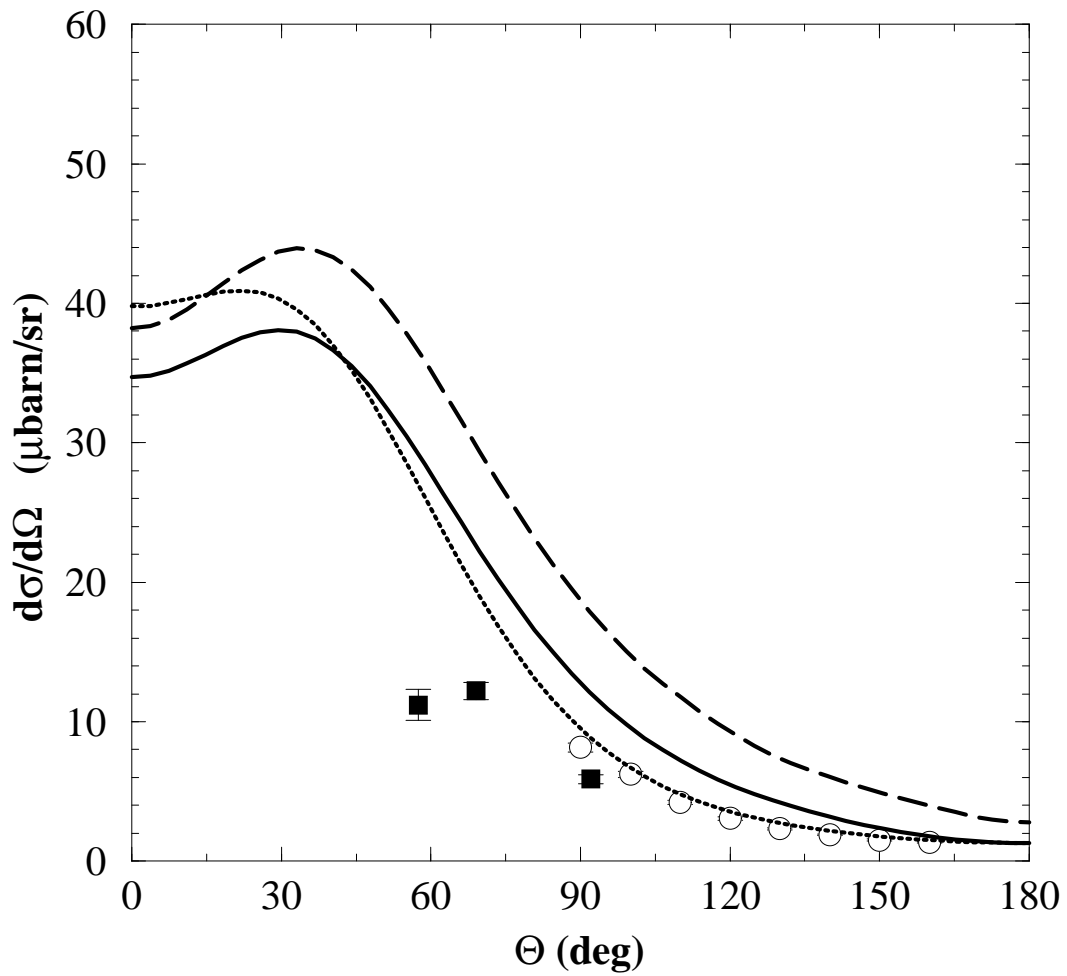


**Fig. 4.10(b).** Differential cross section of photo pionproduction on the deuteron for the photon lab energy  $E_{lab}^{\gamma} = 300$  MeV. The legend corresponds to Fig. 4.10(a).

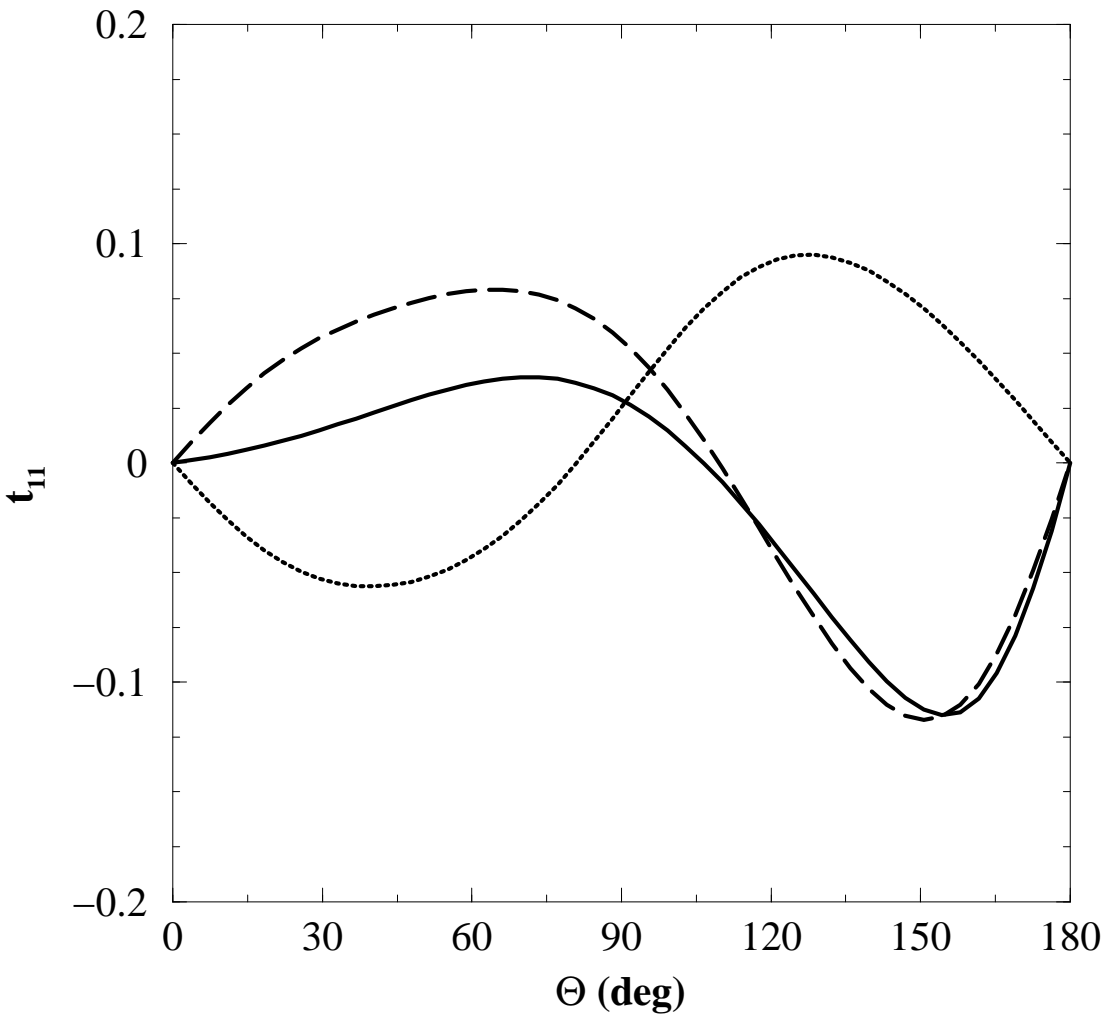


**Fig. 4.11(a).** Vector polarization of photo pionproduction on the deuteron for the photon lab energy  $E_{lab}^\gamma = 260$  MeV. Sensitivity of results on three different choices of the nucleon- $\Delta$  potential in Figs. 1(c) and 1(d) is shown. They were chosen as follows: The nucleon- $\Delta$  potential as described in Subsect. 3.1 is the reference potential (solid line), the two others are based on meson exchange (long-dashed line) and on a nonrelativistic quark model (dotted line). The value of the coupling strength  $G_{M1}^{N\Delta}$  is 5.16.

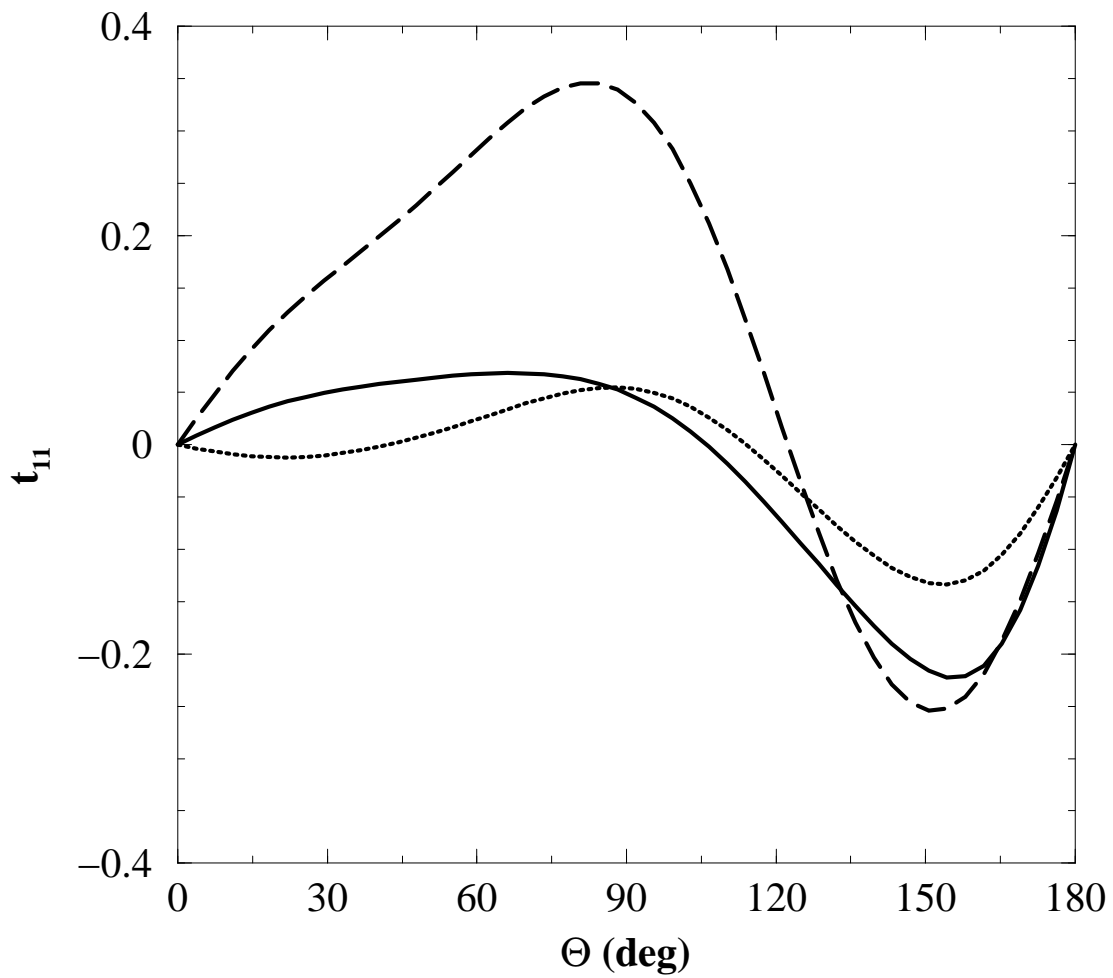


**Fig. 4.11(b).** Vector polarization of photo pionproduction on the deuteron for the photon lab energy  $E_{lab}^\gamma = 300$  MeV. The legend corresponds to Fig. 4.11(a).

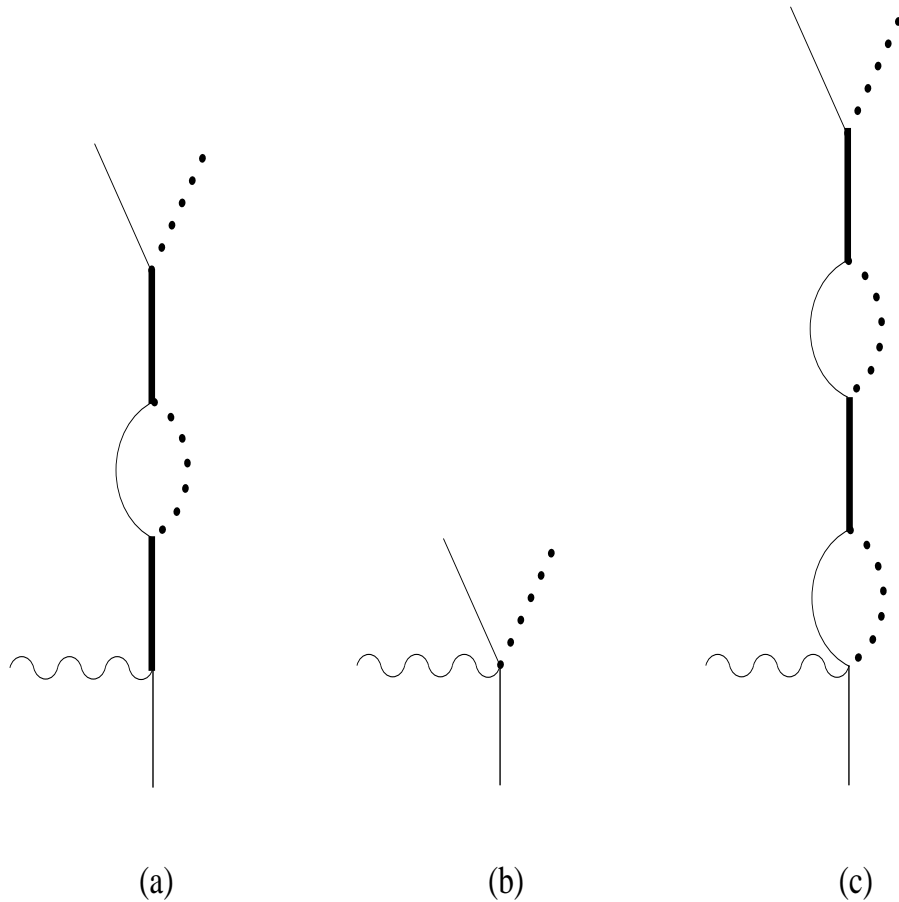


**Fig. C.1.** Processes contributing to photo pionproduction on the single nucleon in the resonant multipole amplitudes  $M_{1+}^{(\frac{3}{2})}$  and  $E_{1+}^{(\frac{3}{2})}$ . The processes correspond to the resonance (a), Born (b) and interference contributions. The hadronic rescattering occurring in the processes (a) and (c) up to infinite order is indicated only in a characteristic low order.

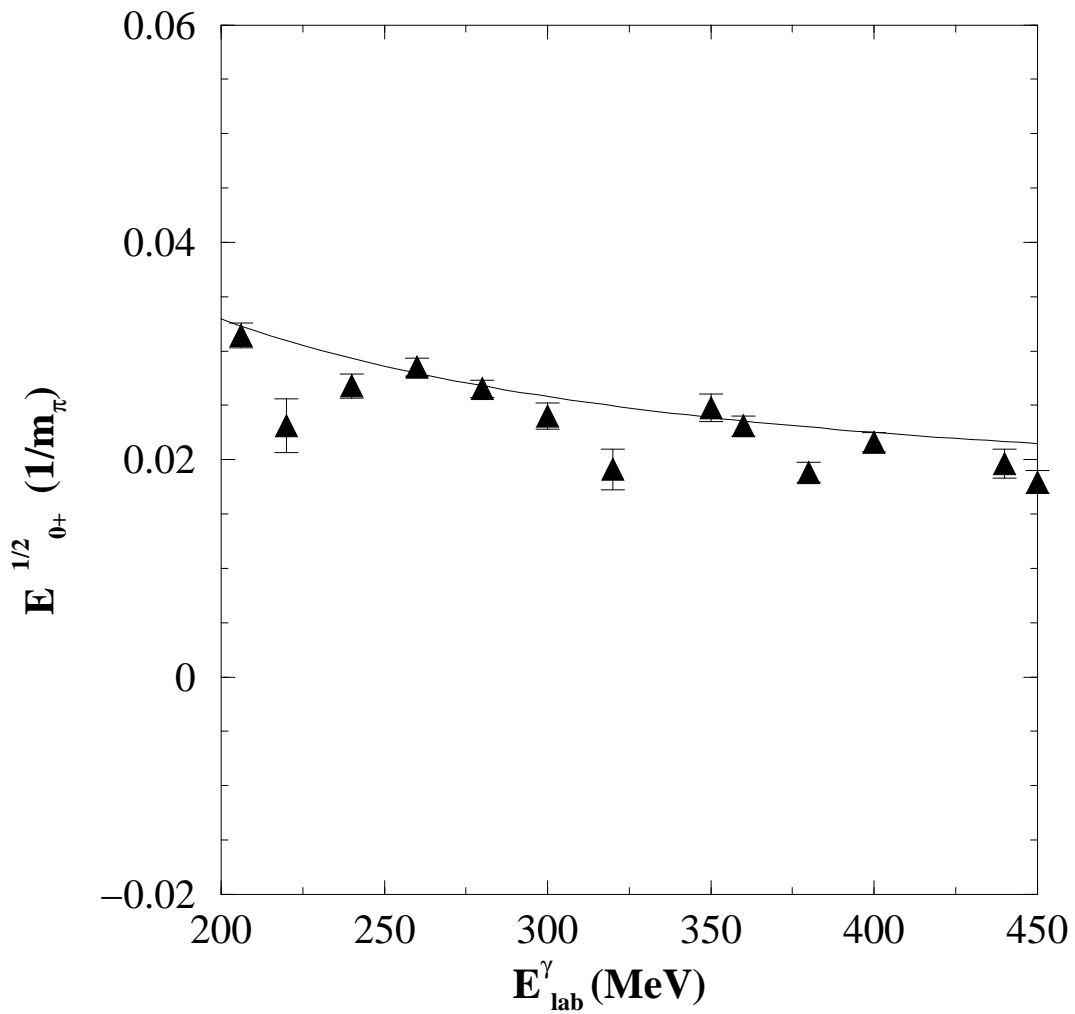


**Fig. C.2.**  $E_{0+}^{1/2}$  multipole of photo pionproduction on the single nucleon. The theoretical fit result (solid line) is compared with the experimental data of Ref. [43].

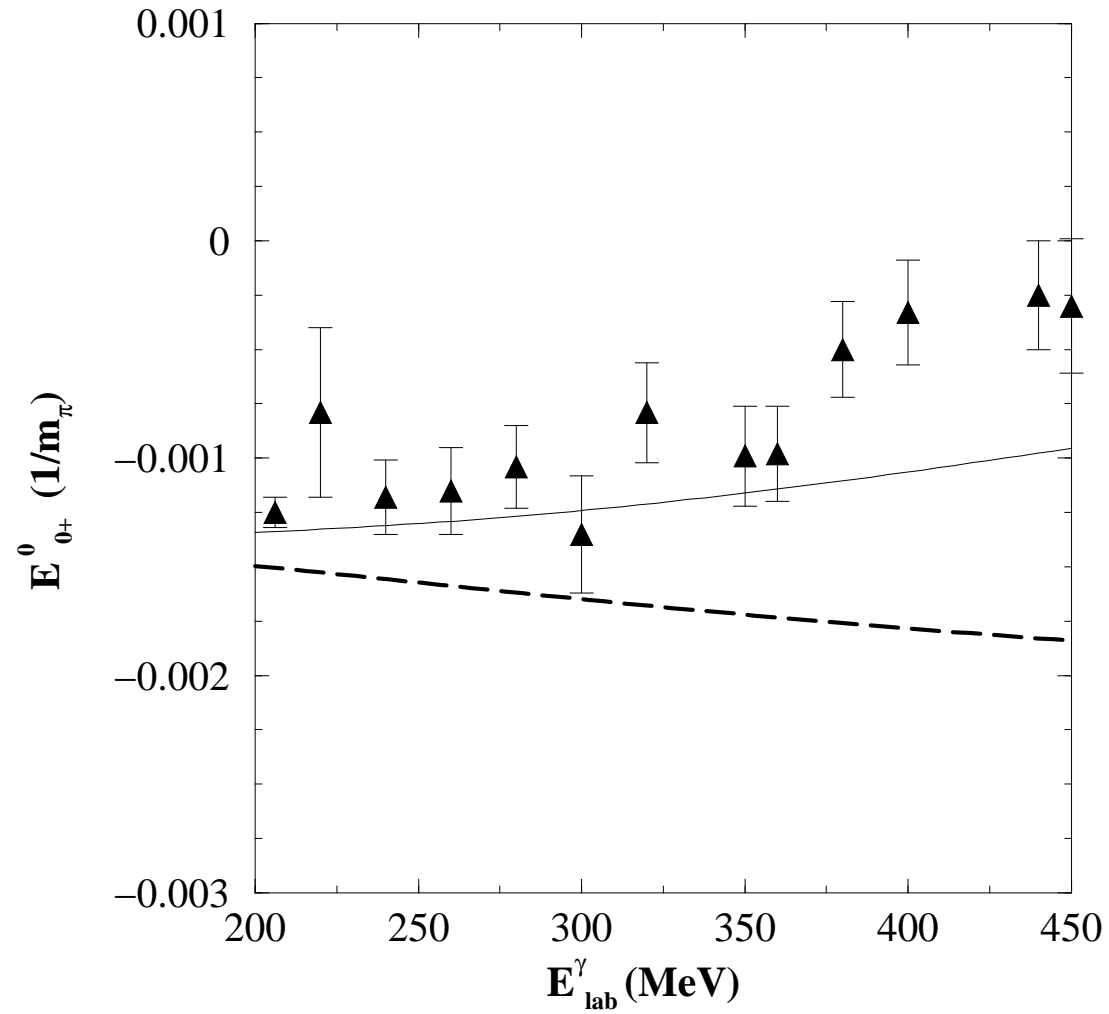


**Fig. C.3.**  $E_{0+}^0$  multipole of photo pionproduction on the single nucleon. The theoretical fit result (solid line) is compared with the experimental data of Ref. [43]. The dashed line represents the result without  $\rho$ -meson contribution.

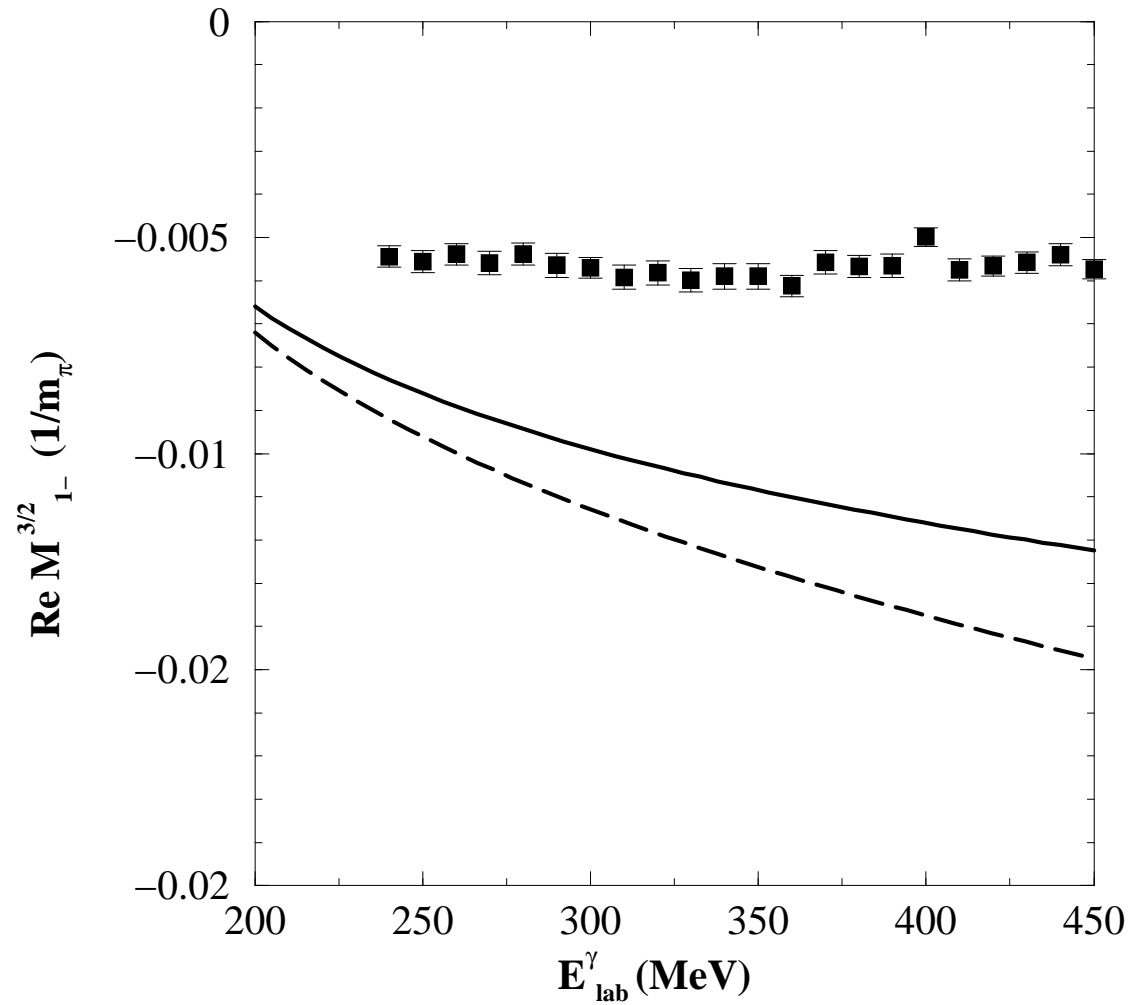


**Fig. C.4.**  $M_{1-}^{3/2}$  multipole of photo pionproduction on the single nucleon. The theoretical fit result (solid line) is compared with the experimental data of Ref. [44]. The dashed line represents the result without  $\omega$ -meson contribution.

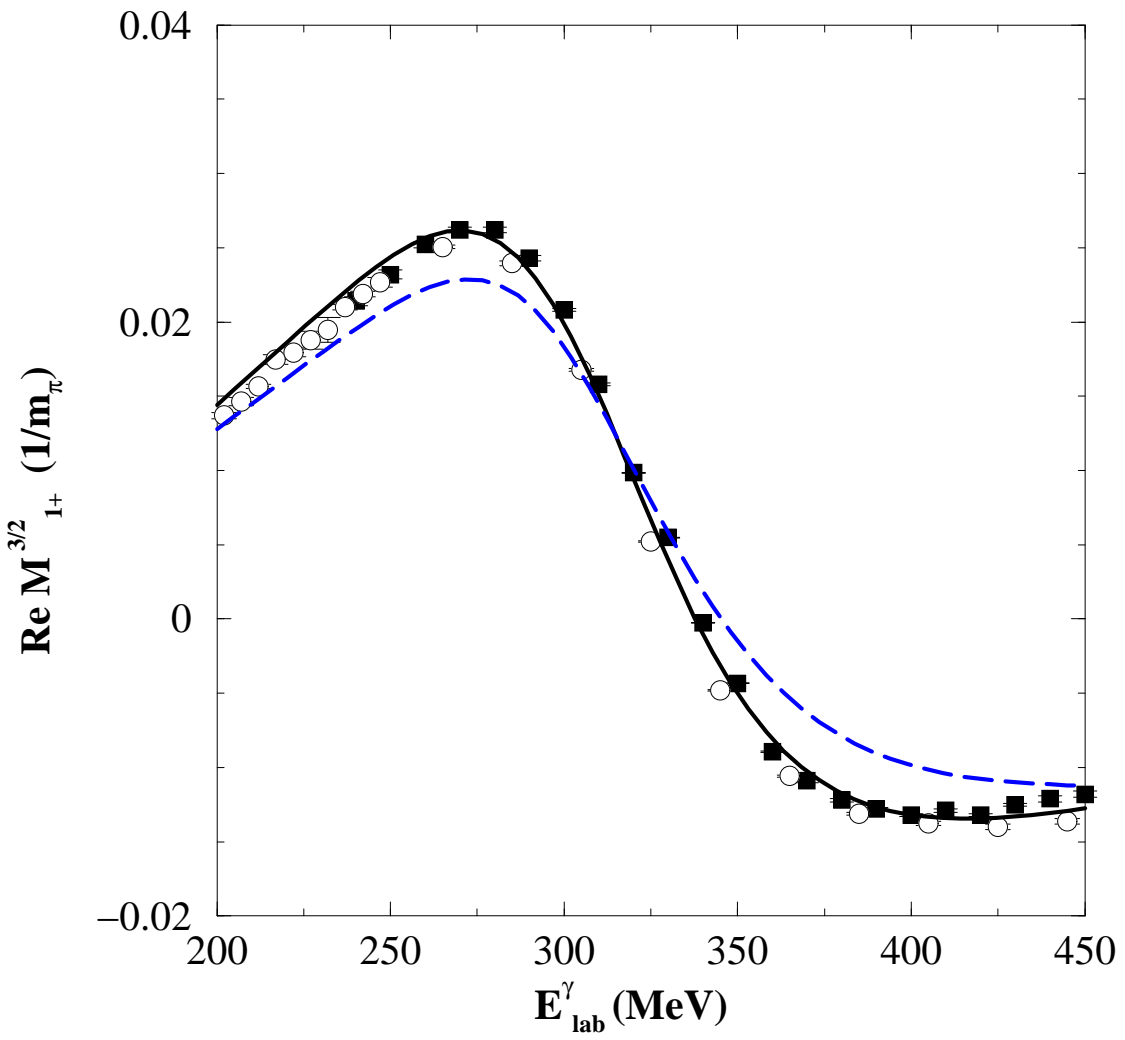


**Fig. C.5.** Real part of  $M_{1+}^{3/2}$  multipole of photo pionproduction on the single nucleon. The theoretical fit result (solid line) is compared with the experimental data of Ref. [44] (filled-in squares) and of Ref. [45] (open circles). The optimized fit parameters are  $G_{M1}^{N\Delta} = 3.65$  and  $\Lambda_B = 245.5$  MeV. The experimental data are from Ref. [44] (squares) and from Ref. [45] (circles). The dashed line corresponds to the result without  $\omega$ -meson contribution.

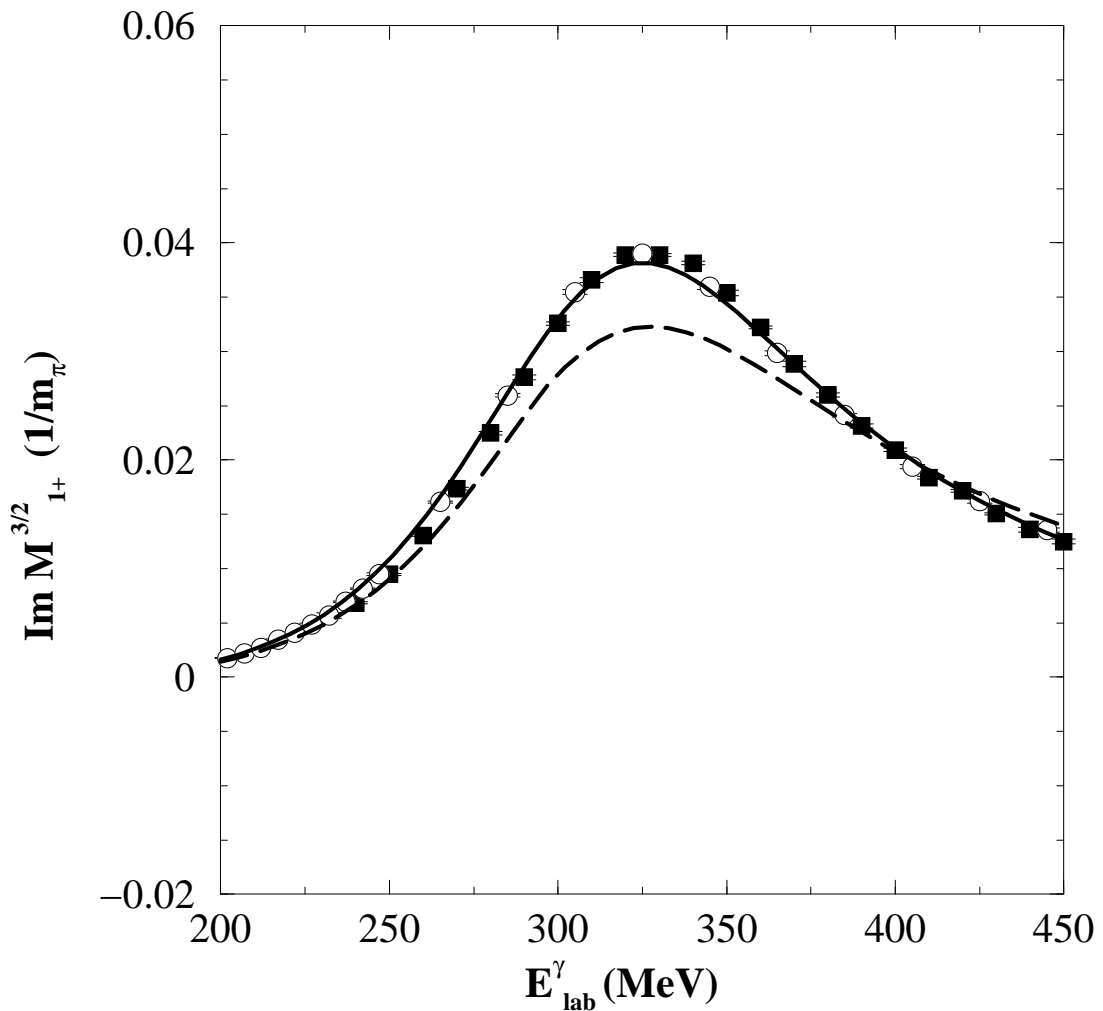


**Fig. C.6.** Imaginary part of  $M_{1+}^{3/2}$  multipole of photo pionproduction on the single nucleon. The legend corresponds to Fig. C.5.

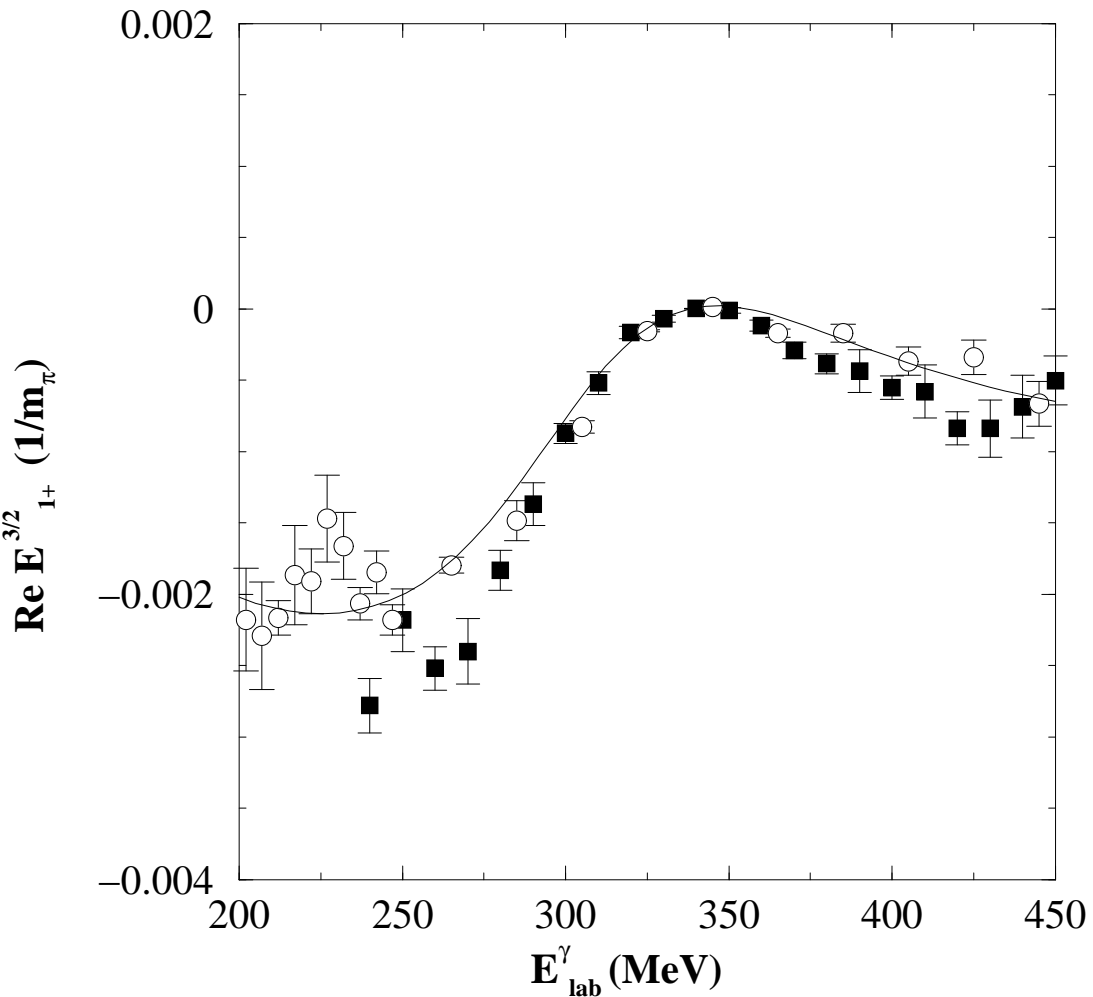


**Fig. C.7.** Real part of  $E_{1+}^{3/2}$  multipole of photo pionproduction on the single nucleon. The theoretical fit result (solid line) is compared with the experimental data of Ref. [44] (filled-in squares) and of Ref. [45] (open circles). The optimized fit parameters are  $G_{E2}^{N\Delta} = 0.1$  and  $\Lambda_B = 379.0$  MeV.

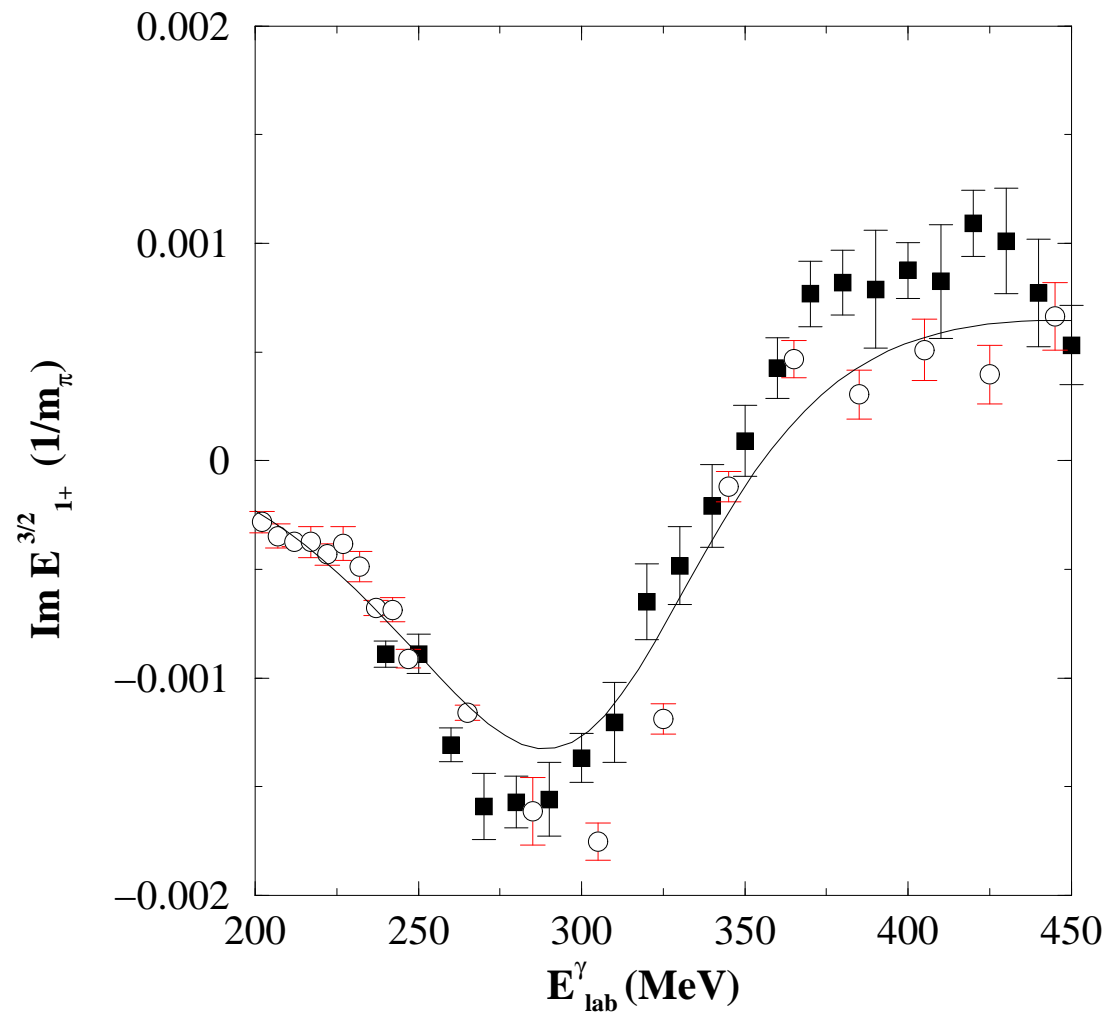


**Fig. C.8.** Imaginary part of  $E_{1+}^{3/2}$  multipole of photo pionproduction on the single nucleon. The legend corresponds to Fig. C.7.